UNIVERSIDADE ESTADUAL DE CAMPINAS
Instituto de Biologia

Mario Ramos de Oliveira Barsottini

Desenvolvimento direcionado de inibidores da enzima mitocondrial Oxidase Alternativa (AOX) com ação antifúngica contra *Moniliophthora perniciosa*, fungo causador da vassoura de bruxa do cacaueiro

CAMPINAS
2019

MARIO RAMOS DE OLIVEIRA BARSOTTINI

Desenvolvimento direcionado de inibidores da enzima mitocondrial Oxidase Alternativa (AOX) com ação antifúngica contra *Moniliophthora perniciosa*, fungo causador da vassoura de bruxa do cacaueiro

Tese apresentada ao Instituto de Biologia da Universidade Estadual de Campinas como parte dos requisitos exigidos para a obtenção do título de Doutor em Genética e Biologia Molecular, na Área de Genética de Microrganismos.

Orientador: Prof. Dr. GONÇALO AMARANTE GUIMARÃES PEREIRA

ESTE EXEMPLAR CORRESPONDE À VERSÃO FINAL DISSERTAÇÃO/TESE DEFENDIDA PELO ALUNO MARIO RAMOS DE OLIVEIRA BARSOTTINI, E ORIENTADA PELO PROF. DR. GONÇALO AMARANTE GUIMARÃES PEREIRA.

CAMPINAS
2019

Agência(s) de fomento e nº(s) de processo(s): FAPESP, 2014/15339-6; CNPq, 142358/2014-2

Ficha catalográfica
Universidade Estadual de Campinas
Biblioteca do Instituto de Biologia
Mara Janaina de Oliveira - CRB 8/6972

B28d

Barsottini, Mario Ramos de Oliveira, 1987-
Desenvolvimento direcionado de inibidores da enzima mitocondrial oxidase alternativa (AOX) com ação antifúngica contra *Moniliophthora perniciosa*, fungo causador da vassoura de bruxa do cacaueiro / Mario Ramos de Oliveira Barsottini. – Campinas, SP : [s.n.], 2019.

Orientador: Gonçalo Amarante Guimarães Pereira.
Tese (doutorado) – Universidade Estadual de Campinas, Instituto de Biologia.

1. Vassoura-de-bruxa (Fitopatologia). 2. *Moniliophthora perniciosa*. 3. Proteínas mitocondriais. 4. Fungicidas. 5. Ensaios de inibição enzimática. I. Pereira, Gonçalo Amarante Guimarães, 1964-. II. Universidade Estadual de Campinas. Instituto de Biologia. III. Título.

Informações para Biblioteca Digital

Título em outro idioma: Rational design of inhibitors of the mitochondrial enzyme alternative oxidase (AOX) with fungicide activity against *Moniliophthora perniciosa*, causal agent of the witches' broom disease of cocoa
Palavras-chave em inglês:
Witches' broom disease
Moniliophthora perniciosa
Mitochondrial proteins
Fungicides
Enzymatic inhibition assays
Área de concentração: Genética de Microorganismos
Titulação: Doutor em Genética e Biologia Molecular
Banca examinadora:
Gonçalo Amarante Guimarães Pereira [Orientador]
Celso Eduardo Benedetti
Juliana Ferreira de Oliveira
Luis Eduardo Soares Netto
Paulo Henrique Conaggin Godoi
Data de defesa: 18-02-2019
Programa de Pós-Graduação: Genética e Biologia Molecular

COMISSÃO EXAMINADORA

Prof. Dr. Gonçalo Amarante Guimarães Pereira

Dr. Celso Eduardo Benedetti

Dra. Juliana Ferreira de Oliveira

Prof. Dr. Luis Eduardo Soares Netto

Dr. Paulo Henrique Conaggin Godoi

Os membros da Comissão Examinadora acima assinaram a Ata de Defesa, que se encontra no processo de vida acadêmica do aluno.

AGRADECIMENTO

Agradeço à minha família pelo incessante apoio a minha formação pessoal e acadêmica.

Agradeço a minha noiva, Mariana, pelo companheirismo e dedicação diários.

Agradeço ao Prof. Dr. Gonçalo A. G. Pereira pela oportunidade e a confiança oferecidas, sem as quais este trabalho não teria se iniciado.

Agradeço ao Dr. Artur T. Cordeiro, à Dra. Silvana A. Rocco e suas equipes, igualmente indispensáveis para a realização deste trabalho.

Agradeço a tantos outros orientadores não oficiais e aos colegas pela solidariedade e ajuda oferecidas em muitos momentos. Em especial, a Renata Baroni, a Bárbara Pires, a Paula Prado e o Gabriel Fiorin.

Agradeço ao Instituto de Biologia da Universidade Estadual de Campinas (IB/UNICAMP) e ao Laboratório Nacional de Biociências do Centro Nacional de Pesquisa em Energia e Materiais (LNBio/CNPEM), instituições de reconhecida excelência científica, pelo acolhimento e apoio fornecidos.

Agradeço à equipe de apoio técnico e administrativo do LGE/IB/UNICAMP e do LNBio/CNPEM, especialmente à Eliane Laranja Dias, ao Welbe Bragança de Oliveira e à Ana Paula Ferreira.

Agradeço à Fundação de Amparo à pesquisa do Estado de São Paulo (FAPESP) e à Coordenação de Aperfeiçoamento de Pessoal de Nível Superior (CAPES) pelo apoio financeiro através das bolsas de doutorado (processo FAPESP n° 2014/15339-6) e de estágio de pesquisa no exterior (processo FAPESP n° 2017/ 12852-2).

Agradeço ao Conselho Nacional de Desenvolvimento Científico e Tecnológico (CNPq) pelo apoio financeiro através do projeto de auxílio à pesquisa Universal processo n° 475535/2013-8 e da bolsa de doutorado processo n° 142358/2014-2.

LISTA DE ABREVIATURAS

AOX: oxidase alternativa.

DAI: dias após a inoculação.

ETC: cadeia transportadora de elétrons.

FAO: Organização das Nações Unidas para a Alimentação e Agricultura.

FRAC: Fungicide Resistance Action Comitee.

NPD: derivado de *N*-fenilbenzamida.

Q_1H_2 / Q_2H_2 / $Q_{10}H_2$: ubiquinol-1 / ubiquinol-2 / ubiquinol-10.

SHAM: ácido salicil-hidroxâmico.

TCA: ácido tricarboxílico.

TMV: vírus do mosaico do tabaco.

VDB / WBD: vassoura de bruxa / witches' broom disease.

RESUMO

A semente do cacaueiro (*Theobroma cacao*) é uma das matérias-primas da indústria chocolateira, contudo doenças fúngicas são uma ameaça à cacauicultura e geram perdas de até 30% na produção mundial. No Brasil, o patógeno mais relevante do cacaueiro é o fungo basidiomiceto *Moniliophthora perniciosa*, que causou enormes prejuízos após atingir as fazendas baianas em 1989. Além de perdas econômicas, a inviabilização da cacauicultura acarretou severos impactos sociais e ecológicos, tais como desemprego, êxodo rural, crescimento urbano desordenado e desmatamento de florestas nativas. *M. perniciosa* causa a doença denominada Vassoura de bruxa do cacaueiro (VDB), a qual é atualmente controlada pelo uso de variedades tolerantes de cacaueiro e práticas de manejo agronômico. Porém, ainda não é possível erradicar a VDB após instalada, o que limita a recuperação das fazendas afetadas. Estudos voltados a elucidar os mecanismos moleculares relacionados à patogenicidade de *M. perniciosa* apontaram para a importância da enzima mitocondrial oxidase alternativa (AOX). A AOX é uma oxidase terminal associada à membrana mitocondrial interna que cria uma ramificação na cadeia transportadora de elétrons no nível do ubiquinol. Apesar de a AOX reduzir a eficiência da síntese de ATP, esta enzima contribui para a homeostase celular em condições normais do desenvolvimento e frente a estresses abióticos e bióticos. Em *M. perniciosa,* a MpAOX atua como um mecanismo de escape frente à resposta de defesa do cacaueiro e a fungicidas comerciais inibidores da via principal da respiração celular, haja vista que a MpAOX permite o funcionamento parcial da mitocôndria e a sobrevivência do patógeno. Assim sendo, este trabalho teve como principal objetivo gerar informações relevantes para o desenvolvimento de novos inibidores da MpAOX com potencial ação fungicida. Os resultados alcançados são organizados em dois capítulos. No primeiro capítulo, apresenta-se o desenvolvimento de um novo modelo experimental baseado na levedura modelo *Pichia pastoris* para a triagem e caracterização funcional de derivados de *N*-fenilbenzamidas (NPD). Através de medições do consumo de oxigênio e da taxa de crescimento de *P. pastoris*, identificou-se ao menos um inibidor da AOX com ação antifúngica *in vitro* e *in planta*. O segundo capítulo aborda a expressão heteróloga, purificação e caracterização funcional da MpAOX. Inibidores do grupo da ascofuranona foram avaliados em ensaios de dose-resposta, permitindo a elucidação de relações estrutura-atividade. Coletivamente, estes resultados representam etapas iniciais para o desenvolvimento de um novo tratamento contra *M. perniciosa* e outros fungos dependentes da AOX, ultimamente contribuindo para o avanço científico-tecnológico do Brasil em áreas estratégicas, tais como a agricultura e a segurança alimentar.

ABSTRACT

The cacao tree seeds (*Theobroma cacao*) are the raw material used in the chocolate industry. However, fungal diseases endanger the world cocoa production and generate losses of 30%. In Brazil, the most important cocoa pathogen is *Moniliophthora perniciosa*, which devastated farms in the state of Bahia after an outbreak in 1989. In addition to economic losses, *M. perniciosa* caused severe social and ecological impacts, such as unemployment, rural exodus and uncontrolled urban growth. *M. perniciosa* is the causal agent of the witches' broom disease (WBD) of cocoa, which is currently controlled with tolerant cacao clones and agronomic management practices. Nonetheless, it is not possible to eradicate WBD, which greatly limits the potential for recovery of Brazilian cacao farms. It has been shown that the mitochondrial enzyme alternative oxidase (AOX) is a potential target for the development of new fungicides against *M. perniciosa*. AOX is a membrane-bound protein associated with the internal membrane in the mitochondria and a terminal oxidase. As such, AOX creates a branching point in the electron transport chain involved in the oxidative phosphorylation, which reduces ATP synthesis, but also confers metabolic plasticity to the cell to resist against a range of abiotic and biotic stresses. In *M. perniciosa*, MpAOX acts as an escape mechanism against the cacao defense response, as well as fungicides widely used in agriculture. Therefore, the main goal of this work was to generate relevant information for the directed development of MpAOX inhibitors with potential antifungal activity, which are presented in two chapters. The first chapter presents the development of a new experimental model based on the *Pichia pastoris* yeast for the functional characterization of *N*-phenylbenzamide derivatives (NPD). Oxygen consumption measurements and growth assays allowed the identification of at least one selective AOX inhibitor with antifungal activity *in vitro* and *in planta*. The second chapter addresses the heterologous expression, purification and functional characterization of MpAOX. Ascofuranone and structurally-related AOX inhibitors were subjected to dose-response assays, which led to the identification of key requirements for favorable ligand interaction with MpAOX and other isoforms. Collectively, those results will assist in the targeted development of a novel antifungal agent targeting *M. perniciosa* and other fungal pathogens dependent on AOX, which will contribute to Brazil's scientific and technological advancement in strategic areas such as agriculture and food security.

SUMÁRIO

INTRODUÇÃO

Moniliophthora perniciosa e a vassoura de bruxa do cacaueiro

O cacaueiro (*Theobroma cacao*) é uma planta perene originária da Bacia Amazônica. Sua principal importância econômica advém da utilização das suas sementes como matéria prima para a produção do chocolate, além de outros produtos, como bebidas e espessantes alimentícios derivados do fruto ou sementes [1]. No entanto, doenças fúngicas representam uma grande ameaça a essa cultura, chegando a causar perdas de 30% na produção global [2].

Em 1989, o Brasil ocupava a segunda posição no *ranking* mundial dos países produtores de amêndoas de cacau (sementes torradas), sendo então responsável por 15% da produção mundial. Das 392 mil toneladas produzidas naquele ano, 27% eram destinadas à exportação (Unidas para a Organização das Nações Alimentação e Agricultura – FAO, 2018). Porém, a chegada da doença vassoura de bruxa do cacaueiro (VDB) no sul do estado Bahia, maior região produtora brasileira, causou um colapso na cacauicultura, associado a forte desemprego, êxodo rural, crescimento urbano desordenado e desmatamento de florestas nativas necessárias para a cacauicultura [1,3]. Desde o início da década de 1990, a produtividade brasileira caiu constantemente até atingir um mínimo de 170 mil T de amêndoas em 2003 (5% da produção mundial), e o Brasil passou a importar essa *commodity*, gerando um déficit na balança comercial de 1,2 bi US$ entre 2007 e 2016 (FAO, 2018) **(Figura 1)**.

O agente etiológico da VDB é o fungo basidiomiceto *Moniliophthora perniciosa*. Também originário da Amazônia, *M. perniciosa* apresenta grande variabilidade e adaptação a diversas espécies vegetais, sendo conhecidos quatro biótipos: B, C, L e S. O biótipo-C ataca o cacaueiro e outras plantas do gênero *Theobroma spp.*, assim como algumas esterculiáceas. O biótipo-S infecta solanáceas, causando sintomas similares de doença. Já o biótipo-H e o biótipo-L, isolados respectivamente de *Heteropterys acutifola* e plantas da família Bignoniaceae, não geram sintomas perceptíveis no hospedeiro [1,4].

M. perniciosa é classificado como um patógeno hemibiotrófico; portanto a VDB é dividida em fases biotrófica e necrotrófica. A fase biotrófica é caracterizada pelo crescimento de *M. perniciosa* no hospedeiro ainda vivo, enquanto que a fase necrotrófica ocorre após a morte dos tecidos vegetais. A infecção se inicia quando basidiósporos de *M. perniciosa* entram em contato com o meristema vegetal (ramos, botões florais ou frutos jovens) e penetram o

hospedeiro através dos estômatos ou ferimentos. Os ramos infectados apresentam sintomas de inchamento e excesso de brotações com perda de dominância apical, resultando assim na formação de estruturas morfologicamente semelhantes a vassouras, denominados de "vassoura-verde". A infecção de botões florais e frutos acarretam no desenvolvimento de flores anormais e frutos partenocárpicos, além do surgimento de deformações e manchas necróticas em frutos em desenvolvimento. De 4 a 8 semanas após a infecção, ocorre a necrose das vassouras, que passam a ser denominadas de "vassoura-secas". O ciclo da doença se completa quando as vassouras ou frutos necrosados e secos são expostos a períodos de alternância entre chuva e estiagem, o que induz a formação de basidiomatas e a liberação de basidiósporos que são distribuídos pelo vento ou chuva [1,5] **(Figura 2 e Figura 3)**.

Igualmente, *M. perniciosa* passa por alterações morfofisiológica durante a progressão da VDB. No início da infecção, suas hifas são convolutas, largas (5 a 20 µm), mononucleadas e sem grampos de conexão, sendo encontradas em baixa densidade no hospedeiro e no espaço intercelular (apoplasto). Já em estágios avançados, observam-se hifas delgadas (1 a 3 µm), regulares, binucleares e com grampo de conexão crescendo extensivamente por todo o tecido vegetal. As hifas mononucleadas são tipicamente associadas ao estágio biotrófico da VDB,

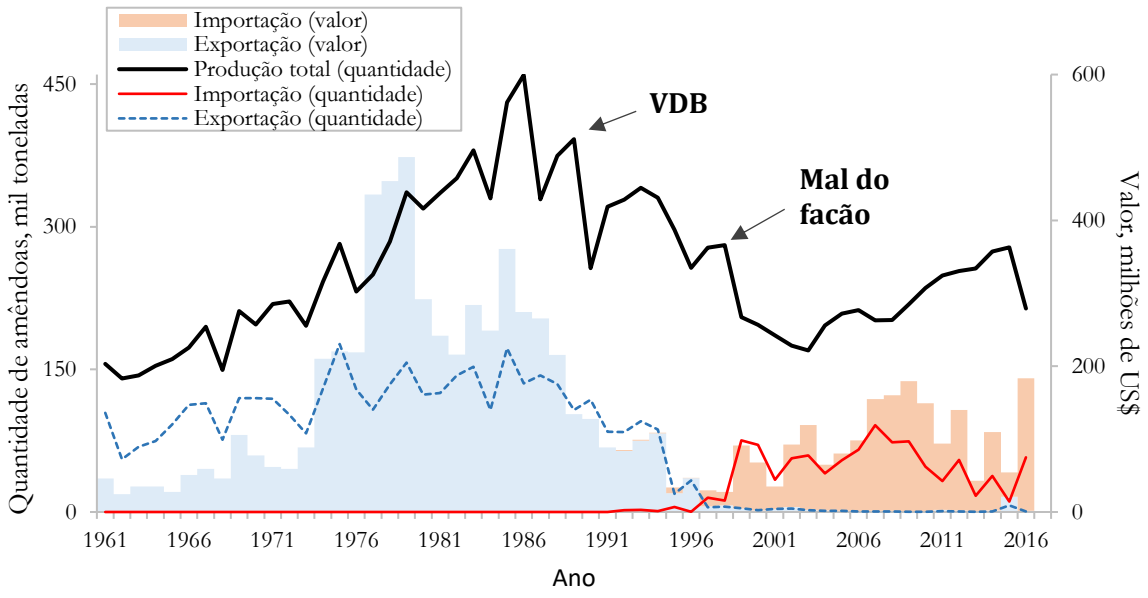

Figura 1. Dados econômicos anuais da produção e comercialização de cacau no Brasil. O primeiro relato da vassoura de bruxa na Bahia é de 1989, enquanto que o mal do facão surgiu em 1997 naquela região. Fonte: Organização das Nações Unidas para a Alimentação e Agricultura (FAO, 2018).

hifas binucleadas são associadas à fase necrotrófica. Porém, há relatos de que ambos os tipos de hifa possam ocorrer ao mesmo tempo em tecidos vivos [1,6].

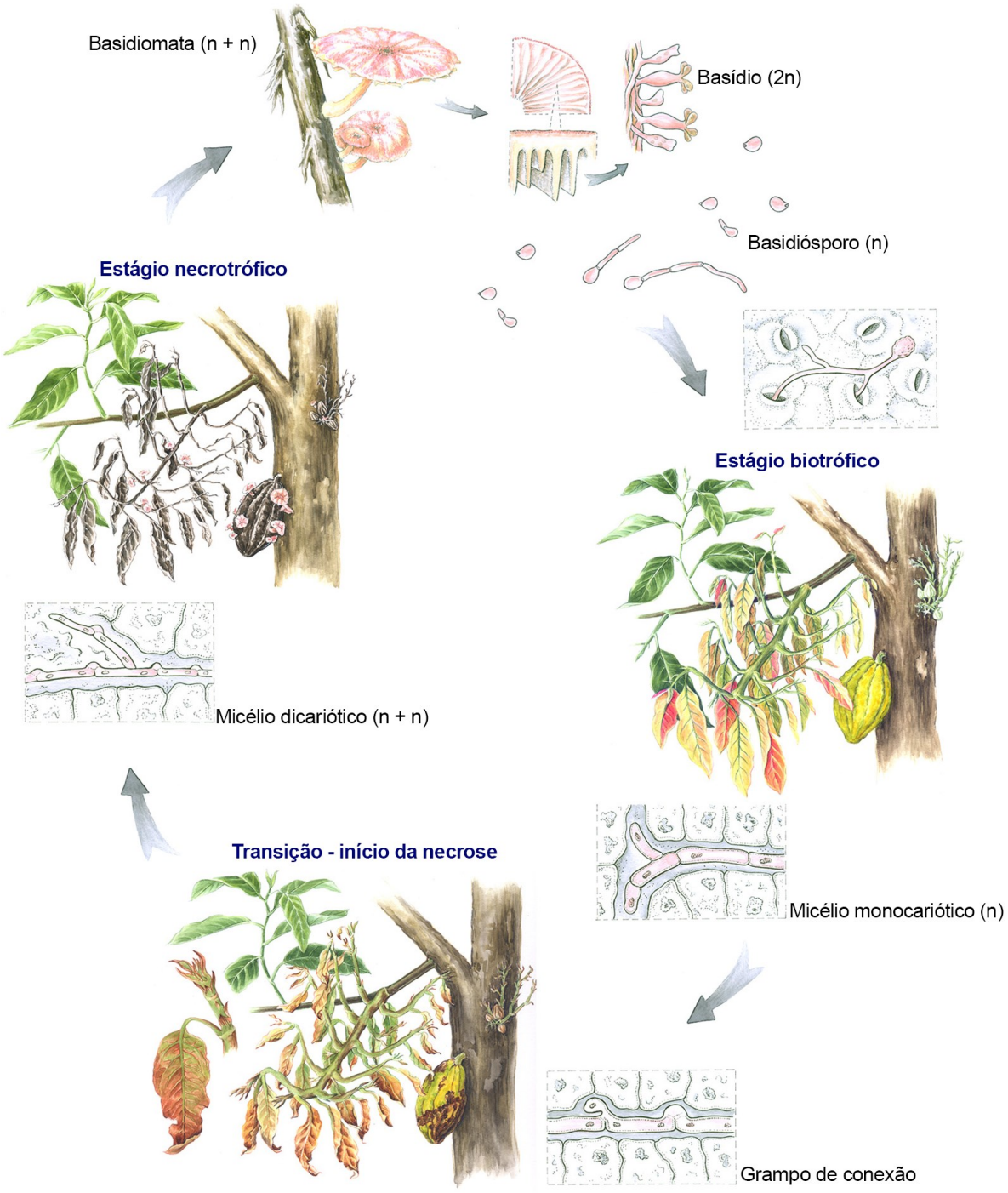

Figura 2. Ciclo de vida de *M. perniciosa*. Basidiósporos carregados pelo vento e chuva entram em contado com tecidos meristemáticos da planta e penetram por aberturas naturais ou ferimentos (topo à direita), dando início à fase biotrófica da vassoura de bruxa. Nesse momento, *M. perniciosa* permanece no espaço intercelular (apoplasto) e com baixa densidade de hifas. Após 2 a 3 meses, ocorre a transição para a fase necrotrófica da infecção e a formação das vassouras secas, nas quais *M. perniciosa* cresce intensamente. Em condições ambientais favoráveis há a formação de cogumelos e a liberação de novos basidiósporos. Adaptado de [163].

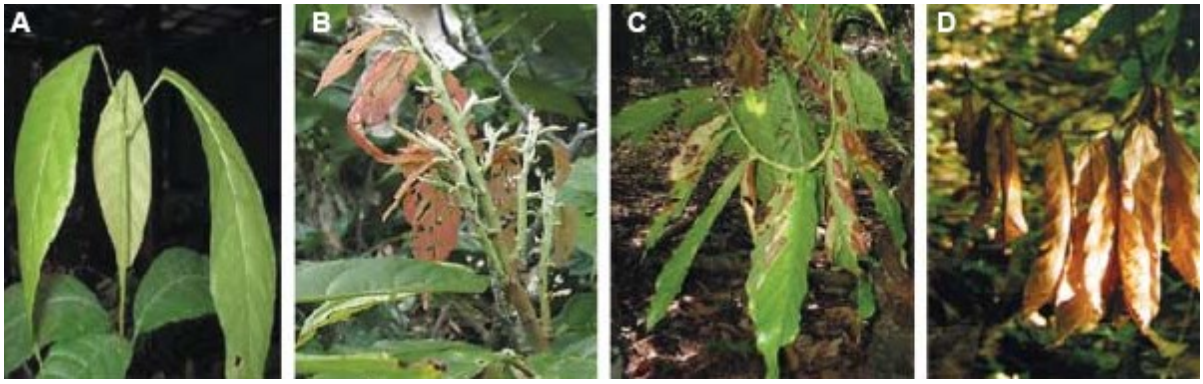

Figura 3. Principais sintomas observados nos ramos do cacaueiro infectado por *M. perniciosa*. **(A)** Cacau sadio. **(B)** Vassoura-verde. **(C)** Início da necrose. **(D)** Vassoura-seca. Retirado de [1].

Até o momento, não se sabe exatamente o que determina a transição da vassoura verde para a vassoura seca, mas alguns eventos em nível molecular já foram investigados. Zaparoli *et al.* (2011) identificaram o aumento do nível de expressão da proteína indutora de necrose MpNEP2 de *M. perniciosa*, pertencente à família das NLPs (*Necrosis and ethylene-inducing peptide 1-like Proteins*), nos estágios avançados da doença, o que poderia contribuir para a morte dos tecidos infectados [7]. Essa mesma proteína é produzida em situações de privação de nutrientes, de modo que pode haver uma relação entre a redução na disponibilidade de açúcares no apoplasto ao final do estágio de vassoura-verde e a sinalização para a mudança de fase no fungo e indução da morte do hospedeiro [8]. A degradação de cristais de oxalato de cálcio, formados no início da infecção de plantas suscetíveis, resulta no acúmulo de H_2O_2. Isso, juntamente com a redução da expressão da enzima detoxificadora APX do cacau, pode contribuir para a morte do hospedeiro ao ativar a via de morte celular programada [6].

A análise de expressão gênica *in planta*, associada a estudos funcionais *ex planta*, indicam que a inibição da respiração celular em *M. perniciosa*, possivelmente através do óxido nítrico produzido como mecanismo de defesa vegetal, pode constituir outra forma de sinalização, mantendo o micélio na fase biotrófica [9]. Isto está de acordo com resultados obtidos com o fungo *Podospora anserina*, no qual a inibição da via respiratória principal retarda o processo de senescência e aumenta sua longevidade cerca de 40 vezes [10].

Apesar de causar a morte dos tecidos infectados, *M. perniciosa* não é letal para o vegetal. Entretanto, as árvores ficam debilitadas e há uma redução na quantidade e qualidade dos frutos produzidos [1]. Muitos métodos para o controle da doença foram testados, e os melhores resultados foram alcançados com uso integrado de práticas agronômicas e fitossanitárias [11],

bem como pela aplicação do fungo *Trichoderma stromaticum* sobre as vassouras secas caídas no solo (*T. stromaticum* é um micoparasita que compete com *M. perniciosa* nos tecidos mortos do cacaueiro) [12]. Ainda assim, não existe uma cura para a VDB após instalada, o que certamente limita o potencial de recuperação da cacauicultura.

No ano de 2000 teve início o Projeto Genoma da Vassoura de Bruxa, coordenado pelo Prof. Dr. Gonçalo A. G. Pereira e envolvendo o LGE (Laboratório de Genômica e Expressão) da Unicamp, a Universidade Estadual Santa Cruz (Ilhéus, BA), a Universidade Federal da Bahia (Salvador, BA) e a Universidade Estadual de Feira de Santana (Feira de Santana, BA). Dentre uma série de trabalhos voltados a investigar as bases moleculares da VDB, identificou-se que a enzima mitocondrial oxidase alternativa de *M. perniciosa* (AOX) é exclusivamente expressa durante a interação com o cacaueiro e é uma fonte de resistência a fungicidas convencionais [9,13,14].

Registra-se aqui que uma segunda doença do cacaueiro atingiu a Bahia em 1997: o mal do facão, causado pelo fungo ascomiceto *Ceratocystis cacaofunesta* [15,16]. *C. cacaofunesta* é um patógeno necrotrófico, que adentra o cacaueiro por aberturas criadas por insetos ou ferramentas de corte contaminadas (originando assim o nome popular da doença). O fungo então se alastra até alcançar o xilema, onde causa lesões necróticas e bloqueia o fluxo de seiva bruta, ultimamente matando o cacaueiro [15,17]. Dado que o primeiro sintoma visível (a murcha das folhas) só surge quando a doença está em estágio avançado, o controle do mal do facão é bastante desafiador e, assim como na vassoura de bruxa, não é possível erradicar o mal do facão das árvores infectadas. Contudo, estudos do nosso grupo indicam que a AOX de *C. cacaofunesta* é expressa do modo constitutivo e igualmente um potencial alvo para o desenvolvimento de fungicidas (dados não publicados).

A enzima mitocondrial oxidase alternativa (AOX) e a cadeia transportadora de elétrons

A fosforilação oxidativa é o processo responsável pela geração de ATP na mitocôndria, a qual depende da energia liberada em reações de oxidorredução catalisadas por complexos proteicos presentes na membrana mitocondrial interna. Primeiramente, cofatores reduzidos durante a glicólise e o ciclo do ácido tricarboxílico (TCA) fornecem elétrons para a cadeia transportadora de elétrons. As enzimas NADH desidrogene tipo I (complexo I) e succinato desidrogenase (complexo II) transferem tais elétrons para o *pool* de ubiquinona/ubiquinol, uma coenzima lipossolúvel na membrana mitocondrial. A citocromo c redutase (complexo III) oxida

o ubiquinol reduzindo o citocromo c, e o citocromo c transfere elétrons para o oxigênio (aceptor final), formando água, pela ação da citocromo c oxidase (complexo IV). Ao longo deste percurso, prótons são translocados da matriz mitocondrial para o espaço intermembrana pelos complexos I, III e IV, e este gradiente quimiosmótico fornece energia necessária para a fosforilação de ADP pela ATP sintase (complexo V) **(Figura 4A)** [18].

Os complexos I a IV são encontrados na grande maioria dos eucariotos e compõem a via principal da cadeia transportadora de elétrons (ETC), porém há outras proteínas que podem modificar o fluxo usual de elétrons. Enzimas conhecidas capazes de reduzir a ubiquinona são a NADH desidrogenases do tipo 2 (NDH-2) interna e externa, a glicerol-3-fosfato desidrogenase mitocondrial (mGPDH), a diidroorotato desidrogenase (DHODH), a *electron-transferring-flavoprotein desidrogenase* (ETFDH), a formato redutase dependente de ubiquinona (UQFDH) e a sulfito:quinona oxidoredutase (SQOR). Já a AOX e a nitrato redutase dissimilatória (dNAR) oxidam o ubiquinol, e os aceptores finais de elétrons são o oxigênio e o nitrogênio, respectivamente **(Figura 4B)** [19–21]. Ao contrário da AOX, que é amplamente distribuída entre os organismos e melhor caracterizada, a dNAR foi descrita apenas em *Fusarium oxysporum* até o momento, e o gene que a codifica não foi identificado. A dNAR pode estar relacionada ao processo de denitrificação do solo por fungos, porém ainda carece de maiores estudos [20–22].

Estas enzimas alternativas não translocam prótons através da membrana mitocondrial, portanto não contribuem diretamente para a síntese de ATP, exceto pela via da FDH e dNAR **(Figura 4B)**. Por outro lado, conferem à célula uma maior plasticidade para a regulação de seus processos metabólicos e fisiológicos, em condições normais ou de estresse, conforme será abordado adiante. Neste momento, destaca-se apenas que a AOX pode manter a ETC operando em casos de disfunção dos complexos III e IV **(Figura 4C)**.

AOX: estrutura, atividade e regulação pós-traducional

A AOX foi identificada primeiramente em plantas e depois em fungos. Porém, com o aumento no número de genomas e meta-genomas sequenciados e disponibilizados, atualmente se reconhecem sequências semelhantes à AOX amplamente distribuídas entre bactérias, fungos, protistas, plantas e animas. Tipicamente, plantas possuem 3 a 5 genes codificantes para a AOX no genoma, agrupados em duas famílias (AOX1 e AOX2), sendo que a AOX2 é encontrada

apenas em dicotiledôneas. Já em fungos e outros organismos, apenas uma isoforma é normalmente encontrada no genoma [23,24].

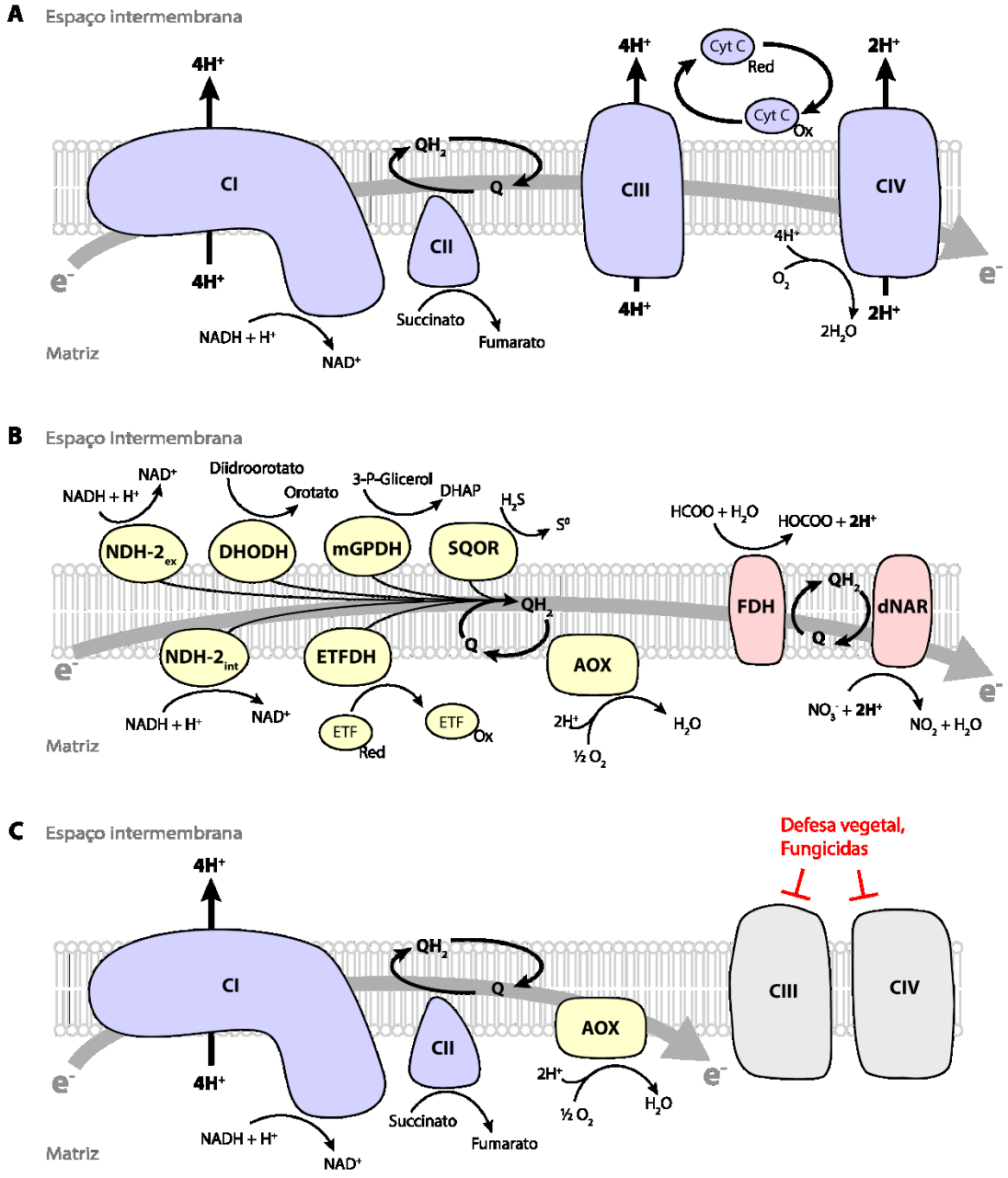

Figura 4. Representação dos componentes da cadeia transportadora de elétrons mitocondrial. **(A)** Via principal, responsável pela geração do gradiente de prótons no espaço intermembrana para a geração de ATP. Brevemente, Cofatores reduzidos NADH (complexo I) ou $FADH_2$ (complexo II) fornecem elétrons para a ubiquinona (cofator Q), gerando ubiquinol (QH_2). Elétrons são então transferidos para o citocromo c através do complexo III e deste para o oxigênio (complexo IV). Os complexos I, III e IV transportam prótons da matriz para o espaço intermembranas. **(B)** Enzimas alternativas podem criar ramificações no fluxo de elétrons no *pool* de ubiquinol. A AOX e a dNAR são as únicas enzimas alternativas em eucariotos capazes de oxidar o ubiquinol. À direita (rosa) está representada a via proposta em *F. oxysporum*, cujo aceptor final é o nitrogênio, em lugar do oxigênio. **(C)** Fluxo de elétrons proposto em *M. perniciosa* na presença de inibidores dos complexos III e IV. Nota-se que a AOX substitui o complexo III e permite o funcionamento mitocondrial nesta condição. Adaptado de [19,20].

Dada a larga distribuição, juntamente com análises genéticas e o fato de que enzimas semelhantes são encontradas no cloroplasto e em bactérias, acredita-se que uma proteína ancestral da AOX já existisse nos procariotos antes dos eventos de endossimbiose que originaram a mitocôndria e o cloroplasto. Ou seja, grupos de organismos que não possuem a AOX, tais como os animais vertebrados, devem tê-la perdido ao longo do processo evolutivo **(Figura 5)** [23,25].

Em eucariotos, a AOX é codificada pelo genoma nuclear e transportada para a mitocôndria após a tradução pelo complexo mitocondrial TOM [26]. Esta enzima tem aproximadamente 40 kDa e pertence à superfamília de proteínas que contêm ferro coordenado por carboxilatos (*diiron carboxylate superfamily*), o que foi primeiramente postulado com base no requerimento por ferro para a sua atividade e pela existência de motivos de aminoácidos E-X-X-H de ligação a ferro. Este fato foi posteriormente confirmado com a resolução da estrutura cristalográfica da AOX de *T. brucei* (TAO) [27,28].

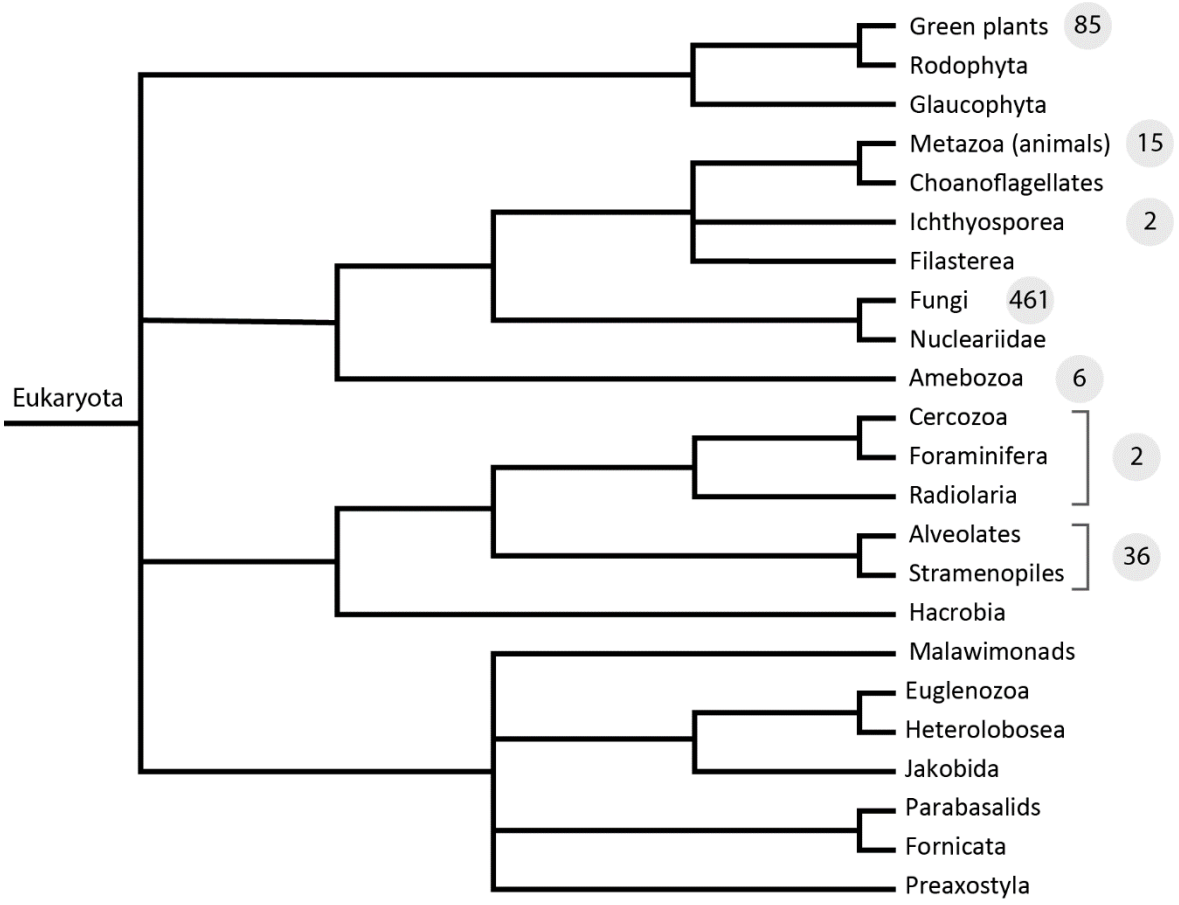

Figura 5. Distribuição filogenética da AOX. Organismos que possuem a AOX de acordo com o banco de dados PFAM (família PF01786) [164]. Bactérias (233 espécies) e vírus (23 espécies) não estão representados.

A TAO é uma proteína compacta, composta por 6 α-hélices longas e 4 α-hélices curtas. Quatro α-hélices antiparalelas (α2, α3, α5 e α6) formam uma cavidade hidrofóbica de ligação ao substrato com 18-20 Å de comprimento. No final desta cavidade se encontram 2 átomos de ferro coordenados por 4 glutamatos, além de outros resíduos possivelmente envolvidos na atividade catalítica da AOX. O ubiquinol, presente na bicamada fosfolipídica, acessa a cavidade hidrofóbica através de uma abertura entre α-hélices α1 e α4 na interface com a membrana, sendo então corretamente orientado por dois resíduos de leucina para sofrer a ação enzimática **(Figura 6)** [28–30].

O mecanismo catalítico da AOX foi parcialmente proposto a partir da estrutura cristalográfica e informações complementares, tais como medidas de ressonância paramagnética eletrônica, mutações sítio-dirigidas e a comparação com outras AOX e oxidases conhecidas [29]. No seu estado basal, a AOX possui dois Fe^{2+} conectados por íon hidroxo (OH). O ciclo catalítico tem início quando o oxigênio molecular se liga a um dos átomos de ferro e o ubiquinol adentra o sítio catalítico. Após uma série de transferências radicalares, é liberada uma molécula de água e uma ubiquinona; no sítio ativo permanecem dois íons Fe^{3+} ligados a um átomo de oxigênio e uma hidroxila. Um segundo ubiquinol entra o sítio catalítico e, por um mecanismo ainda não elucidado, doa seus elétrons, restaurando os Fe^{2+} e liberando mais uma água e uma ubiquinona **(Figura 7)**.

A caracterização bioquímica da AOX é desafiadora, dado que esta é uma proteína de membrana e o substrato natural (ubiquinol-10; $Q_{10}H_2$) é altamente hidrofóbico. Por esta razão, a AOX é purificada na presença de agentes surfactantes, e ensaios enzimáticos são feitos com análogos hidrofílicos do ubiquinol (Q_1H_2 e Q_2H_2) [31–34]. A comparação da atividade específica da AOX recombinante de diversos organismos indica que a TAO é a mais ativa (600 μmol QH_2 min^{-1} mg^{-1}), seguida das AOX das plantas termogênicas *Arum maculatum* e *Sauromatum guttatum* (~35 μmol QH_2 min^{-1} mg^{-1}) e então das AOX do molusco *Ciona intestinallis* e da bactéria *Novosphingobium aromaticivorans* (~3 μmol QH_2 min^{-1} mg^{-1}). Visto que os resíduos responsáveis pela interação com o substrato e a catálise são conservados entre estas proteínas, especula-se que este fenômeno seja explicado por diferenças na abertura da cavidade hidrofóbica. Por exemplo, a TAO tem uma abertura de 7 Å, enquanto que o modelo computacional da AOX de *N. aromaticivorans* exibe uma abertura de 5 Å [35].

Na estrutura cristalográfica da TAO foi observado um homodímero com possível relevância biológica, visto que resíduos de aminoácido hidrofóbicos presentes na interface dos monômeros são conservados entre as AOX **(Figura 6A)** [28]. Em plantas, a dimerização está envolvida na regulação pós-traducional da AOX mediante a formação de uma ponte dissulfeto intermolecular através de um resíduo de cisteína conservado (Cys_I). Na presença de agentes redutores, a ponte é desfeita (o dímero permanece) e a atividade enzimática aumenta, enquanto que o oposto ocorre na presença de agentes oxidantes. Também foi demonstrado que a redução

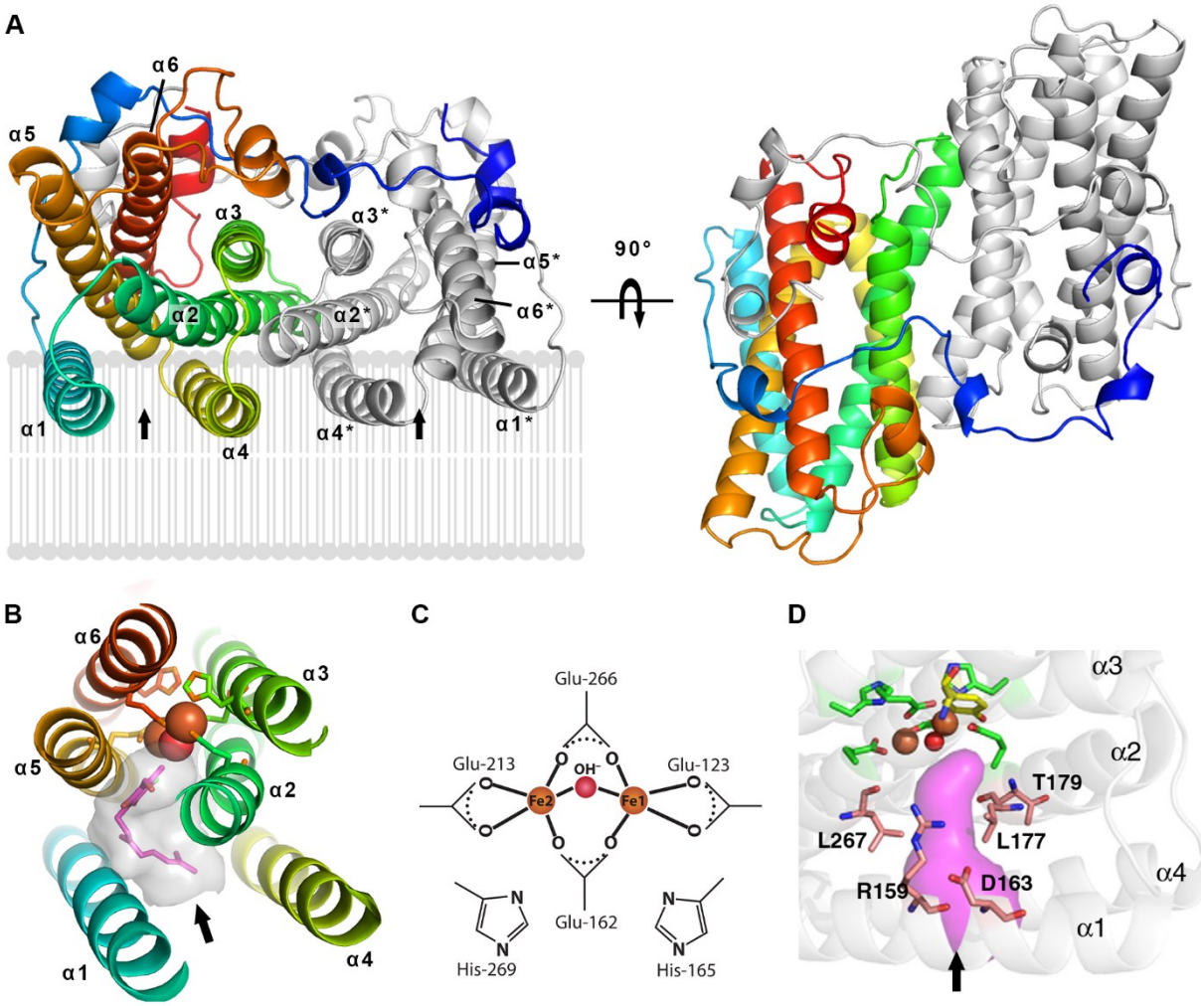

Figura 6. Estrutura da AOX. **(A)** Representação em *cartoon* da estrutura cristalográfica da AOX de *T. brucei* (TAO; PDB ID 3w54) e modelagem da interação com a membrana fosfolipídica. Um dos monômeros está colorido da porção N-terminal (azul) para a C-terminal (vermelho), e o outro monômero está em cinza. Setas indicam a entrada do sítio catalítico voltada para a membrana fosfolipídica. **(B)** e **(C)** Destaque dos íons de ferro e resíduos de aminoácido envolvidos em sua coordenação, bem como o inibidor coletoclorina B (*stick* magenta) dentro do sítio de interação com o substrato (sombreamento cinza). **(D)** Modelo estrutural da AOX de *Sauromatum guttatum*, exibindo o sítio de ligação ao substrato (superfície magenta), os resíduos de coordenação com o ferro (*stick* verde), os resíduos que orientam o substrato para a conformação favorável à reação enzimática (*stick* magenta) e a tirosina envolvida na catálise (*stick* amarelo). Adaptado de [28–30].

da AOX pode ser mediada por tiorredoxinas mitocondriais, o que pode representar uma forma de integração da maquinaria associada à regulação do potencial redox mitocondrial e da cadeia transportadora de elétrons [36,37].

A Cys_I ocorre apenas na AOX de plantas, e esta forma de regulação através da ponte dissulfeto está restrita a este grupo de enzimas [38–40]. Ademais, não foram encontradas evidências de dimerização nas AOX da levedura *Pichia stipis* e do protozoário *Acanthamoeba castellanii* [39,41].

Um segundo mecanismo de regulação descrito em AOX de plantas é a ativação por ácidos orgânicos, tais como piruvato, succinato e glioxilato. Notavelmente, a interação com piruvato ocorre através da cisteína previamente mencionada (Cys_I), havendo sobreposição com o mecanismo de regulação dependente do estado redox da AOX apresentado. Ou seja, apenas na AOX reduzida a cisteína está disponível para a ativação por piruvato [42,43]. Postula-se que

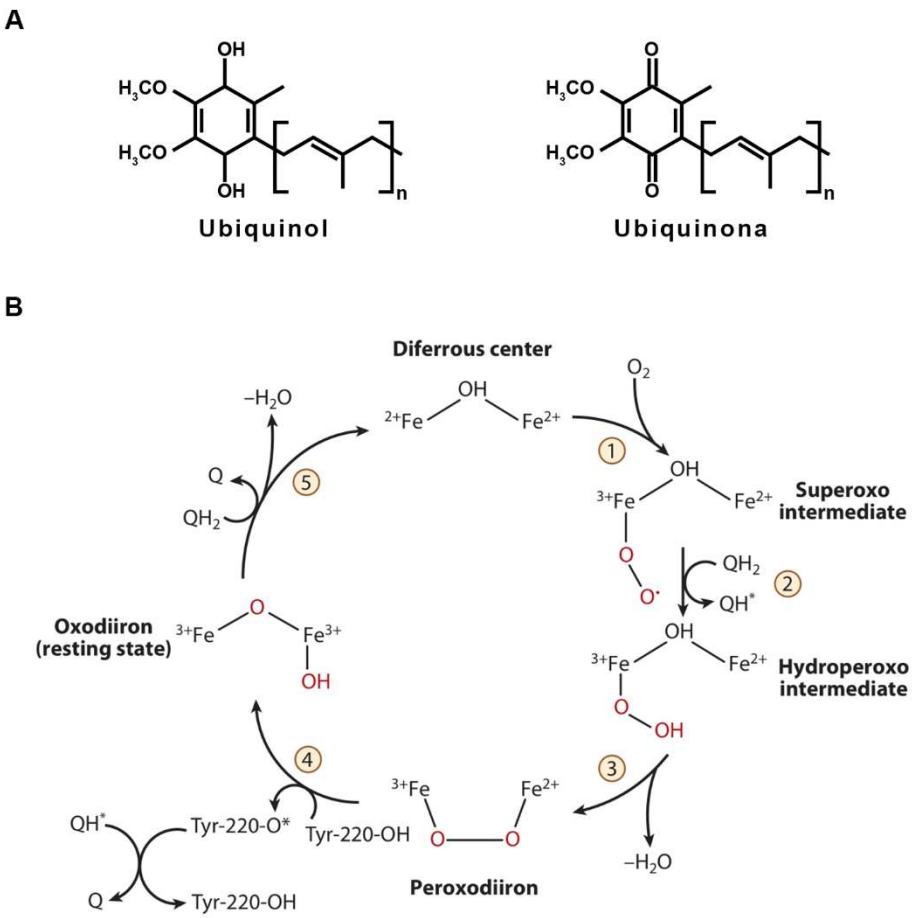

Figura 7. Mecanismo catalítico da AOX. **(A)** Estrutura do ubiquinol e da ubiquinona. Na mitocôndria, as formas mais comuns são com 9 e 10 unidades isoprênicas (Q_9 e Q_{10}). **(B)** Mecanismo catalítico parcialmente proposto. Retirado de [29].

isto ocorra através de modificações estruturais causadas pela adição de uma carga positiva que aumentam a afinidade da AOX pelos substratos (ubiquinol e oxigênio) [40,44–46].

Entretanto, a presença da Cys_I não é suficiente para a regulação por piruvato, haja visto que uma AOX da planta termogênica *S. guttatum* é insensível a este composto e se encontra sempre na forma ativa. A comparação desta com a AtAOX1a (sensível ao piruvato) aponta para certos resíduos de aminoácido que poderiam ser responsáveis por este fenômeno [47].

Já a interação com succinato e glioxilato ocorre através de uma segunda cisteína conservada (Cys_{II}). Ainda que a Cys_{II} não forme uma ponte dissulfeto intermolecular, a ativação por succinato e glioxilato é igualmente abolida na presença de agentes oxidantes. Isto pode ocorrer devido ao bloqueio do acesso destes ativadores à Cys_{II}, ou a dimerização da Cys_I impede a ativação por succinato e glioxilato mesmo que estes se liguem à AOX [40,45,48,49].

AOX de fungos e protozoários são insensíveis ao piruvato, fato que é atribuído à inexistência de um resíduo correspondente à Cys_I de plantas [39,41,50]. Em contrapartida uma série de trabalhos demonstraram que AOX de fungos são ativadas por mono- e difosfato nucleosídeos, tais como ADP, AMP e GMP [39,50–56]. A análise da estrutura primária das AOX de fungos e plantas indica uma inserção de aproximadamente 20 aminoácidos nos fungos, sendo esta uma possível região de interação com nucleosídeos fosfato. Porém, ao menos três AOX de outros organismos também são ativadas por AMP: dos protozoários *Paramecium tetraurelia* e *A. castellanii* [41,57] e da alga *Euglena gracilis* [58], as quais não foram incluídas na comparação de sequência das AOX [39]. *Ustilago maydis* parece ser uma exceção, pois sua AOX é ativada tanto por AMP como por piruvato. Igualmente, a sequência primária da AOX de *U. maydis* não foi analisada [55].

Por fim, a AOX é sensível ao estado redox do *pool* de ubiquinol/ubiquinona, ou seja, a proporção entre estas moléculas na membrana mitocondrial. Ensaios com mitocôndrias isoladas de plantas demonstram que a AOX passa a atuar significativamente quando a proporção é de 40% ubiquinol (na ausência de piruvato) ou 20% ubiquinol (na presença de piruvato). Esses resultados suportam a hipótese de que a AOX atue como um escape de elétrons e evite a hiper-redução dos componentes da ETC caso o fluxo pela via principal não seja suficientemente rápido [38,44,47,59,60]. Resta determinar se a AOX de outros organismos também são sensíveis a este mecanismo de ativação, porém estudos com a mitocôndria de *Candida parapsilosis* e o uso de inibidores específicos para componentes da via principal e alternativa da respiração sugerem que sim [52].

O papel da AOX no controle do metabolismo e na resistência a estresse

Há evidências de que a AOX possa atuar em situações normais de crescimento e desenvolvimento, bem como durante a resposta a estresse biótico e abiótico. Dada a grande diversidade de situações nas quais a AOX é induzida (em nível transcricional ou pós-traducional), fica claro que há mais de uma via de sinalização envolvida.

A AOX foi inicialmente identificada como a enzima responsável pela geração de calor em plantas termogênicas [61]. Por exemplo, o apêndice floral de *Arum maculatum* libera calor durante parte do seu desenvolvimento, podendo atingir 20 °C acima da temperatura ambiente (32°C e 12 °C, respectivamente), o que está correlacionado com uma alta expressão da Aox1e neste órgão [62].

Em fungos ascomicetos, dois fatores de transcrição são necessários para a expressão da AOX (AOD2 e AOD 5 em *Neurospora crassa*), os quais também regulam outros genes relacionados ao metabolismo energético, tais como a fosfoenolpiruvato carboxiquinase, a frutose 1,6-bifosfatase e uma NADH desidrogenase tipo 2, dentre outros genes com função desconhecida [10,63–66]. O envolvimento da AOX na regulação do metabolismo celular também é corroborado pelo fato de que, ao menos em tabaco, a expressão desta enzima é induzida por citrato, um intermediário do ciclo do TCA e precursor da síntese de aminoácidos [67]. Além disso, três isoformas da AOX de *Arabidopsis thaliana* testadas (das cinco existentes) exibem diferentes perfis de ativação pós-traducional por intermediários do ciclo do TCA, tais como piruvato, glioxilato, oxaloacetato e 2-oxoglutarato [68].

Em *P. anserina* ocorre a co-regulação da AOX com genes relacionados ao metabolismo secundário [63], o que está de acordo com o fato de que a deleção da AOX de *Aspergillus nidulans* leva a uma redução da produção da micotoxina sterigmatocistina [69,70]. Já no fungo *Acreonium chrysogenum*, a adição de óleo de soja em meio de cultura causa um aumento na respiração alternativa concomitante com uma maior produção de cefalosporina C [71]. Como compostos secundários são normalmente sintetizados na fase estacionária (na qual não há mais crescimento celular), supõe-se que a AOX suporte o metabolismo anabólico mesmo quando a via principal da ETC esteja reprimida devido à alta concentração de ATP. Caso a entrada de elétrons na ETC ocorra através de uma NADH desidrogenase do tipo 2, ocorre um desacoplamento completo entre a ETC e a oxidação fosforilativa. Ou seja, a AOX e a NADH-2 permitem que cofatores necessários para o metabolismo anabólico sejam regenerados em situações de alta disponibilidade energética (**Figura 4B**).

O fato de a AOX contribuir para a regeneração de cofatores oxidados sugerem um papel desta enzima também no balanço redox mitocondrial e celular. Foi observado em diferentes organismos que a deleção ou *knock-down* da AOX ocasiona um aumento na geração de espécies reativas de oxigênio e de nitrogênio. Isto pode estar associado à hiperredução da ETC e ao consequente escape de elétrons que leva à formação de radicais livres [69,72,73]. Interessantemente, ao menos em plantas, a atividade da AOX pode ser modulada pós-traducionalmente por tiorredoxinas mitocondriais, enzimas com ação antioxidante que participam do sistema de regulação do potencial redox intracelular. Neste caso, a AOX é mais ativa quando está na forma reduzida [36,37].

Como espécies reativas de oxigênio estão intimamente ligadas a vias de sinalização celular, tais como respostas de defesa e de morte celular programada [74], é possível que a AOX auxilie na modulação de tais vias. Em milho e tabaco foi visto que o ácido salicílico (hormônio vegetal e inibidor da oxidação fosforilativa), a antimicina-A (inibidor do complexo III) ou o H_2O_2 induzem a AOX1, juntamente com outros genes envolvidos na apoptose [75–78]. Ademais, ensaios de infecção de *A. thaliana* com a bactéria *Pseudomonas syringae* revelaram uma ativação mais rápida da respiração alternativa durante interações incompatíveis (estirpe avirulenta de *P. syringae*) do que em interações compatíveis (estirpe virulenta); incremento este que se correlacionou com o início da resposta de defesa hipersensitiva (na qual ocorre morte celular programada no hospedeiro). Neste caso, a expressão da AOX1A se mostrou dependente da via de sinalização do etileno [79].

Ainda em relação ao estresse biótico, observou-se que tabaco apresenta níveis elevados de expressão da AOX após a infecção pelo vírus do mosaico do tabaco (TMV) [80], e que a atividade da AOX parece ser essencial para a indução de resistência sistêmica adquirida, mas não para a síntese de proteínas PR, em resposta ao TMV [81,82].

Quanto ao cacaueiro, três isoformas da AOX foram identificadas no Atlas Transcriptômico da Vassoura de Bruxa (http://bioinfo08.ibi.unicamp.br/atlas). O transcrito CGD0008991 é o mais abundante na maioria das condições avaliadas, havendo um nível de expressão constante deste transcrito nos ramos, exceto por uma queda após 111 dias. Porém não houve diferença entre plântulas sadias e infectadas com *M. perniciosa*. Quanto aos outros dois transcritos, a maior alteração causa pela infecção ocorre no fruto, com uma predominância do CGD0025813 na semente e do CGD0015607 na casca (**Figura 8**).

Outra situação em que a AOX pode contribuir é a resistência a estresse abiótico. O promotor do gene *aox1a* de *A. thaliana* possui um elemento de repressão controlado pela via do ácido abscísico (especificamente, reprimido constitutivamente pelo fator de transcrição *abscisic acid insensitive 4*; ABI4), um hormônio vegetal relacionado à senescência e dormência de sementes, bem como à resistência a estresse abiótico [83]. Ensaios funcionais demonstraram que o tratamento com ácido abscísico induz (desreprime) a expressão do gene repórter sob controle daquele promotor [83], o que está de acordo com outros resultados que associam a AOX à resistência ao frio [83,84], à seca [85], ao estresse osmótico [86], à baixa disponibilidade de fósforo [87] e ao ozônio [88].

Por outro lado, a regulação da AOX é intrincada, e seu efeito no metabolismo e no desenvolvimento são complexos. Há grande variabilidade dentre os diferentes sistemas investigados, especialmente em plantas que possuem muitas isoformas da AOX, o que indica, juntamente com a variedade de respostas associadas à AOX previamente mencionados, que exista mais de uma via de sinalização que leva à indução da AOX.

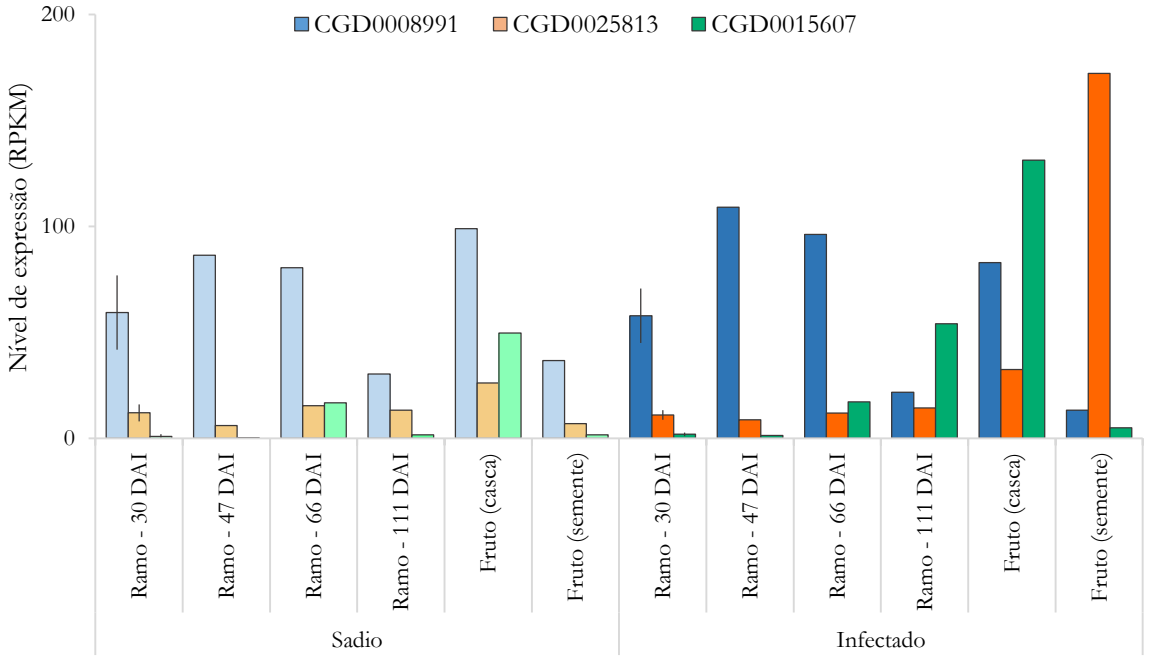

Figura 8. Perfil de expressão das 3 isoformas da AOX em *T. cacao* ao longo da vassoura de bruxa. À esquerda estão representados tecidos sadios de idade correspondente ao infectado. Os ramos foram obtidos em casa de vegetação, e os frutos foram coletados em campo. Apenas amostras de 30 dias após a inoculação (DAI) possuem réplica biológica e, portanto, desvio padrão. Dados extraídos do Atlas Transcriptômico da Vassoura de Bruxa (http://bioinfo08.ibi.unicamp.br/atlas).

A. maculatum possui 7 isoformas da AOX, porém apenas a AOX1e, a qual não necessita de piruvato ou de agentes redutores para a sua completa ativação, está associada à termogênese [62]. Em *A. thaliana* há um controle espacial e temporal da expressão das 5 isoformas (AOX1a, 1b, 1c, 1d e AOX2), podendo inclusive ocorrer a co-expressão em certos órgãos. Por exemplo, AtAOX1d é predominante durante a floração, enquanto que a AtAOX2 é encontrada majoritariamente na semente [89]. Em arroz, a expressão das AOX1a e -1b ocorre na raiz e em folhas maduras; a AOX1c é encontrada em folhas jovens, folhas maduras e na inflorescência, mas não na raiz; e a AOX2 está presente apenas na semente [90,91]. Na soja, a AOX2 é a isoforma predominante em cotilédones jovens, e a AOX 3, em cotilédones mais velhos e na raiz [92,93].

Em relação à resposta ao estresse, *Vigna unguiculata* apresenta expressão diferencial apenas da VuAox2b durante o estresse osmótico, não sendo detectada a expressão da VuAox1 e da VuAox2a. Ainda mais, um cultivar resistente ao estresse osmótico exibe variação no perfil de expressão da VuAox2b dependente do osmólito empregado, havendo uma repressão por NaCl e uma indução por PEG 6000 [86]. Similarmente, as AOX1a e 1b de arroz são induzidas pelo frio, mas não a AOX1c [90].

Outro exemplo de expressão diferencial entre isoformas da AOX é encontrado em milho, no qual mutantes que apresentam disfunção mitocondrial apresentam uma superexpressão da AOX. Contudo, verificou-se um aumento na AOX2 na linhagem deficiente para o complexo I, enquanto que a mutação do complexo III leva a um aumento na AOX3. Já a disfunção da maquinaria de tradução mitocondrial induz a expressão de ambas isoformas [94].

Mesmo em fungos foram encontradas divergências. Por exemplo, a expressão desregulada da AOX (knock-down ou superexpressão) em *Pichia pastoris* leva a uma diminuição na produção de biomassa associado a um aumento na geração de espécies reativas de oxigênio e morte celular [73]. No entanto, a deleção ou superexpressão deste gene em *A. nidulans* não acarretou diferenças perceptíveis no crescimento *in vitro*, mesmo em condições de estresse oxidativo [69].

A AOX como fator de virulência e sobrevivência em patógenos

A AOX é induzida em situações de disfunção mitocondrial, tais como inibição dos complexos respiratórios, inibição da ATP sintase, desacomplamento mitocondrial e a inibição do ciclo do TCA [95,96]. Em especial, a AOX cria uma via paralela aos complexos III e IV, a

partir do pool de ubiquinol, o que pode manter a ETC operando em casos de disfunção destas enzimas **(Figura 4C).**

No caso de *M. perniciosa*, a MpAOX é expressa exclusivamente durante os estágios iniciais da VDB, momento em que o cacaueiro ainda está vivo. Interessantemente, foi detectado um aumento na quantidade de H_2O_2 e de oxido nítrico, um potente inibidor do complexo IV, na vassoura verde quando comparada com plantas não infectadas [6,9].

Além disso, vale destacar que 23% dos 236 fungicidas (princípios ativos) comercializados nos EUA em 2017 consistem de inibidores da respiração celular, sendo que 43% destes são inibidores do complexo III (*Fungicide Resistance Action Comitee*, FRAC, 2018). A azoxistrobina, fungicida da classe das estrobilurinas, é um inibidor do complexo III de enorme sucesso na agricultura. Assim sendo, há grande preocupação quando se identificam espécies ou isolados de fungos resistentes a este fungicida, inclusive pela ação da AOX [97,98].

De fato, o papel da AOX na resistência a estrobilurinas já foi demonstrado para *M. perniciosa*, e outros fitopatógenos que atacam culturas importantes ao redor do globo, tais como *Magnaporthe grisea* [99], *Mycosphaerella graminicola* [100,101], *Sclerotinia sclerotiorum* [102], *Venturia inaequalis* [103], dentre outros [97,104–107]. Ao mesmo tempo, a inibição da AOX foi suficiente para quebrar a resistência em muitos destes casos.

A AOX também pode atuar contra fungicidas com outros modos de ação. Foi demonstrado em *S. sclerotiorum* um aumento na expressão da AOX quando desafiado com procimidona, um fungicida da classe das dicarboximidas e com atividade sobre a via de sinalização por histidina quinases e MAP quinases [108]. Já a AOX de *Candida albicans* parece ter papel relevante na resistência a azóis, inibidores de enzimas envolvidas na síntese de ergosterol, componente da membra celular de fungos [109,110].

Por fim, ressalta-se que a AOX também é encontrada em patógenos de humanos e outros animais, alguns dos quais também se mostraram sensíveis à inibição da AOX. Por exemplo, nos fungos e leveduras *Aspergillus fumigatus, Candida albicans*, *Cryptococcus neoformans* e *Paracoccidioides brasiliensis* [111–114], bem como os protozoários *Trypanosoma brucei*, *Cryptosporidium parvum*, *Toxoplasma gondii* e *Plasmodium falciparum* [115–117].

Assim sendo, o estudo da AOX despertou grande interesse nas áreas da saúde e da fitopatologia, especialmente quanto ao desenvolvimento de novos produtos baseados na sua inibição. No contexto da VDB, espera-se que um inibidor da AOX atue sinergisticamente com

outros princípios que ataquem a via principal da respiração, desta forma sendo possível que o óxido nítrico naturalmente produzido pelo cacaueiro seja suficiente para este fim. Paralelamente, poder-se-ia aplicar um fungicida da classe das estrobilurinas durante o tratamento da VDB (em conjunto com o inibidor da AOX), com a vantagem de que as estrobilurinas já passaram pelas etapas de liberação para uso comercial.

Desenvolvimento de novos inibidores da AOX para o tratamento de doenças

Na década de 1970, derivados do ácido hidroxâmico e do ácido gálico foram identificados como inibidores da respiração alternativa de plantas, ainda que fossem inespecíficos para a AOX. Por exemplo, a ação destes compostos sobre lipooxigenases (que também consomem oxigênio), ocasionou certa dificuldade nos estudos iniciais para a identificação e caracterização da AOX [118–120].

Adicionalmente, a expressão da AOX é um mecanismo de sobrevivência ou virulência em vários microrganismos de interesse humano e ausente em vertebrados. Em particular, esta a única oxidase terminal presente em *T. brucei*, causador da doença do sono em humanos, durante a fase tripomastigota. Assim sendo, a TAO é considerada um potencial alvo para o desenvolvimento de novos agentes tripanossomicidas, conforme já demonstrado em condições de laboratório [115,121] (nota-se que a AOX é encontrada em outras espécies de tripanossoma, mas não em *T. cruzi*, causador da doença de chagas) [121,122].

De fato, demonstrou-se que o ácido salicil-hidroxâmico (SHAM) é eficaz contra *T. brucei in vitro*; porém, a toxicidade aguda em camundongos ocasionada pelas altas doses necessárias para a cura da tripanossomíase inviabilizou seu uso terapêutico [123]. Após extenso trabalho de síntese e caracterização de análogos estruturais, identificou-se que a injeção intraperitoneal de *N*-n-butil-3,4-dihydroxybenzamida (500-600 mg kg^{-1}), em conjunto com a ingestão de glicerol, é altamente eficaz e apresenta baixa toxicidade aguda em camundongos [124–128].

Já em 1997 se descobriu que a ascofuranona, produzida pelo fungo ascomiceto *Acremonium sclerotinogenum*, exibe ação tripanossomicida *in vitro* através da inibição da glicerol-3-fosfato desidrogenase (GAPDH) e da TAO [129,130]. Produtos naturais estruturalmente correlatos (ascoclorina, coletoclorina e ilicicolina A), são igualmente ativos sobre a TAO e a AOX de outros organismos [35] **(Figura 9)**.

Outros inibidores não seletivos da via alternativa da respiração já descritos são a cloroquina [131], o UHDBT [132,133], o ácido linoleico [52,133], a auraquina C [134], derivados do 4-hidroxibenzoato e do 4-alcoxibenzaldeído [135] e a cumarina – esta última inferida pela presença no sítio ativo da TAO após a resolução da estrutura cristalográfica (Protein Databank IDs 5gn7 e 5gn9) **(Figura 9)**.

Ao contrário do reportado para a *N*-n-butil-3,4-dihydroxybenzamida, a injeção intraperitoneal (400 mg kg^{-1}) ou a ingestão (3.200 mg kg^{-1}) da ascofuranona sem a coadministração de glicerol foi capaz de curar camundongos infectados com *T. brucei* [136]. Assim sendo, a ascofuranona é considerada uma forte candidata para o tratamento da tripanossomíase humana. Estudos recentes visaram elucidar as relações estrutura-atividade de análogos da ascofuranona sobre a TAO *in vitro* e *in vivo*, o que é fortemente beneficiado pela

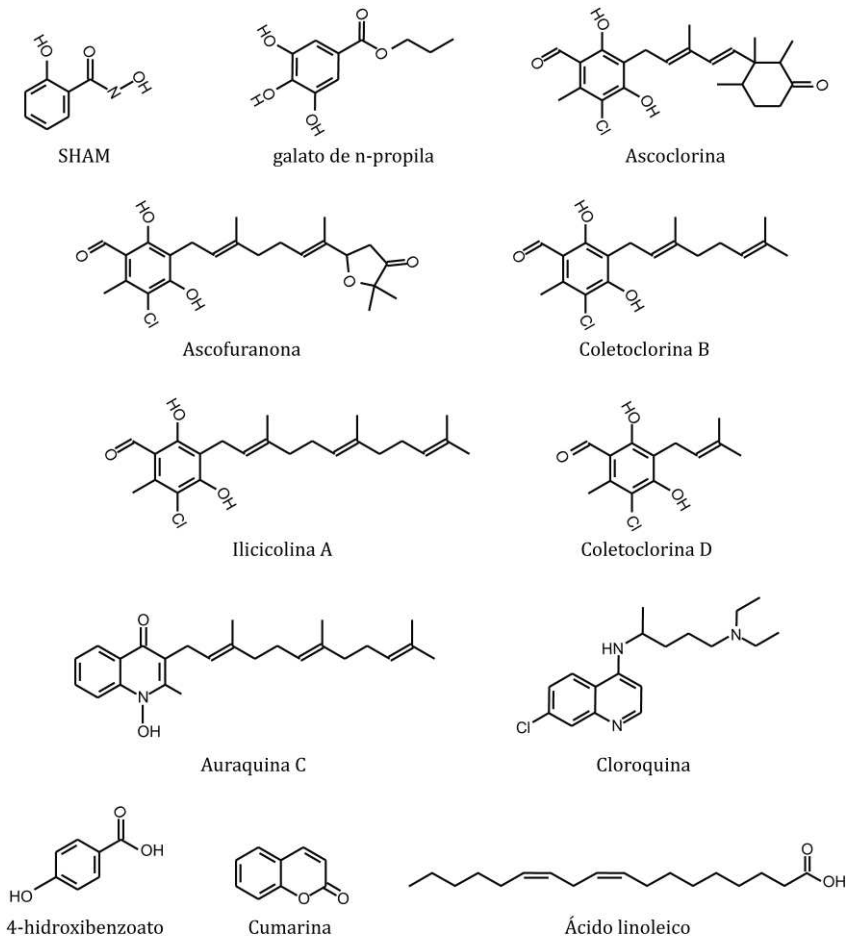

Figura 9. Inibidores conhecidos da AOX. Detalhes e referências bibliográficas são fornecidos ao longo do texto.

disponibilidade de estruturas cristalográficas desta enzima ligada a análogos da ascofuranona (Protein Databank ID 3vva e 3w54 e **Figura 6B**) [137–139].

Em contrapartida, ainda há uma relativa falta de conhecimento sobre as AOX de fungos quando comparadas a protozoários e plantas, mesmo após a descoberta de que inibidores da AOX também poderiam ser empregados no controle de fitopatógenos que ameaçam culturas de importância econômica e a segurança alimentar global [97,98].

Objetivos

Dado o exposto, este trabalho teve por objetivo gerar novas informações relevantes para o desenvolvimento direcionado de fungicidas baseados na inibição da AOX, bem como avaliar o seu efeito em fitopatógenos de interesse. Especificamente:

1. Desenvolver modelos experimentais adequados para a triagem e caracterização funcional de inibidores da AOX de fungos, tanto de compostos já conhecidos como novas entidades químicas;
2. Avaliar o potencial antifúngico de inibidores da AOX sobre *M. perniciosa*, *in vitro* e *in planta*;
3. Purificar a AOX de *M. perniciosa* (MpAOX) recombinante e caracterizá-la funcionalmente quanto à cinética enzimática, ativação pós-traducional e inibição por pequenas moléculas; e
4. Gerar dados úteis para direcionar análises da interação proteína-ligante e estudos de relação estrutura-atividade;

Os resultados obtidos são organizados em dois capítulos. No primeiro capítulo é apresentado o manuscrito intitulado "*Synthesis and testing of novel alternative oxidase (AOX) inhibitors with antifungal activity against Moniliophthora perniciosa (Stahel), the causal agent of witches' broom disease of cocoa, and other phytopathogens*" aceito para publicação no periódico *Pest Management Science* [104]. Neste trabalho, buscou-se desenvolver um modelo celular para a triagem e caracterização funcional de novos inibidores da AOX com ação antifúngica. Dado que a rota sintética estabelecida para a ascofuranona e análogos é laboriosa e de baixo rendimento, foi planejada e sintetizada uma nova classe de inibidores putativos da AOX, em colaboração com a Dra. Silvana A. Rocco do Laboratório Nacional de Biociências/Centro Nacional de Pesquisa em Energia e Materiais (LNBio/CNPEM). Derivados de *N*-fenilbenzamidas (NPD) foram planejados com base na estrutura de ligantes já conhecidos da AOX, o SHAM e o n-propil galato, visando-se manter a capacidade de interação com a enzima, porém modulando a hidrofobicidade do ligante. Em seguida, 74 NPD foram testados na levedura modelo *Pichia pastoris*, a qual possui uma AOX endógena, em ensaios de medição do consumo de oxigênio e de crescimento celular. O composto específico para a AOX e que proporcionou a maior inibição sobre o crescimento de *P. pastoris* (NPD 7J-41) também exibiu

maior potência que o SHAM sobre a AOX recombinante de *M. perniciosa* expressada em *Escherichia coli*. Por fim, testes *in vitro* e *in planta* demonstram que o 7J-41 tem ação antifúngica contra fungos fitopatógenos, inclusive *M. perniciosa*. Tais dados apoiaram a criação de um modelo computacional usado em simulações *in silico* para a elucidação de relações estrutura-atividade para os NPD.

No segundo capítulo, é abordada a expressão, a purificação e a caracterização bioquímica da MpAOX recombinante (rMpAOX), em colaboração com o Dr. Artur T. Cordeiro (LNBio/CNPEM) e o Prof. Dr. Anthony L. Moore (University of Sussex, Reino Unido). Inicialmente, foi avaliada a atividade da rMpAOX ainda associada à membrana celular de *E. coli*. Conforme observado em outras AOX de fungos, a rMpAOX foi ativada por GMP, AMP e ADP. Então, ensaios de dose-reposta foram realizados com a ascofuranona e análogos estruturais, confirmando que esta classe de inibidores também age sobre a MpAOX. Interessantemente, observou-se uma grande diferença na potência da ascoclorina entre a rMpAOX e a TAO e, após a comparação dos resíduos que compõem o sítio de ligação com o ligante destas duas enzimas, identificaram-se dois resíduos da MpAOX que provavelmente desfavorecem a interação com a ascoclorina. Por fim, a cinética enzimática da rMpAOX foi caracterizada em relação ao substrato (ubiquinol-1) e um inibidor (coletoclorina B), permitindo-se obter constantes de Michaelis-Mentes e de inibição para estes compostos. Estes dados compõem um manuscrito em elaboração a ser submetido para publicação.

CAPÍTULO 1

Synthesis and testing of novel alternative oxidase (AOX) inhibitors with antifungal activity against *Moniliophthora perniciosa* (Stahel), the causal agent of witches' broom disease of cocoa, and other phytopathogens

Barsottini *et al.* (2018), **Pest Manag. Sci.**, in press, DOI 10.1002/ps.5243

Research Article

Received: 17 July 2018 Revised: 18 September 2018 Accepted article published: 22 October 2018 Published online in Wiley Online Library:

(wileyonlinelibrary.com) DOI 10.1002/ps.5243

Synthesis and testing of novel alternative oxidase (AOX) inhibitors with antifungal activity against *Moniliophthora perniciosa* (Stahel), the causal agent of witches' broom disease of cocoa, and other phytopathogens

Mario RO Barsottini,[a,b] Bárbara A Pires,[a] Maria L Vieira,[b] José GC Pereira,[b] Paulo CS Costa,[b,c] Jaqueline Sanitá,[b] Alessandro Coradini,[a] Fellipe Mello,[a] Cidnei Marschalk,[a] Eder M Silva,[d] Daniele Paschoal,[d] Antonio Figueira,[d] Fábio HS Rodrigues,[e] Artur T Cordeiro,[b] Paulo CML Miranda,[c] Paulo SL Oliveira,[b] Maurício L Sforça,[b] Marcelo F Carazzolle,[a] Silvana A Rocco[b] and Gonçalo AG Pereira[a*]

Abstract

BACKGROUND: *Moniliophthora perniciosa* (Stahel) Aime & Phillips-Mora is the causal agent of witches' broom disease (WBD) of cocoa (*Theobroma cacao L.*) and a threat to the chocolate industry. The membrane-bound enzyme alternative oxidase (AOX) is critical for *M. perniciosa* virulence and resistance to fungicides, which has also been observed in other phytopathogens. Notably AOX is an escape mechanism from strobilurins and other respiration inhibitors, making AOX a promising target for controlling WBD and other fungal diseases.

RESULTS: We present the first study aimed at developing novel fungal AOX inhibitors. *N*-Phenylbenzamide (NPD) derivatives were screened in the model yeast *Pichia pastoris* through oxygen consumption and growth measurements. The most promising AOX inhibitor (NPD 7j-41) was further characterized and displayed better activity than the classical AOX inhibitor SHAM *in vitro* against filamentous fugal phytopathogens, such as *M. perniciosa*, *Sclerotinia sclerotiorum* and *Venturia pirina*. We demonstrate that 7j-41 inhibits *M. perniciosa* spore germination and prevents WBD symptom appearance in infected plants. Finally, a structural model of *P. pastoris* AOX was created and used in ligand structure-activity relationships analyses.

CONCLUSION: We present novel fungal AOX inhibitors with antifungal activity against relevant phytopathogens. We envisage the development of novel antifungal agents to secure food production.

Supporting information may be found in the online version of this article.

Keywords: Witches' broom disease; *Moniliophthora perniciosa*; Alternative oxidase; fungicide; crop protection; structure-activity relationship (SAR)

1 INTRODUCTION

Moniliophthora perniciosa (Stahel) Aime & Phillips-Mora is the causal agent of the witches' broom disease (WBD) of cocoa (*Theobroma cacao* L.) and a major threat to the multi-billion dollar industry of chocolate production and commercialization. Present in the Americas, this basidiomycete fungus is responsible for a Brazilian crisis after an outbreak in the largest cocoa-producing state (Bahia) in 1989. *M. perniciosa* also risks reaching Africa, where cocoa varieties highly susceptible to WBD are widely used. Thus far, there is no method to eradicate *M. perniciosa* from affected areas and farmers rely upon resistant cacao clones and crop management techniques to reduce WBD's impact.[1,2]

M. perniciosa is a hemibiotrophic pathogen, and WBD is divided in biotrophic and necrotrophic phases. The biotrophic phase starts

* *Correspondence to: GAG Pereira, Genomics and bioEnergy Laboratory, Institute of Biology, State University of Campinas, Campinas, Brazil. E-mail: goncalo@unicamp.br*

a *Department of Genetics, Evolution, Microbiology and Imunology, Genomics and bioEnergy Laboratory, Institute of Biology, State University of Campinas, Campinas, Brazil*

b *Brazilian Biosciences National Laboratory, Brazilian Center for Research in Energy and Materials, Campinas, Brazil*

c *Department of Organic Chemistry, Institute of Chemistry, State University of Campinas, Campinas, Brazil*

d *Center for Nuclear Energy in Agriculture, University of Sao Paulo, Piracicaba, Brazil*

e *School of Life Sciences, University of Warwick - Gibbet Hill Campus, Coventry, United Kingdom*

when basidiospores infect meristems (shoots, flower buds and young fruits) and develop into sparsely growing hyphae inside of the plant organs. This is when crucial host-pathogen interactions occur and lasts 2–3 months, which is unusually long for a phytopathogen. Afterwards, the infected cocoa tissues wither, which hallmarks the start of the necrotrophic phase, and a dense *M. perniciosa* mycelium grows on dead cocoa tissues. The transition between the biotrophic and necrotrophic WBD phases correlates with extensive morphophysiological changes in *M. perniciosa*. Notably, we have identified that the mitochondrial enzyme alternative oxidase (AOX) is exclusively expressed during the biotrophic phase and plays a critical role for *M. perniciosa* virulence, as well as survival to fungicides.[3,4]

AOX is widely distributed among organisms, being found in bacteria, yeasts, fungi, protists, plants and animals.[5,6] It is a membrane protein located in the matrix side of the inner mitochondrial membrane and creates a branching point in the electron transport chain (ETC) at the ubiquinone level. AOX reduces oxygen to water without the engagement of complexes III and IV, thus providing metabolic plasticity to the cell to, among other things, cope with biotic and abiotic stress.[7–10] Here, we highlight AOX as a resistance factor to ETC inhibitors and fungicides, notably strobilurins and Q_O other inhibitors.[11,12] This has been shown in a number of phytopathogens that attack several important crops worldwide, such as *Magnaporthe grisea*,[13] *Moniliophthora perniciosa*,[3] *Mycosphaerella graminicola*,[14,15] *Sclerotinia sclerotiorum*[16] and *Venturia inaequalis*,[17] among others.[18–21]

Derivatives of gallic acid and hydroxamic acid are long known AOX inhibitors, but they have poor pharmacological properties and are not adequate for commercial use.[19,22] Ascofuranone and structural analogues are potent inhibitors of the human parasite *T. brucei* AOX (TAO),[23,24] and current efforts are directed towards improving the pharmacological properties of TAO inhibitors for clinical use.[25–27] However, comprehensive studies on fungal AOX inhibition are scarce, and structure-based drug design of compounds targeting other organisms is limited by the fact that the sole AOX structure available thus far is from TAO. Moreover, synthesizing ascofuranone and derivatives is laborious and demands several reactional steps, which reduces yield and increases cost. In spite of current advances in computational biology, it is imperative to obtain experimental data to direct drug design initiatives targeting fungal AOXs.

Here, we describe a novel class of easily synthesized AOX inhibitors with antifungal activity. *Pichia pastoris* is a robust yeast used for industrial applications that grows aerobically and contains an AOX gene. *P. pastoris* was thus employed to evaluate 74 rationally designed *N*-phenylbenzamide derivatives (NPDs) through measurements of oxygen uptake and growth, providing information on the potency, selectivity and antifungal potential of those compounds. The most potent and selective NPD (7j-41) was then tested against filamentous fungal phytopathogens *M. perniciosa*, *S. sclerotiorum* and *Venturia pirina*, and the three species displayed sensitivity to 7j-41. We further demonstrate that 7j-41 prevents *M. perniciosa* basidiospore germination *in vitro*, as well as the development of WBD symptoms in infected plants. An experimentally validated structural model of *P. pastoris* AOX is presented, which enabled analyses of the structure-activity relationship for the tested NPD library. We envisage that our results will be useful for the study of fungal AOXs, as well as for the development of novel antifungal agents based on AOX inhibitors.

2 MATERIALS AND METHODS

2.1 Reagents and respiration inhibitors

The respiration inhibitors used in this work were potassium cyanide, salicylhydroxamic acid (SHAM) and n-propyl gallate (PG) from Sigma (USA), as well as the commercial preparation of azoxystrobin Amistar WG (Zeneca Brasil LTDA., Brazil; 50% active ingredient). NPDs were obtained through the Schötten–Baumann reaction,[28–30] with the synthesis of amides from amine derivatives and acyl halides in the presence of aqueous bases. Concentrated stock solutions were prepared in DMSO, except for potassium cyanide, which was dissolved in water and had the pH adjusted to 7 with HCl, and stored at −20 °C. For dose-response assays, test compounds were serially diluted in DMSO such that the final concentration of DMSO was constant across every condition.

2.2 Biological material and growth conditions

The organisms used were *P. pastoris* X-33 (Invitrogen, USA), *E. coli* BL21 (DE3) Rosetta 2 (Novagen, USA), *M. perniciosa* biotype-S TIR01, *M perniciosa* biotype-C FA553,[31] *S. sclerotiorum* and *V. pirina*. *P. pastoris* was grown at 30 °C in YP culture medium (5 g L^{-1} yeast extract and 10 g L^{-1} peptone) with either 3% (v:v) glycerol (YPG) or 1% glycerol (YPG 1%), as indicated throughout the text. *E. coli* was grown in Luria-Broth (5 g L^{-1} yeast extract, 10 g L^{-1} peptone and 10 g L^{-1} NaCl) and filamentous fungi were cultivated on malt-agar (17 g L^{-1} mat extract, 5 g L^{-1} yeast extract and 2% agar) at 25–28 °C. *M. perniciosa* spores were germinated in LMCpL+ culture medium[32] at 28 °C in the dark.

2.3 *P. pastoris* growth assay and data processing

Freshly streaked *P. pastoris* colonies were inoculated into YPG liquid medium and grown aerobically for 16–24 h at 30 °C. For growth assays in solid YPG, cells were diluted to an optical density of 0.02 (600 nm) or lower, transferred to YPG supplemented with respiration inhibitors (5 mg L^{-1} AZO and 5 mM SHAM) or 1% DMSO and incubated until the appearance of visible colonies. Growth assays in liquid culture medium were performed in 96-well flat-bottomed microtiter plates under agitation, in which 5 mM SHAM or 500 µM NPD were added, as well as DMSO or 0.5 mg L^{-1} AZO. Internal controls were included in each plate, consisting of 1% DMSO and 1% DMSO plus 0.5 mg L^{-1} AZO. Absorbance readings (600 nm) were performed at 15 min intervals (SpectraMax 384, Molecular Devices, USA) for a total of 72 h, and measured values were converted to real values with Eqn. 1. OCHT® software was used to fit a sigmoidal curve function of determinate growth[33] and the maximum specific growth rate (µMax) was calculated at the inflection point. Growth parameters obtained from each experiment were normalized as a percentage of the internal controls. For dose-response assays, a four-parameter sigmoid function was fitted (Prism Graphpad, Graphpad Software, Inc.).

$$f(x) = 12.092x^4 - 31.353x^3 + 31.371x^2 - 6.4295x + 0.5974 \quad (1)$$

2.4 Cloning of rMpAOX, site-directed mutagenesis and ectopic expression

The DNA-coding sequence for MpAOX (Genebank ID ABN09948.3) had already been sub-cloned and kindly provided by Paula F. Prado. The region corresponding to the mature protein (e.g., without the 40 amino acid residue N-terminal mitochondrial signaling peptide), as predicted in silico by the Signal P server,[34] was amplified by PCR to generate the rMpAOXΔ40 construct. Recognition sites for NdeI and EcoRI restriction enzymes were

included to the 5′ ends of the PCR primers and used for cloning of the PCR product into the pET28a bacterial expression vector (Novagen, USA) with standard molecular biology procedures. Site-directed mutagenesis of rMpAOXΔ40 was performed with the QuikChange II Site-Directed Mutagenesis Kit (Agilent Technologies, USA) and following instructions provided by the manufacturer. Codons coding for threonine 261 and tyrosine 262 in MpAOX (relative to the full-length protein) were changed to valine and phenylalanine, respectively, based on known inactivating mutations of corresponding residues in *T. brucei* AOX.[23] The ectopic expression of rMpAOXΔ40 in *E. coli* was performed essentially as described elsewhere.[25] *E. coli* cells were transformed with pET28a-rMpAOXΔ40 or the empty vector backbone by electroporation and plated in selective LB medium with 25 μg mL^{-1} kanamycin and 50 μg mL^{-1} chloramphenicol. Individual colonies were picked and inoculated in liquid LB medium with antibiotics and grown at 37 °C and 250 rpm for 16 h. The absorbance at 600 nm was measured (Biochrom WPA CO 8000 Cell Density Meter) and aliquots were transferred to fresh LB medium with antibiotics and 50 μM $FeSO_4$ to a final optical density of 0.01. After 2 h at 30 °C and aeration, expression of the recombinant protein was induced by 25 μM isopropyl β-D-1-thiogalactopyranoside (IPTG). The culture was kept under the same conditions for another 8 h and cells were harvested and used immediately for oxygen measurement assays.

2.5 Oxygen consumption measurements

Oxygen consumption measurements were performed with a Clark-type oxygen electrode (Oxygraph Plus, Hansatech Instruments, UK). *P. pastoris* was grown on YPG for 16 h and cells were used directly (non-treated) or subjected 5 mg L^{-1} AZO for 4 h to induce the alternative respiration before measurements. *E. coli* expressing rMpAOX was prepared as described. After growth, *P. pastoris* or *E. coli* cells were washed with fresh YPG (glycerol as respiration substrate) and transferred to the oxygraph chamber. The cell concentration was adjusted to give an oxygen consumption rate of ~40 nmol mL^{-1} min^{-1}. Measurements of the alternative respiration were performed in the presence of 2.5 mM KCN. O_2 uptake was recorded before and after addition of DMSO or the test compounds, and the residual respiration was determined as the ratio between the final and initial respiration rates. For dose-response assays, a four-parameter sigmoid function was fitted (Prism Graphpad, Graphpad Software, Inc.).

2.6 Antifungal activity assays

M. perniciosa basidiospores were diluted with LMCpL+ medium to 10^5 mL^{-1} and 100 μL aliquots were transferred to a 96-well plate. NPD 7j-41 or 7j-78 were added into each well, and basidiospore germination and hyphal development were monitored for 21 days. For mycelial growth assays, agar plugs containing active mycelia from *M. perniciosa*, *S. sclerotiorum* and *V. pirina* were transferred to the center of new culture plates amended with 7j-41 or 7j-78, with or without further addition of 5 mg L^{-1} AZO. Control plates consisted of 0.5% DMSO and 0.5% DMSO plus 5 mg L^{-1} AZO. After 15 days, the mycelial diameter was measured in two orthogonal axes and averaged. For *in planta* assays, 16-day-old seedlings of tomato (*Solanum lycopersicum*) cultivar Micro-Tom (MT) were inoculated with 10^6 basidiospores of *M. perniciosa* S-biotype isolate TIR01 as described elsewhere.[35] 7j-41 at 200 μM or DMSO were mixed with the basidiospore suspension during inoculation, and non-inoculated plants were equally treated. Symptoms were evaluated by measuring the stem diameter[35] at 5, 15, 25 and 35 days after inoculation. The experiment was completely randomized, with 30 plants per treatment, and results were analyzed with Student's *t*-test (R x64 3.4.3).

2.7 PpAOD molecular modeling and docking

The PpAOD structure was modeled with YASARA,[36] using TAO structures with bound ligands as templates (PDB ID 3VVA and 3W54).[23] Each chain from those structures was individually used as templates. After comparative modeling, the position of the hydroxide ion was optimized in solution through a steep descent and simulated annealing minimization using AMBER14 force field (ff14).[37] Each PpAOD model was used as input to a molecular docking routine in AutoDock (v. 4.2.5.1)[38] and the best pose of each ligand was obtained after five runs. Model performance was evaluated through the BEDROC metric[39] by comparing their biological activity and docking scores. For this purpose, the 30 PpAOD-selective NPD were ranked and the first quartile (eight compounds) was defined as active, whereas the rest was considered inactive. The BEDROC function was implemented in MatLab R2011a (Mathworks) with alpha values of 6 and 20. The cavity volume was generated with KVFinder.[40]

3 RESULTS

3.1 *Pichia pastoris* as a fungal model for AOX inhibitor characterization

It has been previously shown that *P. pastoris* possesses a functional AOX (PpAOD), although not constitutively expressed.[41] Here, we demonstrate that PpAOD is induced by the fungicide and ETC inhibitor azoxystrobin (AZO), which shifts the O_2 uptake from a cyanide-sensitive (main respiration) to a cyanide-insensitive (alternative respiration) pathway. Accordingly, classic AOX inhibitors SHAM and n-propyl gallate blocked the alternative respiration and demonstrate that AOX allows oxygen consumption to continue in the presence of AZO (Fig. 1(A)). PpAOD also contributes to *P. pastoris* growth on AZO, albeit at a lower speed, and only the combination of AZO and SHAM abolished the formation of visible colonies (Fig. 1(B)).

P. pastoris grows to high cell densities in liquid culture, which interferes with automated absorbance readings. To avoid this problem, the glycerol concentration in YP medium was reduced to 1% to limit cell growth. Furthermore, a standard curve with known *P. pastoris* cell densities was generated and used to determine the correct absorbance of unknown samples. The maximal specific growth rate (μMax) in liquid culture medium was thus determined and provided an accurate estimate of *P. pastoris* growth capacity before and after the inhibition of cellular respiration (Fig. S1).

Next, AZO-treated *P. pastoris* was employed to functionally characterize 74 NPDs synthesized by our group in search of novel fungal AOX inhibitors. DMSO-treated *P. pastoris* was used as a control to evaluate the selectivity of those compounds with respect to the alternative respiration (Fig. 2). At 500 μM, the tested NPDs exerted little effect upon the main respiration, with an average inhibition of 8 ± 9% in O_2 uptake and 13 ± 21% of growth rate. On the other hand, the alternative respiration was inhibited by 65 ± 21%, and the PpAOD-driven growth by 40 ± 29%. There was a marked difference in activity of some NPDs after comparison of respiration and growth measurements, such as 7j-07, 7j-25, 7j-42 and 7j-91 to name a few. This suggests that (i) toxic/unspecific compounds active only in growth assays may have off-targets other than ETC components and (ii) the cellular environment greatly

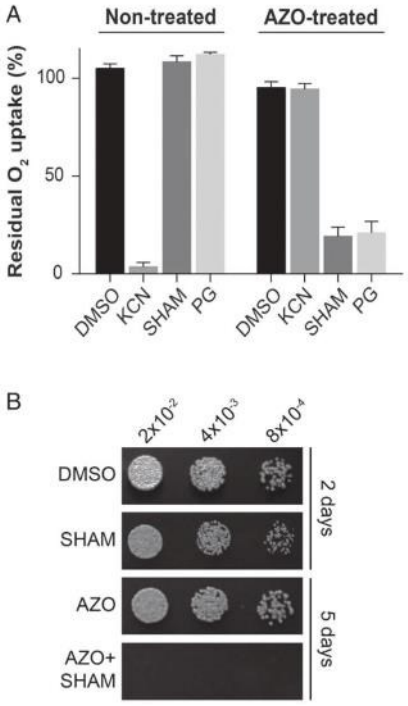

Figure 1. *P. pastoris* alternative respiration and growth. (A) Azoxystrobin induces the alternative respiration in *P. pastoris*. *P. pastoris* was treated (AZO-treated) for 4 h with 5 mg L^{-1} AZO or not (non-treated) before each measurement. Bars depict mean ± SD ($n = 3$). KCN: 2.5 mM potassium cyanide (main respiration inhibitor); SHAM and PG: 5 mM salicylhydroxamic acid and 1 mM n-propyl gallate (AOX inhibitors). (B) *P. pastoris* growth in solid culture medium. *P. pastoris* cells from a pre-culture were transferred to YPG medium amended with 5 mg L^{-1} AZO, 5 mM SHAM or both. Cell density is indicated on top. The alternative respiration sustains *P. pastoris* growth on AZO, albeit at a slower rate, and AZO plus SHAM abolished cellular growth.

influences the biological effect of NPDs, possibly due to the cellular metabolism of xenobiotics. For instance, some AOX-targeting NPDs did not reduce cell growth, which might be explained by cytochrome P450 metabolism or detoxification through efflux pumps, two known mechanisms of drug resistance in fungi.[42,43]

Overall, 69 of the 74 tested NPDs led to statistically significant inhibition of the alternative respiration. However, 42 of those 74 also interfered with either the O_2 uptake or the cellular growth in control conditions (without AZO). Of the 31 NPDs exclusively active after AZO treatment, 12 affected the alternative respiration and not the cellular growth, one reduced cellular growth and not the alternative respiration, and 16 selectively inhibited both the alternative respiration and cellular growth. Only one NPD, 7j-78, had no appreciable effect in any circumstance. These data are fully available in Table S1 and at PubChem bioassay database (PubChem AID: 1259412).

From the set of selective PpAOD inhibitors active in both O_2 uptake and cellular growth assays, 7j-41 was the most potent *P. pastoris* growth inhibitor. Therefore, 7j-41 was selected for further characterization and compared with SHAM. Both compounds displayed similar IC_{50} values on *P. pastoris* alternative respiration (208.9 µM and 261.8 µM, respectively) (Fig. 3(A)), but 7j-41 was remarkably a more potent growth inhibitor than SHAM (respective IC_{50} of 40.7 µM and 367.6 µM; Fig. 3(B)). In order to evaluate those compounds on a different fungal AOX, the recombinant *M. perniciosa* AOX (rMpAOX) was expressed in *E. coli* and O_2 consumption was measured. Indeed, rMpAOX expression created a cyanide-insensitive respiration in *E. coli*, which was not seen either in the negative control (empty vector backbone) or after the expression of mutated rMpAOX versions containing known inactivating amino acid substitutions[23] (Fig. S2). The IC_{50} of 7J-41 on rMpAOX was 178.9 µM, comparable to PpAOD. Conversely, rMpAOX was less responsive to SHAM, which inhibited only 20% of the cyanide-insensitive O_2 uptake at 2.5 mM. At 10 mM SHAM, 60% inhibition was achieved; however, off-target effects of the same magnitude were seen on *E. coli* main respiration (Fig. 3(C)). Thus, we have shown that 7j-41 possess better activity than SHAM on *P. pastoris* growth and on rMpAOX.

3.2 NPD 7j-41 displays antifungal activity against filamentous fungal phytopathogens

The next step was to assess the antifungal activity of 7J-41 against filamentous fungi. We selected three phytopathogens for which AOX is involved in resistance to ETC inhibitors. *M. perniciosa* and *S. sclerotiorum* have been described elsewhere,[3,16] and we demonstrate here that the same phenomenon occurs in *V. pirina*. A BlastP search performed against the *V. pirina* genome[44] in JGI Mycocosm Portal and MpAOX as query returned one AOX-coding sequence, namely, Protein Model 209839 in Scaffold 14 with 57.4% identity. It was also seen that *V. pirina* is able to grow on AZO, but not in the combination of AZO and SHAM (Fig. S3). Hence, we investigated the effect of 7j-41 alone or with AZO on the mycelial development of the three selected phytopathogens. NPD 7j-78 (Fig. 4(A)), which did not display any activity on *P. pastoris*, was evaluated as well. As shown in Fig. 4(B), a combination of AZO and 500 µM 7j-41 reduced the *in vitro* radial growth of *M. perniciosa*, *S. sclerotiorum* and *V. pirina* when compared to AZO alone. Remarkably, *V. pirina* was sensitive to SHAM and 7J-41 alone in the absence of AZO (Fig. 4(B) and Fig. S3).

During the WBD of cocoa, MpAOX is highly expressed in early developmental stages of *M. perniciosa*, and the biotrophic-like mycelium is sensitive to SHAM *in vitro* even in the absence of AZO.[3] In agreement, we observed a complete inhibition of *M. perniciosa* basidiospore germination with 125 µM 7j-41, while the inert 7j-78 did not exert any effect up to the maximal tested concentration of 250 µM (Fig. 4(C)). For comparison, SHAM abolished *M. perniciosa* basidiospore germination only at 5 mM (Fig. S4), which is the same concentration used previously in *in vitro* mycelial growth assays.[3]

Finally, the antifungal activity of 7j-41 was evaluated *in planta* against *M. perniciosa* (Fig. 5). We observed that 200 µM 7j-41 completely prevented WBD symptom appearance in infected tomato (*Solanum lycopersicum*) plants, which usually consist of stem swelling, axillary shoot growth and leaf distortion.[35] Even 35 days after inoculation, no difference was seen in stem diameter between non-inoculated plants and inoculated, 7j-41-treated plants (Fig. 4(D)). 7j-41 did not exert appreciable effects on non-inoculated control plants. Here, we demonstrated that 7j-41 is active against filamentous fungi that are threats to crops worldwide, including *M. perniciosa*, for which there is currently no chemical treatment available.

3.3 A PpAOD structural model provides insights on NPD structure-activity relationships

In order to enlighten the NPD structure-activity relationship and gain insights for the development of antifungal agents based

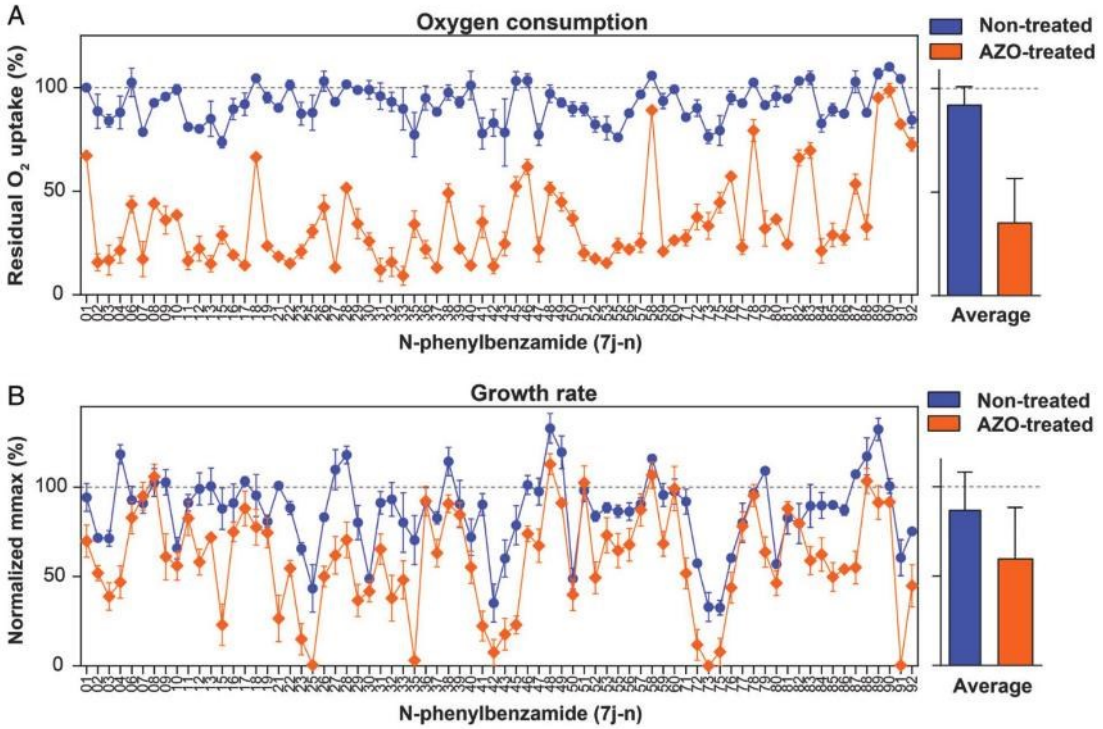

Figure 2. N-Phenylbenzamide functional characterization. (A) Effect on oxygen consumption rate of each tested NPD (left; mean ± SEM) and mean ± SD of all measurements (right). Main respiration: blue spheres; alternative respiration: orange diamonds. (B) Maximal growth rates in liquid culture medium sustained by the main (non-treated) and the alternative respiration (AZO-treated) in the presence of each NPD (left; mean ± SEM) and mean ± SD of all values (right). Full data is presented in Table S1.

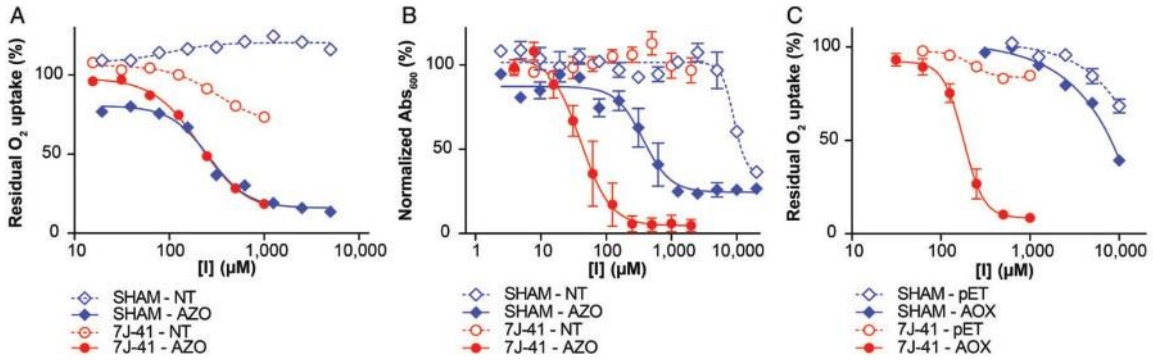

Figure 3. Dose-response assays with SHAM and 7j-41. (A) *P. pastoris* O_2 uptake after addition of SHAM or NPD 7j-41 at varying concentrations, before (NT) or after (AZO) treatment. (B) Relative growth of *P. pastoris* in liquid culture medium, as measured by the final optical density after 72 h of growth, normalized by the control condition (not treated). (C) O_2 uptake of whole *E. coli* cells transformed with rMpAOXΔ40 (AOX) or the pET28 empty backbone (pET).

on AOX inhibition, we compared the NPD biological activity on *P. pastoris* and their modeled interactions with PpAOD. Initially we generated 21 distinct PpAOD structural models based on TAO (46.2% sequence identity). We selected as templates TAO structures bound with the ascofuranone derivative AF2779OH (PDB ID: 3VVA) and with colletochlorin B (PDB ID: 3W54).[23] The apo TAO structure (PDB ID: 3VV9) was not used because the volume of the binding site is smaller than the NPD. Subsequently, 30 NPDs that were selective inhibitors of *P. pastoris* alternative respiration were docked into each PpAOD structural model. Model performance was evaluated with the BEDROC metric and two distinct α values[39] (Fig. S5), and the PpAOD model that generated the highest correlation with experimental data was selected for investigation (Fig. 6). Thus, NPD structure-activity relationships and protein-ligand interactions are discussed below.

PpAOD inhibitors show a clear preference for polarizable and bulkier halogen atoms from higher periods, such as Cl, Br and I. Their greater volumes allow for more points of contact, which

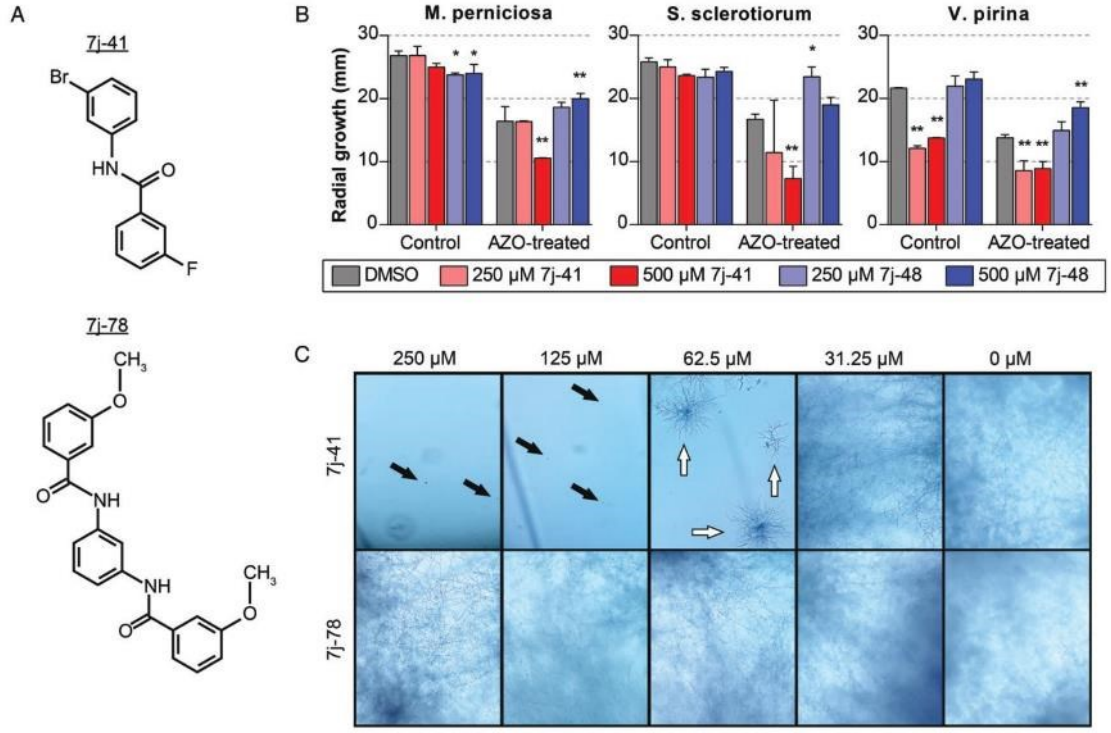

Figure 4. *In vitro* antifungal activity of NPD 7j-41. (A) Phytopathogens *M. perniciosa*, *S. sclerotiorum* and *V. pirina* were grown with the active NPD 7j-41 and the inert NPD 7j-78, with or without further addition of 5 mg L^{-1} AZO. (B) Bars depict the radial growth of the mycelia (mean ± SD; $n = 3$) after 15 days. Asterisks indicate results statistically different from DMSO treatment (with or without AZO, as pertinent). *$P < 0.05$; **$P < 0.01$. For the three tested fungal species, 500 μM 7j-41 increased their sensitivity to AZO. Notably, *V. pirina* is sensitive to 7j-41 even in the absence of AZO. (C) *M. perniciosa* basidiospores germination assay. After 21 days, fully developed mycelium was observed in every condition with 7j-78, whereas 7j-41 exhibited inhibitory effects on spore germination from 62.5 μM. Black arrows, non-germinated spores; white arrows, partially developed mycelium.

leads to a higher affinity to the PpAOD active site. Moreover, NPD with F and Cl substitutions were more effective growth inhibitors, which is explained by the fact that such atoms may prevent drug degradation by the cellular metabolism.[45] In general, the *meta* position of the aromatic ring bonded to the amide nitrogen atom favors electronegative substituents for better antifungal activity.

Substituents R_1 and R_2 (Table S1) define which of the two benzene rings will be positioned more internally with respect to the PpAOD active site. F, Cl and I favor the insertion of the benzene ring to which they are attached, which is due to their interaction with the region corresponding to Phe134, Leu137, Glu138 and Tyr235. These resides are in the vicinity of the PpAOD diiron center, and the hydroxide radical bridging the two iron atoms may also interact with *meta* substituents in some NPDs. The NPD carbonil group is usually directed towards Arg97 and an electrostatic interaction is predicted, although the geometry of this interaction does not permit the establishment of a hydrogen bond. The nitrogen atom of the NPD amide interacts with PpAOD α-helix 5 – following TAO's structure nomenclature[23] – and it is possible for a hydrogen bond to occur between that nitrogen and the Glu230 backbone carbonyl group.

Van der Walls forces also play an important role in protein-ligand interaction. A π stacking interaction occurs between benzene rings from NPD and Phe100, which are positioned orthogonally with respect to each other. Additionally, we observed ligand interactions with Met93, Arg97, Trp130, Arg133 and Thr234. R2 substituents, when directed towards the outside of the active site, are positioned according to their size. For instance, F atoms interact with a small hydrophobic cavity formed by Met93, Leu227 and C_β and C_γ of Glu230. Bulkier atoms, such as Cl, Br and I, do not interact with that small hydrophobic cavity and are instead directed towards the entrance of the active site. NPDs with poor biological activity and low docking scores usually exhibit either polar substituents in close proximity to hydrophobic regions, or fewer points of interaction due to small substituents, such as hydrogen (Fig. S6).

In their most stable conformation, NPDs present a delocalized π electronic system. However, the ligand's aromatic rings are reoriented when inside the PpAOD active site in order to favor the protein-ligand interaction. Substituents that intensify the electronic delocalization, such as NO_2, disfavor that rearrangement and, therefore, are weak ligands. Furthermore, NO_2 is a polar group that interacts weakly with hydrophobic residues in the active site.

4 DISCUSSION

AOX is a desirable target for the development of new antiparasitic and antifungal agents, with clear potential impacts on human health and food security, since AOX inhibitors might be used to treat human fungal pathogens[46–49] as well as

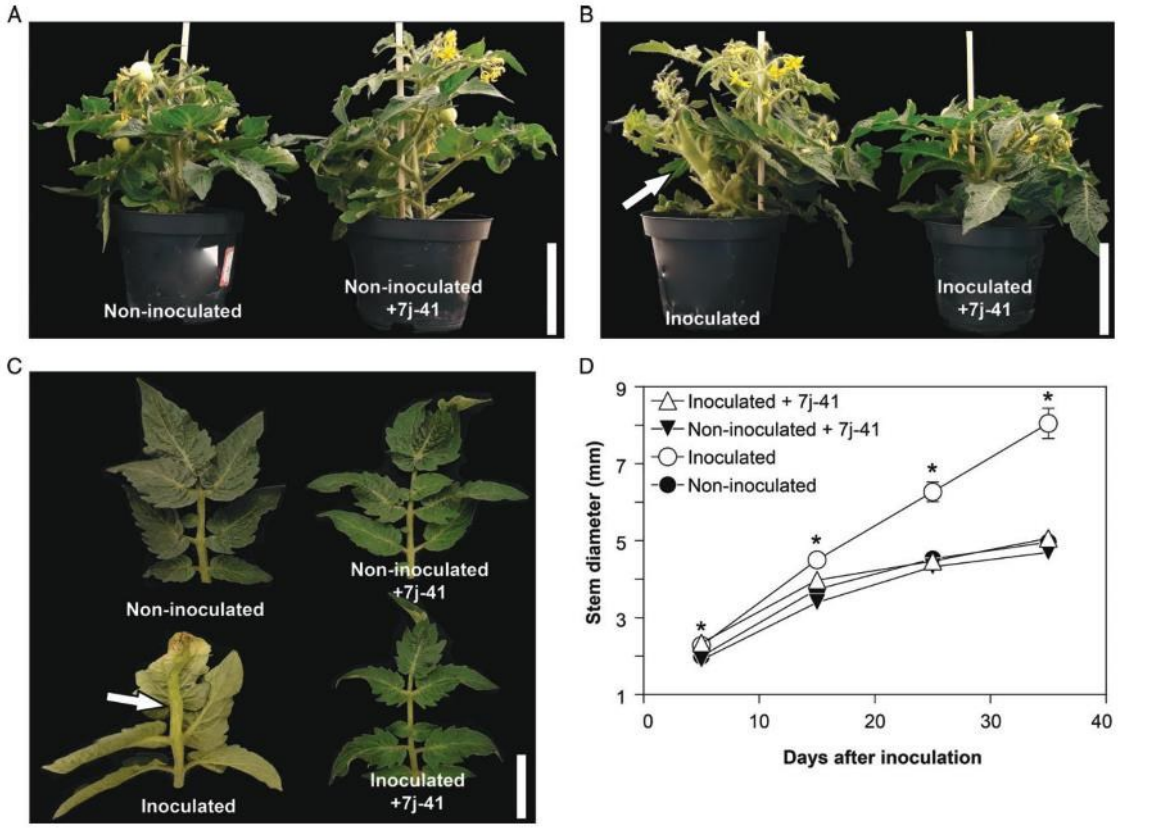

Figure 5. *In planta* antifungal activity of NPD 7j-41 against *M. perniciosa*. MT plants 35 days after inoculation with spores from S-biotype isolate of *M. perniciosa* were compared with the control treatment. (A) Left, non-inoculated MT (treated only with DMSO). Right, non-inoculated MT treated with 7j-41. No differences were observed between them (controls). (B) Left, MT inoculated with *M. perniciosa* displaying stem swelling. The arrow shows the abnormal axillary outgrowth (broom). Right, plant inoculated together with 7j-41 displaying no symptoms. (C) MT leaves inoculated with *M. perniciosa* displaying petiole swelling compared with the other treatments which present no symptoms. (D) Mean of stem diameter from MT inoculated with *M. perniciosa* biotype-S, non-inoculated, inoculated with *M. perniciosa*, treated with 7j-41 molecule and non-inoculated treated with 7j-41 molecule at 5, 15, 25 and 35 days after inoculation (average ± SD; $n = 30$). Asterisks indicate results statistically different from the non-inoculated control. *$P < 0.05$. Scale bars: 6 cm (A, B), 2 cm (C).

phytopathogens.[3,14–17] Here, we present the first comprehensive study on fungal AOX inhibition by small molecules and provide new tools to aid the development of novel fungicides.

Here, the yeast *Pichia pastoris* was employed as a fungal model to assess the antifungal potential of those compounds. Usually, *Saccharomyces cerevisiae* is used as a host for heterologous expression of fungal AOXs because it lacks its own AOX.[50–52] However, our experience shows that *S. cerevisiae* was not a robust model for testing AOX-driven growth (data not shown), and we reason that this is because *S. cerevisiae* lacks a functional ETC complex I, the only ETC component that contributes to ATP synthesis when AOX is the sole terminal oxidase. The AOX-expressing *P. pastoris*, on the other hand, can readily grow on a non-fermentable carbon source, such as glycerol, using complex I to generate ATP. This allowed us to functionally characterize our NPD library and identify the selective PpAOD inhibitor 7j-41. Overall, 7j-41 was more potent than SHAM as an antifungal agent and was effective against three non-model filamentous fungi that are threats to crops worldwide, *M. perniciosa*, *S. sclerotiorum* and *V. pirina*. Finally, an experimentally validated structural model of PpAOD was generated, which provided useful information on protein-ligand interactions and NPD structure-activity relationships.

M. perniciosa was the first phytopathogen for which compelling evidence has been obtained on the relevance of AOX during host infection. Throughout the *M. perniciosa* life cycle, MpAOX is overexpressed in the biotrophic phase, when the living cocoa produces large amounts of the potent ETC inhibitor nitric oxide. Indeed, parallels were drawn between *M. perniciosa* and the human parasite *T. brucei* with respect to the dependence on the alternative respiration for virulence and survival.[3] Here, we demonstrated that AOX inhibitor 7j-41 alone was enough to prevent *M. perniciosa in vitro* spore germination and abolished the appearance of WBD symptoms in infected plants. Notably, SHAM has been shown to prevent *M. grisea* and *Botrytis cinerea* spore germination *in vitro*,[53,54] suggesting that AOX activity is a common feature needed for spore germination in these fungi.

On the other hand, disease development is not always dependent on AOX, since *M. grisea* AOX knock-out strains displayed similar virulence levels in barley leaves as did the wild-type.[13] However, the relevance of fungal AOX in agricultural settings is also related to AOX's contribution to fungicide resistance. Strobilurins

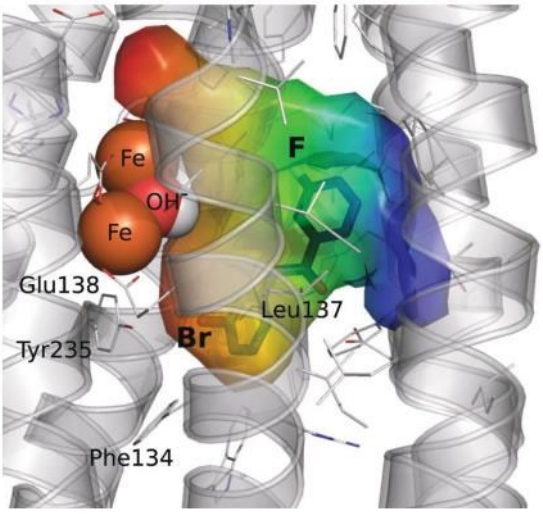

Figure 6. PpAOD structural model and docking of 7j-41. The best docking pose is shown. The color range represents from the aperture of the cavity to the solvent (blue) until the region farthest from that aperture (red). Residues Phe134, Leu137, Glu138 and Tyr235 make up the bromine interaction subsite.

are quinone outside (complex III) inhibitors successfully employed as agrochemicals for more than 20 years,[55] and the escape mechanism through the alternative respiration has been thoroughly discussed and exemplified.[11,19] Moreover, the non-ETC targeting fungicide procymidone has been shown to induce AOX expression in *S. sclerotiorum*[16] and *Candida albicans* AOX provides resistance against azole fungicides.[12,56] This is in accordance with studies on yeasts demonstrating that mitochondrial function as a whole plays a great part in fungal virulence and resistance to antifungal agents.[57] Collectively, those results indicate that AOX plays a broader role in fungal development and expands the scenarios in which AOX-targeting molecules can be effectively employed to treat fungal diseases (i.e., in combination with other AOX-inducing molecules).

Overall, our data demonstrate that 7j-41 is more potent and selective than SHAM against *M. perniciosa*, which is evidenced by the difference in concentrations used (10–20 times higher for SHAM than 7j-41) and by non-specific effects in *E. coli* membranes with SHAM. We envisage that our results and the uncovered NPD structure-activity relationship will guide AOX-targeting fungicide development against *M. perniciosa* and other fungal threats to crops worldwide.

ACKNOWLEDGEMENTS

This work was supported by the São Paulo Research Foundation (FAPESP) through research grants 2015/07653-5 and 2016/10498-4, and scholarships 2014/15339-6, 2015/09870-3, 2015/06677-8 and 2017/17000-4. This work was also supported by the National Council for Scientific and Technological Development (CNPq) grant 475535/2013-8 and scholarship 142358/2014-2. The authors also acknowledge the Brazilian Biosciences National Laboratory (LNBio-CNPEM/MCTI), specifically the Nuclear Magnetic Resonance and Chemistry and Natural Products Laboratories. The authors thank Rafael Guido for his valuable support on the rational design studies and to Paula F. Prado for providing the sub-cloned MpAOX DNA sequence.

AUTHOR CONTRIBUTION

Wrote the manuscript: M.R.O.B., J.G.C.P., P.C.S.C., S.A.R.; NPD synthesis and structural characterization: M.L.V., J.S., F.H.S.R., M.L.S., S.A.R.; *P. pastoris* and antifungal assays *in vitro*: M.R.O.B., B.A.P., A.C., F.M., A.T.C., M.F.C., G.A.G.P.; *in planta* assays: S.E.M., D.P., A.F.; structural modeling and structure-activity relationship determination: J.G.C.P., P.C.S.C., P.C.M.L.M., P.S.L.O., M.F.C.; conceptualization: G.A.G.P.

SUPPORTING INFORMATION

Supporting information may be found in the online version of this article.

REFERENCES

1 Meinhardt LW, Rincones J, Bailey BA, Aime MC, Griffith GW, Zhang D *et al.*, *Moniliophthora perniciosa*, the causal agent of witches' broom disease of cacao: what's new from this old foe? *Mol Plant Pathol* **9**:577–588 (2008).
2 Teixeira PJPL, Thomazella DP and Pereira GAP, Time for chocolate: current understanding and new perspectives on cacao witches' Broom disease research. *PLoS Pathog* **11**:1–8 (2015).
3 Thomazella DPT, Teixeira PJPL, Oliveira HC, Saviani EE, Rincones J, Toni IM *et al.*, The hemibiotrophic cacao pathogen *Moniliophthora perniciosa* depends on a mitochondrial alternative oxidase for biotrophic development. *New Phytol* **194**:1025–1034 (2012).
4 Teixeira PJPL, Thomazella DPDTDT, Reis O, do Prado PFV, do Rio MCS, Fiorin GL *et al.*, High-resolution transcript profiling of the atypical biotrophic interaction between *Theobroma cacao* and the fungal pathogen *Moniliophthora perniciosa*. *Plant Cell* **26**:4245–4269 (2014).
5 McDonald AE and Vanlerberghe GC, Origins, evolutionary history, and taxonomic distribution of alternative oxidase and plastoquinol terminal oxidase. *Comp Biochem Physiol Part D Genomics Proteomics* **1**:357–364 (2006).
6 McDonald AE, Alternative oxidase: What information can protein sequence comparisons give us? *Physiol Plant* **137**:328–341 (2009).
7 Rogov AG, Sukhanova EI, Uralskaya LA, Aliverdieva DA and Zvyagilskaya RA, Alternative oxidase: Distribution, induction, properties, structure, regulation, and functions. *Biochem* **79**:1615–1634 (2014).
8 Gupta KJ, Mur LAJ and Neelwarne B, *Alternative Respiratory Pathways in Higher Plants*. John Wiley & Sons, Ltd, Chichester, UK (2015).
9 Taiz L and Zeiger E, Respiration and Lipid Metabolism, in *Plant Physiology and Development*, ed. by Taiz L and Zeiger E. Sinauer Associates, Sunderland, pp. 223–258 (2003).
10 Del-Saz NF, Ribas-Carbo M, McDonald AE, Lambers H, Fernie AR and Florez-Sarasa I, An in vivo perspective of the role(s) of the alternative oxidase pathway. *Trends Plant Sci* **23**:206–219 (2017).
11 Fernández-Ortuño D, Torés JA, de Vicente A and Pérez-García A, Mechanisms of resistance to Qol fungicides in phytopathogenic fungi. *Int Microbiol* **11**:1–9 (2008).
12 Yan L, Li M, Cao Y, Gao P, Cao Y, Wang Y *et al.*, The alternative oxidase of *Candida albicans* causes reduced fluconazole susceptibility. *J Antimicrob Chemother* **64**:764–773 (2009).
13 Avila-Adame C and Köller W, Disruption of the alternative oxidase gene in *Magnaporthe grisea* and its impact on host infection. *Mol Plant Microbe Interact* **15**:493–500 (2002).
14 Affourtit C, Heaney SP and Moore AL, Mitochondrial electron transfer in the wheat pathogenic fungus *Septoria tritici*: on the role of alternative respiratory enzymes in fungicide resistance. *Biochim Biophys Acta - Bioenerg* **1459**:291–298 (2000).
15 Miguez M, Reeve C, Wood PM and Hollomon DW, Alternative oxidase reduces the sensitivity of *Mycosphaerella graminicola* to QOI fungicides. *Pest Manag Sci* **60**:3–7 (2004).
16 Xu T, Wang Y-T, Liang W-S, Yao F, Li Y-H, Li D-R *et al.*, Involvement of alternative oxidase in the regulation of sensitivity of *Sclerotinia sclerotiorum* to the fungicides azoxystrobin and procymidone. *J Microbiol* **51**:352–358 (2013).

17 Olaya G, Zheng D and Köller W, Differential responses of germinating *Venturia inaequalis conidia* to kresoxim-methyl. *Pestic Sci* **54**:230–236 (1998).
18 Joseph-Horne T, Wood PM, Wood CK, Moore AL, Headrick J and Hollomon D, Characterization of a split respiratory pathway in the wheat 'take-all' fungus, *Gaeumannomyces graminis* var. tritici. *J Biol Chem* **273**:11127–11133 (1998).
19 Wood PM and Hollomon DW, A critical evaluation of the role of alternative oxidase in the performance of strobilurin and related fungicides acting at the Qo site of complex III. *Pest Manag Sci* **59**:499–511 (2003).
20 Walker AS, Auclair C, Gredt M and Leroux P, First occurrence of resistance to strobilurin fungicides in *Microdochium nivale* and *Microdochium majus* from French naturally infected wheat grains. *Pest Manag Sci* **65**:906–915 (2009).
21 Hayashi K, Watanabe M, Tanaka T and Uesugi Y, Cyanide-insensitive respiration of phytopathogenic fungi demonstrated by antifungal joint action of respiration inhibitors. *J Pestic Sci* **21**:399–403 (1996).
22 Menzies SK, Tulloch LB, Florence GJ and Smith TK, The trypanosome alternative oxidase: a potential drug target? *Parasitology* **145**:175–183 (2018).
23 Shiba T, Kido Y, Sakamoto K, Inaoka DK, Tsuge C, Tatsumi R *et al.*, Structure of the trypanosome cyanide-insensitive alternative oxidase. *Proc Natl Acad Sci* **110**:4580–4585 (2013).
24 May B, Young L and Moore AL, Structural insights into the alternative oxidases: are all oxidases made equal? *Biochem Soc Trans* **45**:731–740 (2017).
25 Saimoto H, Kido Y, Haga Y, Sakamoto K and Kita K, Pharmacophore identification of ascofuranone, potent inhibitor of cyanide-insensitive alternative oxidase of *Trypanosoma brucei*. *J Biochem* **153**:267–273 (2013).
26 West RA, O'Doherty OG, Askwith T, Atack J, Beswick P, Laverick J *et al.*, African trypanosomiasis: Synthesis & SAR enabling novel drug discovery of ubiquinol mimics for trypanosome alternative oxidase. *Eur J Med Chem* **141**:676–689 (2017).
27 Ebiloma GU, Ayuga TD, Balogun EO, Gil LA, Donachie A, Kaiser M *et al.*, Inhibition of trypanosome alternative oxidase without its N-terminal mitochondrial targeting signal (ΔMTS-TAO) by cationic and non-cationic 4-hydroxybenzoate and 4-alkoxybenzaldehyde derivatives active against *T. brucei* and *T. congolense*. *Eur J Med Chem* **150**:385–402 (2018).
28 Baumann E, Ueber eine einfache Methode der Darstellung von Benzoësäureäthern. *Berichte der Dtsch Chem Gesellschaft* **19**:3218–3222 (1886).
29 Schotten C, Ueber die Oxydation des Piperidins. *Berichte der Dtsch Chem Gesellschaft* **17**:2544–2547 (1884).
30 Kurti L and Czako B, *Strategic Applications of Named Reactions in Organic Synthesis*, 1st edn. Elsevier Academic Press, San Diego, CA (2005).
31 Mondego JMC, Carazzolle MF, Costa GGL, Formighieri EF, Parizzi LP, Rincones J *et al.*, A genome survey of *Moniliophthora perniciosa* gives new insights into Witches' Broom Disease of cacao. *BMC Genomics* **9**:548 (2008).
32 Meinhardt LW, Bellato CDM, Rincones J, Azevedo RA, JCM C and GAG P, In vitro production of biotrophic-like cultures of *Crinipellis perniciosa*, the causal agent of witches' broom disease of *Theobroma cacao*. *Curr Microbiol* **52**:191–196 (2006).
33 de Mello F da SB, Coradini ALV, Tizei PAG, Carazzolle MF, Pereira GAG, and Teixeira GS, Static microplate fermentation and automated growth analysis approaches identified a highly-aldehyde resistant Saccharomyces cerevisiae strain. *Biomass and Bioenergy* **120**:49–58 (2019).
34 Petersen TN, Brunak S, von Heijne G and Nielsen H, SignalP 4.0: discriminating signal peptides from transmembrane regions. *Nat Methods* **8**:785–786 (2011).
35 Deganello J, Leal GA, Rocha ML, Peres LEP and Figueira A, Interaction of moniliophthora perniciosa biotypes with micro-tom tomato: A model system to investigate the witches' broom disease of *Theobroma cacao*. *Plant Pathol* **63**:1251–1263 (2014).
36 Krieger E, Joo K, Lee J, Lee J, Raman S, Thompson J *et al.*, Improving physical realism, stereochemistry, and side-chain accuracy in homology modeling: Four approaches that performed well in CASP8. *Proteins Struct Funct Bioinforma* **77**:114–122 (2009).
37 Maier JA, Martinez C, Kasavajhala K, Wickstrom L, Hauser KE and Simmerling C, ff14SB: Improving the accuracy of protein side chain and backbone parameters from ff99SB. *J Chem Theory Comput* **11**:3696–3713 (2015).
38 Morris GM, Huey R, Lindstrom W, Sanner MF, Belew RK, Goodsell DS *et al.*, AutoDock4 and AutoDockTools4: Automated docking with selective receptor flexibility. *J Comput Chem* **30**:2785–2791 (2009).
39 Truchon J-F and Bayly CI, Evaluating virtual screening methods: good and bad metrics for the "Early Recognition" Problem. *J Chem Inf Model* **47**:488–508 (2007).
40 Oliveira SH, Ferraz FA, Honorato RV, Xavier-Neto J, Sobreira TJ and de Oliveira PS, KVFinder: steered identification of protein cavities as a PyMOL plugin. *BMC Bioinformatics* **15**:197 (2014).
41 Kern A, Hartner FS, Freigassner M, Spielhofer J, Rumpf C, Leitner L *et al.*, *Pichia pastoris* 'just in time' alternative respiration. *Microbiology* **153**:1250–1260 (2007).
42 Anderson JB, Evolution of antifungal-drug resistance: mechanisms and pathogen fitness. *Nat Rev Microbiol* **3**:547–556 (2005).
43 Shin J, Kim J-E, Lee Y-W and Son H, Fungal cytochrome P450s and the P450 complement (CYPome) of *Fusarium graminearum*. *Toxins (Basel)* **10**:112 (2018).
44 Cooke IR, Jones D, Bowen JK, Deng C, Faou P, Hall NE *et al.*, Proteogenomic analysis of the *Venturia pirina* (pear scab fungus) secretome reveals potential effectors. *J Proteome Res* **13**:3635–3644 (2014).
45 Murphy CD and Sandford G, Recent advances in fluorination techniques and their anticipated impact on drug metabolism and toxicity. *Expert Opin Drug Metab Toxicol* **11**:589–599 (2015).
46 Martins VP, Dinamarco TM, Soriani FM, Tudella VG, Oliveira SC, Goldman GH *et al.*, Involvement of an alternative oxidase in oxidative stress and mycelium-to-yeast differentiation in *Paracoccidioides brasiliensis*. *Eukaryot Cell* **10**:237–248 (2011).
47 Guedouari H, Gergondey R, Bourdais A, Vanparis O, Bulteau AL, Camadro JM *et al.*, Changes in glutathione-dependent redox status and mitochondrial energetic strategies are part of the adaptive response during the filamentation process in *Candida albicans*. *Biochim Biophys Acta - Mol Basis Dis* **1842**:1855–1869 (2014).
48 Magnani T, Soriani FM, Martins VDP, Policarpo ACDF, Sorgi CA, Faccioli LH *et al.*, Silencing of mitochondrial alternative oxidase gene of *Aspergillus fumigatus* enhances reactive oxygen species production and killing of the fungus by macrophages. *J Bioenerg Biomembr* **40**:631–636 (2008).
49 Akhter S, McDade HC, Gorlach JM, Heinrich G, Cox GM and Perfect JR, Role of alternative oxidase gene in pathogenesis of *Cryptococcus neoformans*. *Infect Immun* **71**:5794–5802 (2003).
50 Magnani T, Soriani FM, Martins VP, Nascimento AM, Tudella VG, Curti C *et al.*, Cloning and functional expression of the mitochondrial alternative oxidase of *Aspergillus fumigatus* and its induction by oxidative stress. *FEMS Microbiol Lett* **271**:230–238 (2007).
51 Huh W-K and Kang S-O, Characterization of the gene family encoding alternative oxidase from *Candida albicans*. *Biochem J* **356**:595–604 (2001).
52 Robertson A, Schaltz K, Neimanis K, Staples JF and McDonald AE, Heterologous expression of the *Crassostrea gigas* (Pacific oyster) alternative oxidase in the yeast *Saccharomyces cerevisiae*. *J Bioenerg Biomembr* **48**:509–520 (2016).
53 Avila-Adame C and Köller W, Impact of alternative respiration and target-site mutations on responses of germinating conidia of *Magnaporthe grisea* to Qo-inhibiting fungicides. *Pest Manag Sci* **59**:303–309 (2003).
54 Inoue K, Tsurumi T, Ishii H, Park P and Ikeda K, Cytological evaluation of the effect of azoxystrobin and alternative oxidase inhibitors in *Botrytis cinerea*. *FEMS Microbiol Lett* **326**:83–90 (2012).
55 Bartlett DW, Clough JM, Godwin JR, Hall AA, Hamer M and Parr-Dobrzanski B, The strobilurin fungicides. *Pest Manag Sci* **58**:649–662 (2002).
56 Strippoli V, D'Auria FD, Tecca M, Callari A and Simonetti G, Propyl gallate increases in vitro antifungal imidazole activity against *Candida albicans*. *Int J Antimicrob Agents* **16**:73–76 (2000).
57 Shingu-Vazquez M and Traven A, Mitochondria and fungal pathogenesis: drug tolerance, virulence, and potential for antifungal therapy. *Eukaryot Cell* **10**:1376–1383 (2011).

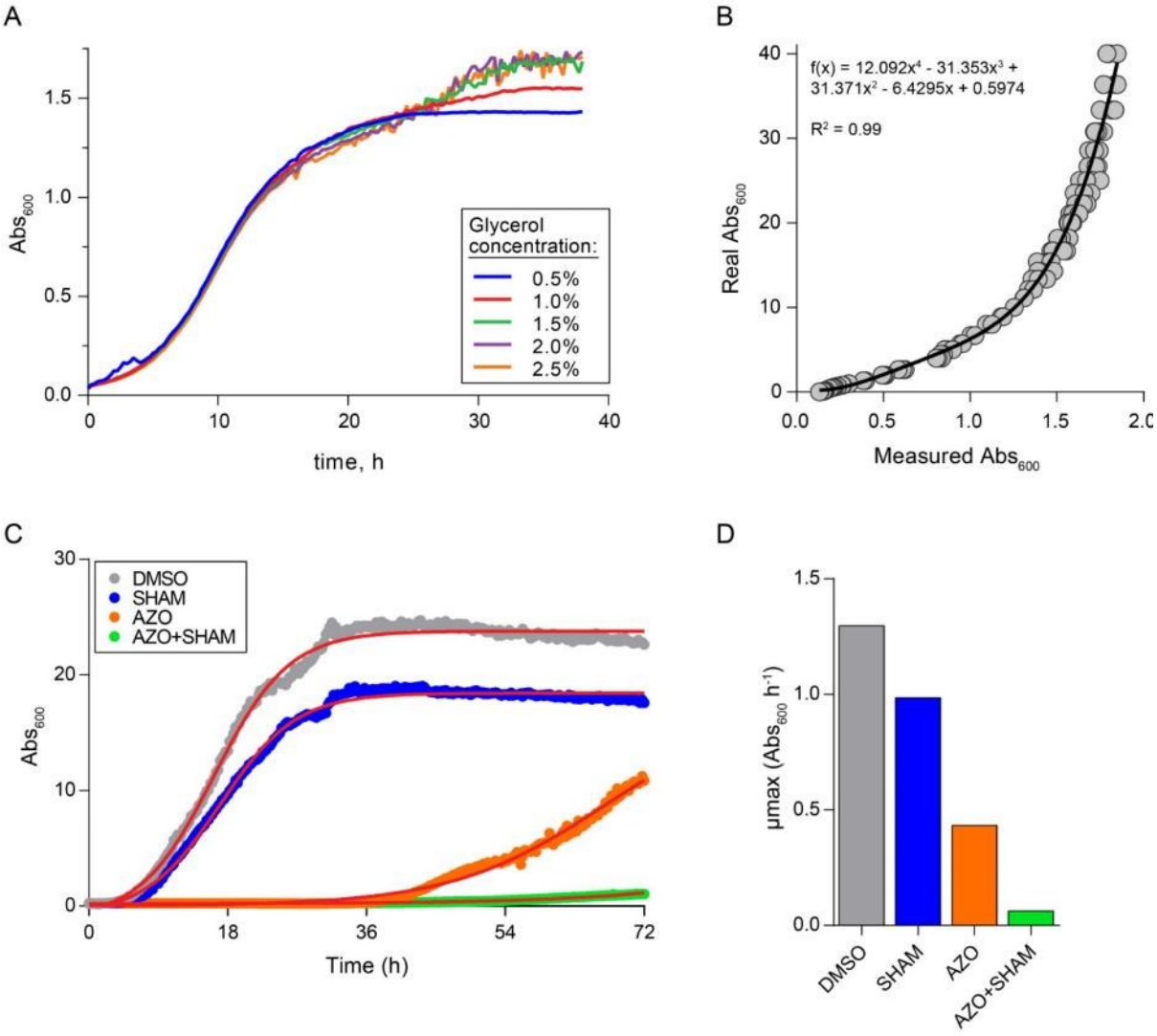

S1 Fig. *P. pastoris* growth measurement in 96-well microtiter plates. (A) Comparison between different starting concentrations of glycerol. Above 1% glycerol, absorbance measurements exhibit high noise at values higher than 1.5 a.u. **(B)** Correlation between measured (X axis) and real (Y axis) optical density of *P. pastoris* cells. A polynomial function was fitted to the data (black line), which was used to correct subsequent measurements before data processing. **(C)** Growth curves in the presence of respiration inhibitors (5 mg L-1 AZO and 5 mM SHAM). **(D)** Maximum specific growth rates (µMax) determined from (C).

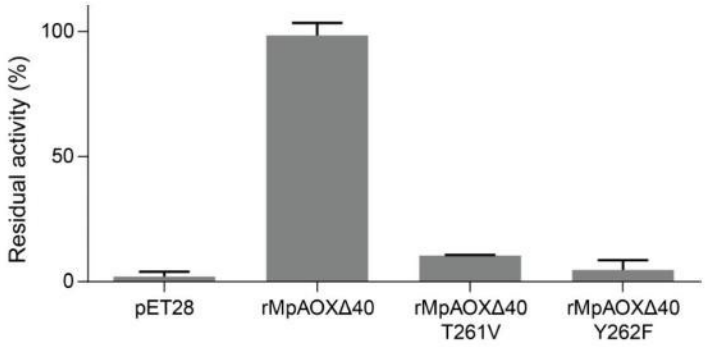

S2 Fig. Residual oxygen consumption rate of E. coli cells transformed with either the pET28a empty backbone, rMpAOXΔ40 or two inactive mutants in the presence of 2.5 mM KCN. Clearly, only the active rMpAOX construct promotes a cyanide-insensitive respiration.

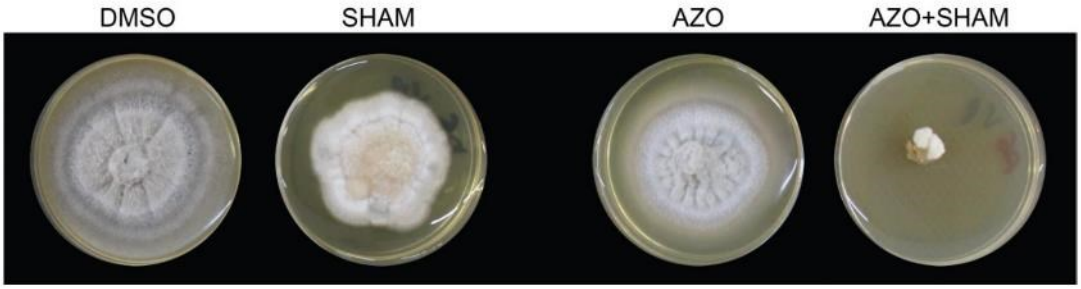

S3 Fig. *In vitro* treatment of *V. pirina* with respiration inhibitors. *V. pirina* was cultivated with AZO, SHAM and a combination of AZO and SHAM for 15 days, whereupon the mycelial growth was recorded and representative results are shown. The fact that SHAM increased *V. pirina's* sensitivity to AZO, as observed for other AOX-containing fungal species, indicates that V. pirina also has a functional AOX. Furthermore, SHAM alone induced morphological changes and reduced fungal radial growth, which, together with results obtained with the *N*-Phenylbenzamide derivative 7j-41 (Figure 5 in the main text), suggests that AOX also plays a developmental role.

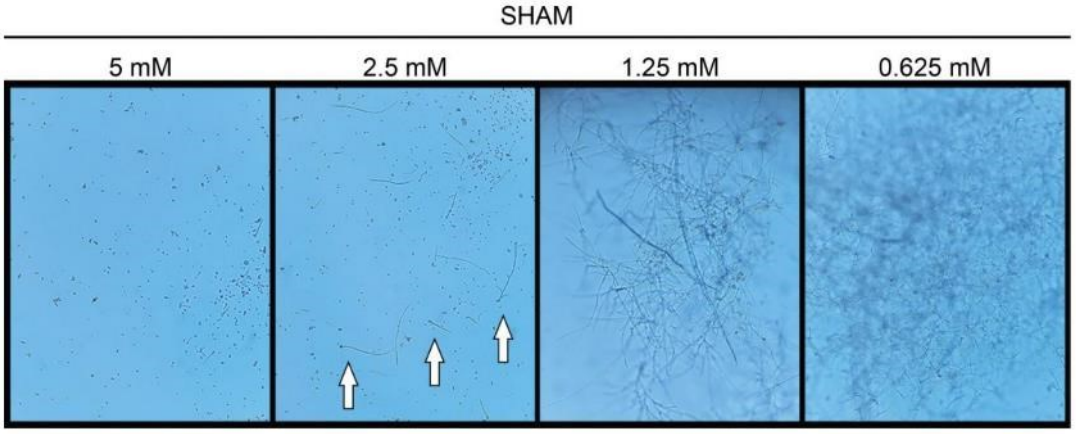

S4 Fig. *In vitro M. perniciosa* spore germination assay with SHAM. *M. perniciosa* spores were left to germinate with varying concentrations of the AOX inhibitor SHAM. Only at 5 mM did this compound completely inhibited spore germination, while the mycelial development was greatly reduced at 2.5 mM (white arrows). At lower SHAM concentrations, fully developed mycelium is observed.

	Template	
Model	PDB ID	Chain
R1	3wa	B
R2	3wa	B
R3	3wa	B
R4	3wa	B
R5	3wa	B
R6	3wa	C
R7	3wa	C
R8	3wa	C
R9	3wa	D
R10	3wa	D
R11	3wa	D
R12	3w54	A
R13	3w54	A
R14	3w54	A
R15	3w54	A
R16	3w54	A
R17	3w54	C
R18	3w54	C
R19	3w54	C
R20	3w54	C
R21	3w54	C

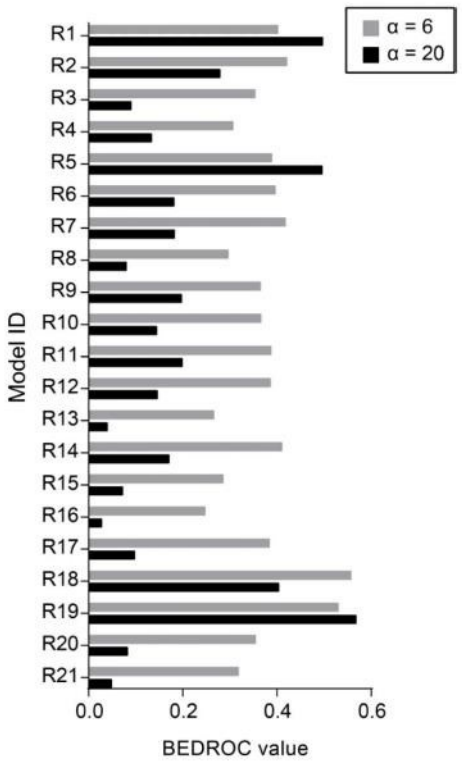

S5 Fig. Details for PpAOD model generation (left) and validation (right). The BEDROC metric indicates the performance of each model in predicting the biological activity outcome for 30 selective NPDs.

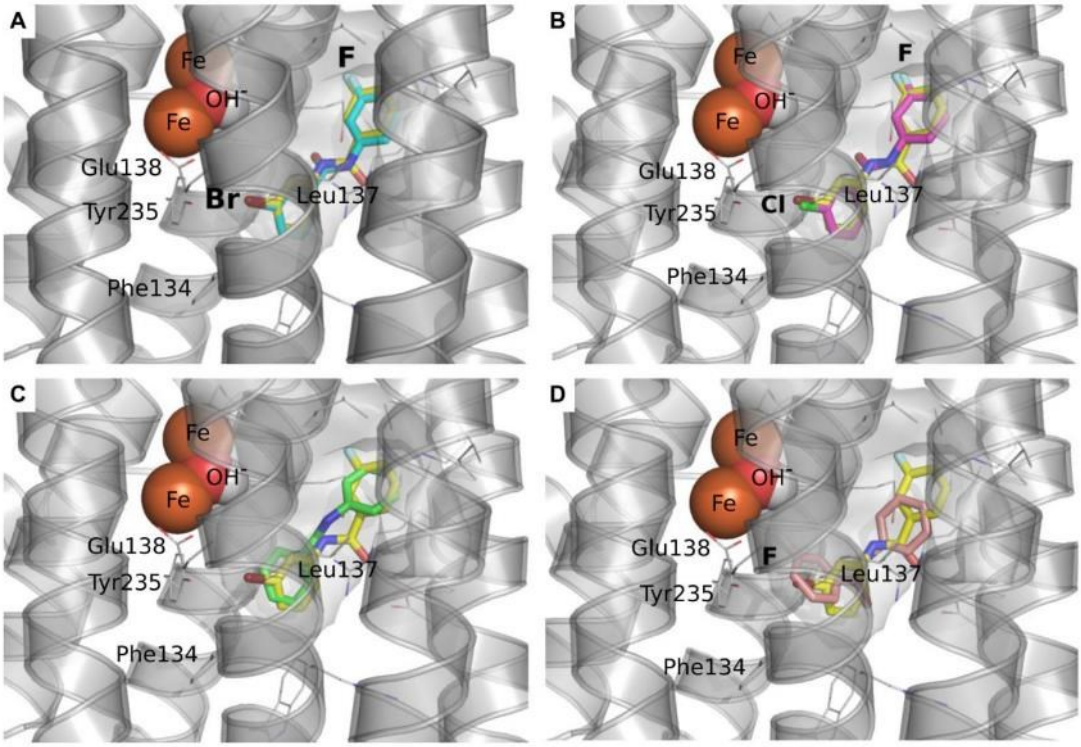

S6 Fig. PpAOD structural model and docking of different NPDs. 7j-41 (yellow stick) was superimposed onto other NPDs for comparison: **(A)** 7j-15 (blue sticks); **(B)** 7j-35 (pink sticks); **(C)** 7j-01 (green sticks); and **(D)** 7j-46 (rose sticks).

Table S1. Summary data of the functional characterization for *N*-Phenylbenzamide derivatives.

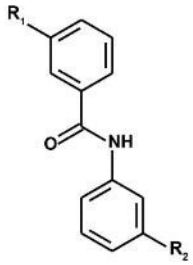

NPD code	Substituents		Control								AZO-treated							
			Residual oxygen consumption				Normalized growth rate				Residual oxygen consumption				Normalized growth rate			
	R1	R2	Average	SEM	n	t-test [a]	Average	SEM	n	t-test [b]	Average	SEM	n	t-test [a]	Average	SEM	n	t-test [b]
7J-01	H	H	99.93	0.75	3		94.28	7.76	5		67.16	0.65	3	*	69.81	9.00	4	*
7J-02	H	Br	88.55	8.25	3		71.62	1.53	3	*	15.73	4.17	3	*	51.89	4.26	3	*
7J-03	H	CF_3	84.02	3.09	3	*	71.38	4.35	3		16.80	7.26	3	*	38.87	7.70	4	*
7J-04	H	Cl	88.01	7.96	3		118.38	5.42	3		21.47	6.11	3	*	46.92	8.97	4	*
7J-06	H	F	102.49	6.87	3		92.84	7.79	5		43.57	4.00	3	*	82.95	9.00	4	
7J-07	H	I	78.57	1.86	3	*	91.03	5.63	4		17.29	8.52	3	*	94.95	7.73	3	
7J-08	H	NH_2	92.56	1.47	3	*	102.64	7.73	3		44.04	2.37	3	*	105.95	6.99	3	
7J-09	H	NO_2	95.61	0.95	3		102.71	7.09	4		36.02	6.78	3	*	61.13	12.94	5	
7J-10	H	N-(1,3-Benzodioxol-5-yl methyl)	99.07	2.35	3		65.84	6.11	3	*	38.59	0.99	3	*	56.08	8.02	4	*
7J-11	Br	Br	81.02	0.95	3	*	91.31	4.72	3		16.46	4.31	3	*	82.52	9.63	4	
7J-12	Br	CF_3	80.15	1.64	3	*	99.07	8.97	3		22.31	5.98	3	*	58.10	7.24	3	*
7J-13	Br	Cl	84.97	8.50	3		100.54	10.22	3		14.99	3.87	3	*	71.84	0.95	3	*
7J-15	Br	F	73.67	2.74	4	*	88.05	11.72	4		28.72	4.32	3	*	23.06	11.71	7	*
7J-16	Br	H	89.64	5.05	3		91.11	10.75	5		19.29	0.93	3	*	74.97	5.49	3	*
7J-17	Br	I	92.01	5.42	3		103.27	2.63	3		14.31	1.81	3	*	88.18	9.79	3	
7J-18	Br	NH_2	104.51	0.38	3		95.32	11.74	4		66.46	2.47	3	*	77.57	10.04	5	

NPD code	Substituents		Control								AZO-treated							
			Residual oxygen consumption				Normalized growth rate				Residual oxygen consumption				Normalized growth rate			
	R1	R2	Average	SEM	n	t-test [a]	Average	SEM	n	t-test [b]	Average	SEM	n	t-test [a]	Average	SEM	n	t-test [b]
7J-19	Br	NO_2	95.14	2.55	3		80.84	3.52	3	*	23.57	2.49	3	*	74.53	8.58	5	*
7J-21	H_3C	Br	90.23	2.12	3	*	100.80	1.73	3		18.55	1.92	3	*	26.61	12.97	6	*
7J-22	H_3C	CF_3	101.12	2.37	3		88.39	3.66	3		15.15	0.73	3	*	54.49	4.60	4	*
7J-23	H_3C	Cl	87.43	5.60	3		65.61	3.38	5	*	20.85	3.38	3	*	14.88	8.78	6	*
7J-25	H_3C	F	87.82	8.58	3		43.37	13.30	6	*	30.69	3.27	3	*	0.51	0.49	4	*
7J-26	H_3C	H	103.08	4.84	3		83.25	2.41	4	*	42.31	5.93	3	*	49.98	5.77	4	*
7J-27	H_3C	I	93.16	1.89	3	*	109.93	11.23	3		13.30	1.06	3	*	61.87	10.55	6	*
7J-28	H_3C	NH_2	101.51	0.76	3		118.04	4.97	3		51.56	2.15	3	*	70.53	9.99	4	
7J-29	H_3C	NO_2	98.84	0.61	3		80.17	9.54	4		34.26	7.24	3	*	36.72	9.11	5	*
7J-30	H_3C	N-(1,3-Benzodioxol-5-yl methyl)	98.98	4.47	3		48.80	0.44	3	*	25.81	3.98	3	*	41.65	5.97	3	*
7J-31	Cl	Br	95.90	6.37	3		91.27	6.29	3		12.02	5.57	3	*	65.39	8.53	3	
7J-32	Cl	CF_3	93.20	4.63	3		93.16	9.43	4		15.79	7.00	3	*	37.94	12.95	6	*
7J-33	Cl	Cl	89.76	10.30	3		80.21	16.64	5		9.19	4.64	3	*	48.09	10.64	5	*
7J-35	Cl	F	77.25	10.75	4		70.32	13.91	4		34.09	6.34	4	*	3.11	2.00	3	*
7J-36	Cl	H	94.94	5.82	3		91.81	7.97	5		21.97	4.20	3	*	92.29	8.44	4	
7J-37	Cl	I	88.31	2.14	3	*	82.78	3.41	5	*	13.16	0.62	3	*	63.13	7.68	5	*
7J-38	Cl	NH_2	97.66	3.73	3		114.40	8.03	5		49.18	4.43	3	*	90.70	4.99	5	
7J-39	Cl	NO_2	92.97	2.68	3		90.56	13.30	5		22.31	2.20	3	*	84.54	6.77	3	
7J-40	Cl	N-(1,3-Benzodioxol-5-yl methyl)	101.03	6.80	3		72.01	10.29	5		14.22	1.46	3	*	55.29	9.03	5	*
7J-41	F	Br	77.87	7.51	5		90.38	6.22	6		35.11	7.72	3	*	22.28	8.42	5	*
7J-42	F	CF_3	82.96	6.40	3		35.17	10.65	5	*	13.82	3.64	3	*	7.63	7.28	4	*
7J-43	F	Cl	78.32	16.27	3		60.10	10.44	4	*	24.62	5.80	3	*	17.75	9.01	3	*
7J-45	F	F	103.11	4.50	3		78.72	10.94	5		52.28	4.72	4	*	22.98	5.09	3	*
7J-46	F	H	103.45	3.17	4		101.27	5.36	5		61.76	3.63	3	*	73.89	4.39	5	*
7J-47	F	I	77.29	5.17	4	*	97.54	7.52	5		21.94	5.97	3	*	67.18	9.35	6	*

NPD code	Substituents		Control								AZO-treated							
			Residual oxygen consumption				Normalized growth rate				Residual oxygen consumption				Normalized growth rate			
	R1	R2	Average	SEM	n	t-test [a]	Average	SEM	n	t-test [b]	Average	SEM	n	t-test [a]	Average	SEM	n	t-test [b]
7J-48	F	NH_2	97.03	4.22	3		132.93	8.36	5	*	51.31	3.07	3	*	112.82	5.94	5	
7J-49	F	NO_2	92.71	2.27	3	*	119.57	9.24	5		44.79	4.30	3	*	91.10	3.10	3	
7J-50	F	N-(1,3-Benzodioxol-5-yl methyl)	89.61	3.37	3		48.82	5.89	3	*	36.90	3.51	3	*	39.77	8.77	4	*
7J-51	I	Br	89,56	3,08	3		98,07	6,31	4		20,19	3,78	3	*	102,51	9,40	6	
7J-52	I	CF_3	82.18	3.73	3	*	83.82	2.97	3	*	17.52	2.48	3	*	49.37	8.93	5	*
7J-53	I	Cl	80,45	5,63	4		88,57	2,81	3		15,40	2,06	4	*	73,05	9,83	3	
7J-55	I	F	75.99	1.32	3	*	86.49	3.44	3		23.74	3.57	3	*	64.54	9.56	4	*
7J-56	I	H	87.66	0.27	3	*	86.39	5.01	3	*	21.93	2.04	3	*	67.84	9.18	6	*
7J-57	I	I	96.73	1.12	3		90.61	3.60	4	*	25.10	4.66	3	*	87.35	9.03	6	
7J-58	I	NH_2	105.71	2.10	3		116.02	2.40	3	*	89.01	0.29	3		106.77	7.46	4	
7J-59	I	NO_2	93.54	3.72	3		95.62	6.48	3		20.99	1.61	3	*	68.37	6.94	3	*
7J-60	I	N-(1,3-Benzodioxol-5-yl methyl)	99.11	1.02	3		97.52	6.97	4		26.29	1.61	3	*	99.20	12.46	5	
7J-71	CH_3O	Br	85,79	0,56	3	*	91,97	6,97	5		27,48	3,82	3	*	51,85	8,59	5	*
7J-72	CH_3O	CF_3	90,15	4,05	3		57,44	0,89	3	*	37,57	6,12	3	*	11,82	8,65	4	*
7J-73	CH_3O	Cl	76,3	3,37	3	*	32,95	8,04	3	*	33,2	6,54	4	*	0	0	3	*
7J-75	CH_3O	F	79,25	7,19	3		32,57	4,05	3	*	44,53	4,94	4	*	7,84	7,63	3	*
7J-76	CH_3O	H	95,07	3,19	3		60,37	2,07	3	*	57,13	2,87	3	*	43,83	8,69	3	*
7J-77	CH_3O	I	92,46	1,04	3	*	80,05	11	4		23,02	3,54	3	*	78,22	7,96	4	
7J-78	CH_3O	NH_2	102,43	1,01	3		96,75	0,75	3		79,24	5,37	3		95,41	6,24	3	
7J-79	CH_3O	NO_2	91,52	1,89	3	*	109,16	2,15	3	*	31,95	8,44	3	*	63,72	8,46	4	*
7J-80	CH_3O	N-(1,3-Benzodioxol-5-yl methyl)	95,78	5,02	3		56,96	0,83	3	*	36,4	2,91	3	*	46,41	6,95	3	*
7J-81	Br	N-(1,3-Benzodioxol-5-yl methyl)	94,72	1,25	3	*	82,81	8,96	4		24,43	2,11	3	*	87,96	3,71	3	

NPD code	Substituents		Control								AZO-treated							
			Residual oxygen consumption				Normalized growth rate				Residual oxygen consumption				Normalized growth rate			
	R1	R2	Average	SEM	n	t-test [a]	Average	SEM	n	t-test [b]	Average	SEM	n	t-test [a]	Average	SEM	n	t-test [b]
7J-82	CN	N-(1,3-Benzodioxol-5-yl methyl)	103,12	0,77	3		79,68	11,24	3		66,11	3,94	3	*	79,62	1,63	3	*
7J-83	CN	H	104,7	3,12	3		89,54	12,09	5		69,61	3,79	4	*	58,86	7,83	4	*
7J-84	CN	Br	82,64	4,21	3		89,74	7,27	3		21,26	5,93	3	*	62,36	9,32	3	*
7J-85	CN	CF_3	89,3	2,93	3	*	90,09	1,42	3	*	28,86	5,7	3	*	49,72	8,08	4	*
7J-86	CN	Cl	87,4	1,83	3	*	87,12	2,97	3	*	27,57	3,61	3	*	54,11	1,36	3	*
7J-87	CN	F	102,85	5,35	3		107,29	2,5	3		53,46	4,74	4	*	55,15	9,22	3	*
7J-88	CN	I	87,81	1,51	3	*	117,19	10,41	4		32,64	5,97	3	*	103,47	7,05	3	
7J-89	CN	NH_2	106,66	2,48	3		132,39	6,35	3	*	95,1	1,09	3		91,38	9,5	4	
7J-90	CN	NO_2	109,96	1,42	3		100,75	4,17	5		98,69	3,26	4		91,73	1,96	4	*
7J-91	H	*p*-$C_3H_3N_2$	104,17	0,91	3		60,55	10,08	5	*	82,32	1,23	3	*	0,31	0,16	3	*
7J-92	Br	*p*-$C_3H_3N_2$	84,36	3,78	3		75,34	2,28	3	*	72,57	3,17	3	*	44,89	11,84	5	*

[a] Asterisks indicate statistically different values from DMSO-treatment; p-value < 0.01

[b] Asterisks indicate statistically different values from internal plate control; p-value < 0.05

CAPÍTULO 2

Heterologous expression, purification and characterization of the alternative oxidase from the fungal phytopathogen *Moniliophthora perniciosa*

Manuscrito em elaboração.

Heterologous expression, purification and characterization of the alternative oxidase from the fungal phytopathogen *Moniliophthora perniciosa*

Mario R. O. Barsottini[a,b], Luke Young[c], Renata M. Baroni[a], Anthony L. Moore[c], Artur T. Cordeiro[b], Gonçalo A. G. Pereira[a,*]

[a] Genomics and bioEnergy Laboratory, Institute of Biology, State University of Campinas, Campinas, Brazil

[b] Brazilian Biosciences National Laboratory, Brazilian Center for Research in Energy and Materials, Campinas, Brazil

[c] Biochemistry & Biomedicine, University of Sussex, Brighton, United Kingdom

[*]Corresponding author: goncalo@unicamp.br (GAGP)

Abstract

Background: *Moniliophthora perniciosa* a fungal pathogen that causes the witches' broom disease of cocoa (WBD). WBD is a threat to the chocolate industry and cannot be eradicated after infection occurs. The membrane-bound mitochondrial enzyme alternative oxidase (MpAOX) is crucial for pathogen survival and is a desirable target for fungicide development. However, little is known about MpAOX inhibitors.

Methods: Recombinant MpAOX was used for biochemical investigations. Dose-response assays with activators and inhibitors were performed with the membrane-bound MpAOX, followed by experiments the kinetic characterization of purified rMpAOX. A structural model was created and compared to AOX from *Trypanosoma brucei* (TAO).

Results: Maximum rMpAOX activation was seen with 5'-GMP (10-fold increase). A range of responses was observed with the tested inhibitors, with colletochorin B (IC_{50} = 14.8 nM) being

350 as potent as ascochlorin (IC_{50} = 5,246 nM), which have not been observed on TAO. This fact, alongside sequence and structural comparisons between MpAOX and TAO, led to the identification of key substitutions in the MpAOX ligand binding pocket that are likely responsible for the poor interaction of ascoclhorin. Finally, kinetic parameters were determined for rMpAOX with regard to the substrate ubiquinol-1 (K_M = 53.4 μM) and colletochlorin B (K_I = 14.8 nM).

Conclusions: MpAOX has similar kinetics towards the substrate and activators as other AOXs. However, differences in the ligand binding pocket lead to striking differences in affinity to inhibitor, specially ascochlorin.

General significance: Those results will be useful for the development of novel AOX-targeting antifungal agents.

Highlights

- MpAOX is activated by 5'-GMP and inhibited by colletochlorin B and analogues
- Two residues in the binding pocket most likely prevent interaction with ascochlorin
- Our results will support the development of novel WBD treatments

Keywords

Moniliophthora perniciosa; alternative oxidase; antifungal agent; membrane protein; AOX inhibition

Abbreviations

5'-ADP: Adenosine 5'-diphosphate; 5'-AMP: Adenosine 5'-monophosphate; 5'-GMP: Guanosine 5'-monophosphate; AC: ascochlorin; AF: ascofuranone; ALA: 5-aminolevulinic acid; AOX: alternative oxidase; C12E8: octaethylene glycol monododecyl ether; CB: colletochlorin B; CD: colletochlorin D; FC-12: fos-choline-12; Q_1: ubiquinone; Q_1H_2: ubiquinol-1; SHAM: salicylhydroxamic acid; TAO: Trypanosoma brucei alternative oxidase; WBD: Witches' broom disease of cocoa

1. Introduction

The cocoa tree (*Theobroma cacao*) is a perennial plant originated from the Amazon River basin in Central America. Cocoa beans are the main raw material used in the multi-billion dollar chocolate industry, and the cocoa pod may be used in cosmetics, food thickeners, beverages, and others. However, fungal pathogens are one of the main causes of production losses in cocoa plantations, which is estimated at 30% worldwide. The basidiomycete fungus *Moniliophthora perniciosa* is the causal agent of the Witches' Broom Disease of cocoa (WBD) present in Latin America, and a WBD outbreak in Brazil's main cocoa producing region – the state of Bahia – in 1989 led to a significant loss in Brazilian competitiveness. Therefore, Brazil shifted from net exporter to net importer of cocoa beans, with major economic and social losses [1].

M. perniciosa is a hemibiothtophic pathogen with a complex life-style and two physiologically distinct life stages. The infection begins when *M. perniciosa* basidiospores reach meristematic cocoa tissues, whereupon infective hyphae penetrate through stomata and wounds. Initially, *M. perniciosa* develops without killing its host, the biothrophic stage of WBD. Most prominent infection symptoms during the biotrophic stage are hypertrophy and hyperplasia of affected tissues, along with loss of apical dominance in shoots. After 2-3 months, WBD advances to the necrothophic stage and infected tissues wither and die. Cycles of rain and drought induce the formation of basidiomata and basidiospores, which are carried by wind and rain.

M. perniciosa exhibits large morphological and physiological differences between the biotrophic and necrotrophic stages, as well as an unusually long biothrophic stage when compared to other known phytopathogens [1,2]. Of particular interest is the identification an alternative oxidase (AOX)-coding gene, which is highly expressed during the *M. perniciosa*-cocoa interaction and most likely critical for WBD development [3,4].

The AOX is an enzyme that participates in the cellular respiration, a process during which reducing equivalents are transferred from carbon sources to oxygen. The main respiratory path way consists of four multi-enzyme complexes (I to IV) and two small components (ubiquinone and cytochrome C) in the inner mitochondrial membrane, which utilizes the chemical energy to translocate protons to the mitochondrial intermembrane space that, in turn, drives ATP synthesis. AOX is a terminal oxidase that creates a branching point at

the ubiquinone level, thereby bypassing complex III and complex IV, which reduces the generation of ATP. The chemical energy is released as heat instead [5].

On the other hand, there is substantial evidence that the AOX ensures some level of metabolic plasticity to the cell, both during regular metabolic conditions and in stressful events. Such an event is the inhibition of complexes III or IV, which halts cellular respiration, ATP production and other upstream processes. The oxidative imbalance also leads to the generation of harmful reactive oxygen species. In the presence of AOX, however, excess reducing equivalents can be used to reduce oxygen to water, thereby partially maintaining energy production through complex I.

It has been shown that infected cocoa plants produce nitric oxide, a potent complex IV inhibitor, and we have recently demonstrated that chemical inhibition of AOX abolishes *M. perniciosa* infection, making AOX inhibitors putative antifungal crop protection agents [4,6]. Furthermore, *M. perniciosa* AOX (MpAOX) is a key resistance factor to commercial fungicides known as strobilurins, which are inhibitors of Complex III [4], and the same was observed in other fungal plant pathogens, such as *Botrytis cinerea*, *Magnaporthe grisea*, *Monilinia fructicola*, *Mycosphaerella graminicola*, *Pyricularia oryzae* and *Venturia inaequalis* [7,8].

Therefore, in order to gain further insights on MpAOX function and inhibitors, we have heterologously expressed and purified this enzyme. We demonstrate that the recombinant MpAOX (rMpAOX) is active in *Escherichia coli* membrane, which was used to evaluate colletochlorin B (CB) and structurally related AOX inhibitors in dose-response assays. Moreover, an analysis of an MpAOX structural model and comparison with the known structure of *Trypanosoma brucei* AOX (TAO) allowed the identification of key amino acid residues that influence protein-ligand affinity. Finally, we present and discuss the kinetic characterization of the purified rMpAOX. We hope that those results will aid the development of novel antifungal agents against *M. perniciosa* and other fungal pathogens.

2. Methods

2.1. Chemicals and reagents.

Ubiquinonol-1 (Q_1H_2) was obtained after the chemical reduction of ubiquinone-1 (Q_1; Sigma), as described elsewhere [9]. In summary, 10 mg ubiquinone-1 were dissolved in 5 mL ethanol, to which 4 g $Na_2S_2O_4$ in 30 mL of water were added. The reaction was left for one hour in the dark and ubiquinol-1 was extracted three times with 20 mL n-hexane. The n-hexane was

washed with 20 mL water, dried with solid $MgSO_4$ and filtered. The n-hexane was removed by evaporation and the solid residue was ressuspended with $CDCl_3$ for Nuclear Magnetic Resonance spectroscopy to confirm the identity and purity of ubiquinol-1. The chloroform was removed by evaporation and ubiquinol-1 was dissolved with acidified DMSO and stored at -80 °C until use. To determine the concentration of ubiquinol-1, it was diluted 100-fold in water and left to spontaneously oxidise for 24 h, after which the absorbance at 278 nm was determined (ε_{278} = 15 mM^{-1} cm^{-1}). Detergents were obtained from Anatrace.

2.2. rMpAOX cloning and expression.

The MpAOX gene used in this work corresponds to UniProt ID A8QJP8 [4], which was cloned without the predicted mitochondrial leading sequence (hereafter referred to as rMpAOX), as assessed with the Signal P server [10]. Strep-tagged rMpAOX was synthesized and cloned into the pET15a plasmid in which the poly-histag was substituted by a twin-streptag. For the HIS-tagged rMpAOX construct, the DNA-coding sequence was PCR-amplified from a *M. perniciosa* cDNA library with flanking NdeI and EcoRI restriction sites and cloned into the pET28a (Novagen) backbone with standard molecular biology techniques. Both rMpAOX constructs were confirmed by DNA sequencing. rMpAOX expression, *E. coli* membrane fraction preparation and protein purification were performed essentially as described for TAO and *Sauromatum guttatum* AOX [11,12]. FN102 *E. coli* cells transformed with pET15b:rMpAOX plasmid were used to inoculate 10 mL of L-broth supplemented with 100 μg mL^{-1} ampicillin, 100 μg mL^{-1} kanamycin and 50 μg mL^{-1} 5-aminolevulinic acid (ALA). This was left to grow overnight at 37 °C. On the following day, 1 mL of overnight culture was transferred to 50 mL of L-broth supplemented with 100 μg mL^{-1} ampicillin, 100 μg mL^{-1} kanamycin, 50 μg mL^{-1} ALA, 0.2 % (w/v) glucose, 50 μg mL^{-1} $MgSO_4$, 25 μg mL^{-1} $FeSO_4$, and 25 μg mL^{-1} $FeCl_3$. The starter culture was left at 37 °C in a shaking incubator (180 rpm) until the OD_{600} reached 0.6. The cells were harvested and the cell pellet was resuspended with ~5 mL of fresh K-broth and used to inoculate 4 L of K-broth supplemented with 100 μg mL^{-1} carbenicilin, 100 μg mL^{-1} kanamycin, 50 μg mL^{-1} $MgSO_4$, 25 μg mL^{-1} $FeSO_4$, 25 μg mL^{-1} $FeCl_3$ and 0.2 % (w/v) glucose, with an starting OD_{600} of 0.01. The culture was incubated at 30 ˚C with 180 rpm shaking until the OD reached ~0.6, then 50 μM IPTG was added for induction of rMpAOX expression. Cultures were left at 30 ˚C for 14-16 hours before cell harvesting. The pET28a:rMpAOX-his-tag plasmid was transformed into the *E. coli* strain BL21 (DE3) Rosetta 2 (Novagen) which were plated on selective L-broth with 50 μg mL^{-1} kanamycin and 50 μg mL^{-1} cloramphenicol. A pre-starter culture was grown overnight at 37 °C and used on the

following day to inoculate 10 L of LB added of kanamycin, cloranphenicol and 50 μM Fe_2SO_4 to an starting OD of 0.01. The culture was grown at 30 °C until the OD_{600} reached 0.1, when 50 μM IPTG was added. Cells were harvested after 10 h.

2.3. *E. coli* membrane fraction preparation.

E. coli membrane preparation were performed as described [12], with minor modifications. The cell pellet was thoroughly resuspended in 10 mL per gram of cells of 65 mM MOPS buffer pH 7.5 supplemented with protease inhibitor tablets (Roche; 1 tablet per 50 mL), 2.5 U mL^{-1} of benzonase and 100 mM $MgSO_4$. The cells were disrupted using two passes at 30 kPa through a pre-cooled Constant cell disruption system (Constant Systems Ltd). The lysate was centrifuged for 15 minutes at 16,000 rcf, and the pelleted unbroken cells and large cell debris were discarded. The supernatant was centrifuged for 90 minutes at 200.000 rcf to collect the fragmented membranes. After centrifugation the supernatant was discarded and the membrane pellets were thoroughly resuspended with 65 mM MOPS pH 7.5 with the aid of a Dounce homogenizer.

2.4. rMpAOX purification.

The *E. coli* membrane fraction was prepared as described and resuspended with 50 mM Tris-HCl pH 7.5, 20% glycerol, 200 mM $MgSO_4$ and 1% Fos-Choline-12 (FC-12) instead of MOPS buffer. The sample was left under gentle rocking for 1 h at 4°C, after which it was centrifuged at 200.000 rcf for 30 min. The supernatant was then subjected to immobilized metal affinity chromatography with the Ni-NTA Superflow resin (Quiagen) loaded with Ni^{2+} for purification of his-tagged rMpAOX, which was performed gravimetrically at 4 °C. The resin was equilibrated with 50 mM Tris-HCl pH 7.5 before passing the sample, after which the resin as washed with 10 volumes of buffer A (20 mM Tris-HCl pH7.5, 50 mM $MgSO_4$, 60 mM NaCl, 20% glycerol and 0.05% DDM unless otherwise stated) with 100 mM imidazole. rMpAOX elution was carried out with 3 resin volumes of buffer A added of 250 mM imidazole. Protein purification was followed by SDS-PAGE and coomassie brilliant-blue staining [13], as well as western blot with AOX antibody. Protein content was estimated through the Bradford method [14] and bovine serum albumin as standard.

2.5. Enzymatic activity measurements

AOX activity measurements were performed essentially as described elsewhere for other AOXs [12,15]. Oxygen uptake from membrane-bound rMpAOX was measured in an Oxygraph-2k (Oroboros Inc.) high-resolution respirometer in 65 mM MOPS pH 7.5 with 1.25

mM NADH and 0.1 mg mL^{-1} potassium cyanide. Respiration rates were recorded before and after the addition of putative MpAOX activators 5'-ADP, 5'-AMP, 5'-GMP, glyoxylate, oxaloacetate, pyruvate or succinate. NADH oxidation measurements membrane-bound rMpAOX were performed spectrophotometrically (ε_{340} = 6.22 mM^{-1} cm^{-1}), with KCN, 1 mM GMP and 300 µM NADH. For the pure rMpAOX, Q_1H_2 oxidation was measured spectrophotometrically (ε_{284} = 14.1 mM^{-1} cm^{-1}) with 100 ng enzyme in 50 µL of 20 mM tris-HCl pH 7.5 and 0.0125% octaethylene glycol monododecyl ether (C12E8). Absorbance readings were performed in microtiter plates in triplicate periodically during 20 minutes, and a blank reaction (substrate without enzyme) was included in every assay and was used to determine the baseline substrate oxidation rate (background). The background was subtracted from the enzymatic reaction rate. When tested, inhibitors were preincubated with the enzyme in reaction buffer for 2-5 minutes before starting the reaction by the addition of the substrate. GraphPad Prism 7.0 (GraphPad Software Inc.) was used for model fitting.

2.6. MpAOX sequence alignment and structural modelling

The amino acid sequence of AOXs used in this work were from *Trypanosoma brucei* (GenBank ID BAB72245.1), *Moniliophthora perniciosa* (ABN09948.3), *Septoria tritici* (XP_003851917.1), *Neurospora crassa* (XP_962086.1), *Aspergillus niger* (BAA32033.2), *Arabidopsis thaliana* (NP_188876.1), *Oryza sativa* (XP_015635413.1) and *Zea mays* (NP_001105180.1). The sequence alignment was performed in JalView [16] software with the built-in MUSCLE routine and default parameters. The MpAOX protein sequence was used as input in the SWISS-MODEL protein structure modelling server [17] and TAO crystal structures PDB ID 3vv9 and 3w54 [18] were selected as templates. The quality of the output model was checked within parameters provided by SWISS-MODEL server. The MpAOX model and TAO structure 3w54 were aligned with PyMOL molecular viewer version 1.8.x (Schrödinger, LLC) and visually inspected, in particular residues that form the active site in TAO and residues with known functions [5]. The volume of the ligand-binding pocket was calculated with the KVfinder plugin [19] with "probe in" and "probe out" parameters respectively set as 1.1 Å and 5 Å.

3. Results and Discussion

3.1.Membrane-bound rMpAOX

The rMpAOX construct used in this work corresponds to the mature MpAOX enzyme without the predicted mitochondrial leading peptide (first 40 N-terminal amino acid residues),

which is cleaved after import to the mitochondria [20]. The removal of the mitochondrial leading sequence has been shown to increase recombinant TAO stability [21], which we also observed for rMpAOX (data not shown).

Initial characterizations of membrane-bound rMpAOX were performed with the high-resolution oxygraph Oroboros 2k. It has been shown that fungal AOXs are activated by mono- and diphosphate nucleosides, such as AMP, GMP and ADP, while plant AOXs display higher activity in the presence of organic acids, such as pyruvate, succinate and others [22,23]. Accordingly, GMP increased membrane-bound rMpAOX oxygen uptake 9.8 times, to a maximum of 669.2 ± 210.2 nmol O_2 min^{-1} mg total $protein^{-1}$, followed by AMP (8.5 times) and ADP (5.9 times). No activation by organic acids was observed **(Fig. 1A)**. GMP dose-response assays revealed that GMP EC_{50} and EC_{90} are 153 µM and 1422 µM, respectively **(Fig. 1B)**.

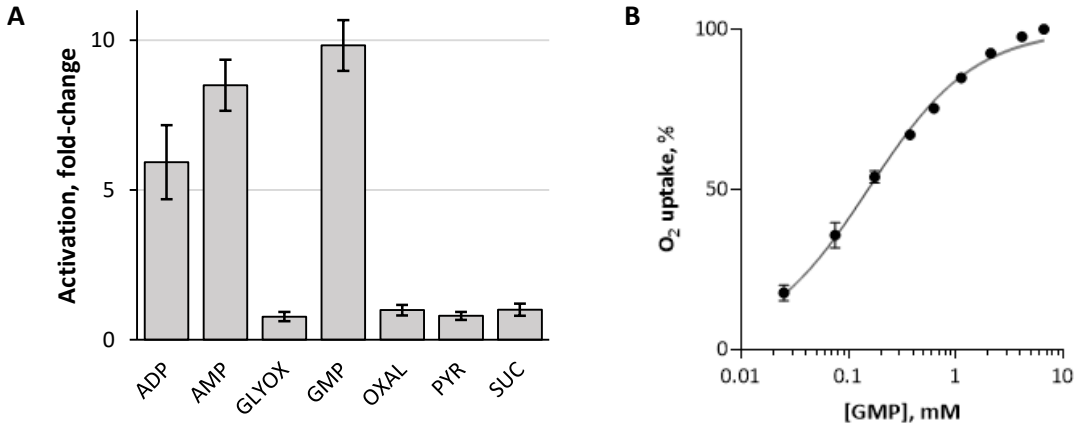

Fig. 1. Testing of rMpAOX activators. **(A)** Fold-change in membrane-bound rMpAOX O_2 uptake after addition of putative activators: ADP, AMP, glyoxylate, GMP, oxaloacetate, pyruvate and succinate (1 mM each). GMP caused the greatest increase in enzymatic activity. **(B)** Dose-response assay with GMP. The continuous line indicate the best fit for a 4-parameter sigmoid function. EC_{50} = 153 ± 9 µM.

Next, 6 known AOX inhibitors were evaluated on membrane-bound rMpAOX. For that, NADH consumption was monitored spectrophotometrically in the presence of varying concentrations of each inhibitor. As shown in **Fig. 2B**, salicylhydroxamic acid (SHAM) did not exert any appreciable effect up to the maximal tested concentration of 25 µM, while IC_{50} values

were successfully determined for ascochlorin (AC), ascofuranone (AF), colletochlorin B (CB), colletochlorin D (CD) and octyl gallate (OG). Interestingly, AC, AF, CB and CD possess identical head groups, allowing one to isolate the effect of distinct carbonic tail on inhibitor potency. Amongst those 4 analogues, AF and CB exhibited the lowest IC_{50} (8.8 nM and 14.8 nM, respectively), followed by CD (114.9 nM) and AC (5,246 nM).

3.2. MpAOX structural model

In order to gain further insights on MpAOX inhibition, we compared our results with published data from TAO. Of particular interest were the crystal structure of TAO bound to CB and structure-activity relationships of CB analogues [15,18]. In TAO, AC has an IC_{50} 7.5 times higher than CB, however that ratio is 350 in rMpAOX. Since a sequence alignment between MpAOX and TAO revealed a complete conservation in amino acid residues involved in binding to CB **(Supplementary fig. S1)**, an MpAOX structural model was generated based on the TAO crystal structure PDI ID 3w54 **(Fig. 2C)**. The predicted tertiary structure of MpAOX is in good agreement with TAO, with a Cα root mean square deviation of 1.6 Å between both proteins. Importantly, the AOX core composed of six α-helices that accommodate the hydrophobic substrate binding cavity and the catalytic site are highly conserved, and the main differences between MpAOX and TAO were found in the N-terminus region, as well as in the 18-residue insertion present in fungal AOXs between α-helices α1 and α2.

A comparison of the residues that make up the AOX hydrophobic cavity revealed six substitutions in MpAOX **(Fig. 2D** and **Table 1)**. In general, the MpAOX residues are bulkier than their TAO counterparts, making the MpAOX cavity volume (165.89 $Å^3$) smaller than TAO (225.72 $Å^3$). A visual inspection of CB bound to TAO crystal structure shows that the end of the isoprenyl tail is close to V125 and M190, which in MpAOX correspond to I167 and F232, respectively. With this, the bulky trimethylated cyclohexanone ring in AC can potentially clash with MpAOX residues and explain the drop in potency.

Conversely, AF displayed a similar relative potency on both AOXs, approximately 1.5 times lower than CB. This indicates that differences seen in the MpAOX hydrophobic cavity did not significantly affect the interaction with the furanone ring in AF. Given the longer isoprene tail in AF, it is possible that the furanone ring is positioned farther away from I167 and F232, being positioned outside of the hydrophobic cavity. Finally, CD has the shortest isoprene tail, which led to an increase in IC_{50} in MpAOX. This is in accordance with results with TAO, for which longer carbon chains increase inhibitor potency [15,24,25].

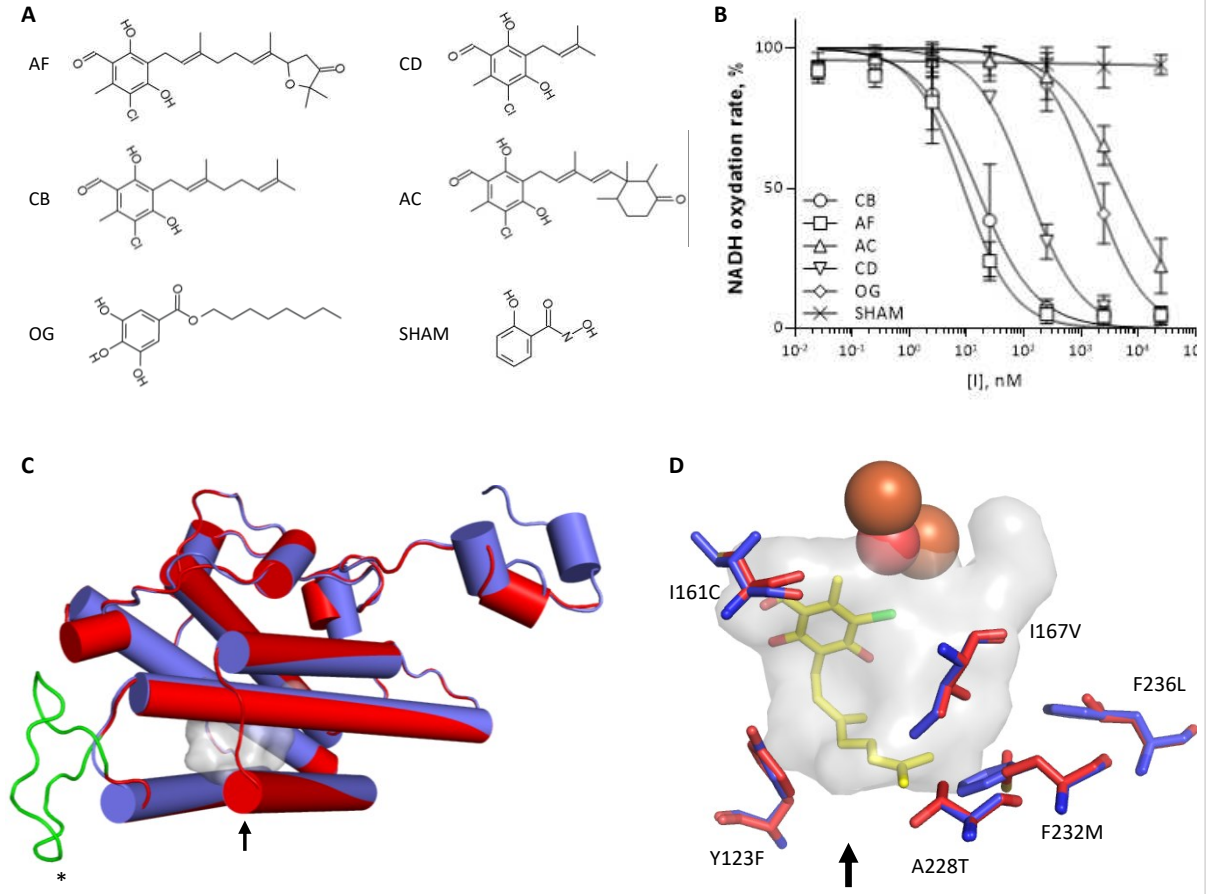

Fig. 2. Structure-activity relationship of MpAOX inhibitors. **(A)** Molecular strucutre of ascofuranone (AF), colletochorin D (CD), colletochlorin B (CB), ascochlorin (AC) octyl gallate (OG) and salycilhydroxamic acid (SHAM). **(B)** Dose-response assay with membrane-bound rMpAOX. Symbols represent the mean and standard deviation of three independent measurements. The continuous line is the best fit of a 4-parameter sigmoid function used to determine IC_{50} values. **(C)** Overview of MpAOX (red; computer-generated) and TAO (bue; PBB ID 3w54) structures. The asterisk marks an insertion of 18 residues in MpAOX (green loop) found in fungal AOXs and likely necessary for activation by GMP. The arrow indicates the entrance to the substrate binding pocket (gray shading) **(D)** Analysis of MpAOX and TAO binding pocket composition. Amino acid residues that are different between those enzymes are shown as red (MpAOX) and blue (TAO) sticks, and listed in **Table 1**. MpAOX residue numbering is used as reference. Yellow sticks depict CB present in the TAO crystal structure, and orange and red spheres represent two Fe^{2+} and one OH^- in TAO.

Table 1. Diference in amino acid composition in the substrate binding pocket between MpAOX and TAO.

MpAOX	TAO
Y123	F99
I161	C119
I167	V125
A228	T186
F232	M190
F236	L194

3.3.rMpAOX purification and kinetic characterization

The purification of his-tagged rMpAOX was performed essentially as described for TAO and SgAOX [11,12]. An initial detergent screening indicated that DDM and FC-12 were the most efficient for membrane protein extraction whilst retaining rMpAOX activity, and those detergents were selected for further evaluation. C12E8, which improved TAO activity when included in the enzyme reaction buffer [11], was also tested. As seen in **Fig. 3A**, using 1% FC-12 during protein solubilization yielded the highest rMpAOX enzymatic activity, regardless of the detergent subsequently used for purification. Based on those results, we selected 1% FC-12 for membrane protein solubilization and 0.05% DDM for downstream steps. Therefore, a highly pure protein of the expected size for the his-tagged rMpAOX construct (40.7 kDa) was seen after SDS-PAGE and was also detected by western blot with an AOX-specific antibody **(Fig 3B)**.

Next, rMpAOX was characterized with respect to ubiquinol-1 (Q_1H_2). A titration of C12E8 in the reaction buffer showed that 0.0125% led to maximal enzymatic activity **(Supplementary fig. S2A)**. Subsequently, the K_M and V_{Max} for rMpAOX and Q_1H_2 were successfully determined as 53.4 ± 6.5 μM and 432.4 ± 19.3 nmol Q_1H_2 min^{-1} mg^{-1} respectively **(Fig. 3C)**. In contrast to results obtained with the membrane-bound rMpAOX, GMP exerted no

effect on this enzyme after solubilization **(Supplementary Fig. S2B)**. This suggests that 1) either the hydrophobic phospholipid environment, or a yet unknown intermediate or interaction partner is required for AOX activation by GMP; or 2) rMpAOX is at maximum capacity and the reaction rate cannot be increased.

The purified rMpAOX was then used to further characterize the inhibition by CB in dose-response assays **(Fig. 3D)**. The IC_{50} of this compound is 59.3 ± 24.4 nM, which is similar to the value observed previously with the membrane-bound enzyme. Since the IC_{50} for CB is within a 10-fold difference with respect to the enzyme concentration (approximately 50 nM), CB was considered a tight binder and the Morrison equation was used to calculate K_I [26], which was determined as 14.8 ± 2.3 nM.

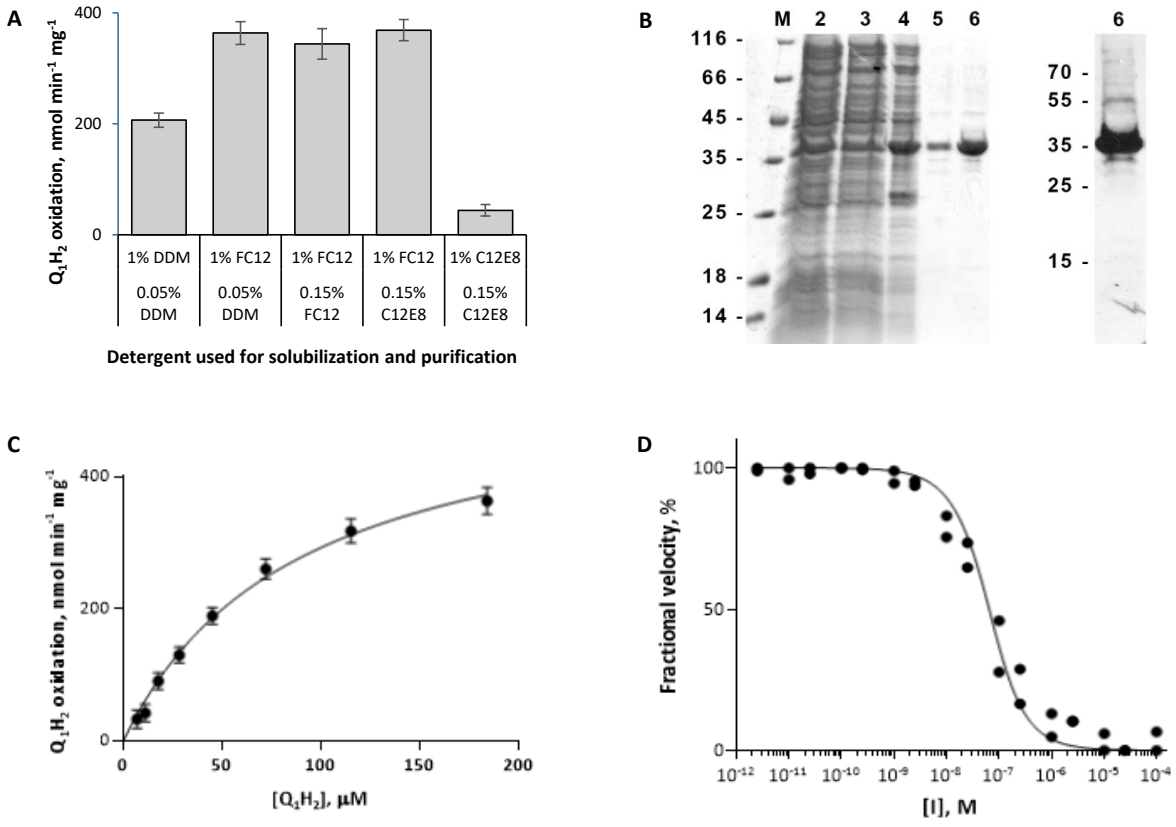

Fig. 3. Purification and kinetic characterization of rMpAOX. **(A)** Effect of detergents DDM, FC12 and C12E8 on pure rMpAOX activity. Each bar depict the Q_1H_2 oxidation rate of rMpAOX purified with the indicated detergents during membrane protein solubilization (top label) and affinity chromatography (bottom label). Membrane protein solubilization with FC12 allowed for the highest rMpAOX activity, regardless of the detergent employed in downstream steps. **(B)** Coomassie-brilliant blue-stained SDS-PAGE (left) and western blot (right) of protein samples collected during rMpAOX purification. M: molecular weight marker; 2: total *E. coli* protein; 3: clarified cell lysate; 4: *E. coli* membrane faction; 5: affinity chromatography flow-through; 6: affinity chromatography eluate. **(C)** Kinetic characterization of rMpAOX with respect to ubiquinol-1 (Q_1H_2). The assay was performed in 50 µL 20 mM tris-HCl buffer with 0.0125% C12E8 and 100 ng rMpAOX. The continuous line is the best fit for the Michaelis-Menten kinetic model. **(D)** Dose response assay with CB and 100 µM Q_1H_2. Points represent two independent measurements and the continuous line is the best fit for the Morrison equation [26].

4. Discussion

For the first time, we present the heterologous expression, purification and kinetic characterization of a fungal AOX. It has been shown that AOXs from other fugal species *Neurospora* are activated by GMP and other nucleotides in the mitochondria [23,27,28], which was also observed here with *E. coli* membrane-bound rMpAOX. Moreover, the fact that AMP induces a greater effect than ADP is in agreement with previous reports. However, GMP activation was abolished after removal of rMpAOX from the cell membrane, suggesting that the hydrophobic environment is required for interaction or that GMP exerts its effect on AOX through an yet unknown intermediate. It is noteworthy that MpAOX, as other fungal AOXs, contains an insertion between α-helices 1 and 2 of approximately 20 amino residues that is proposedly related to GMP activation [28].

Six AOX inhibitors were subjected to dose-response assays on the membrane-bound rMpAOX. SHAM did not show any effect up to 25 μM, which is in accordance with results showing that SHAM has a high IC_{50} on rMpAOX in the milimolar range in intact *E. coli* cells [6]. Interestingly, AF and CB displayed similar relative potencies on rMpAOX, TAO and SgAOX [12,15], with AF being twice as active than CB, as assessed by IC_{50} measurements. On the other hand we have identified key differences in MpAOX that may explain the poorer effect of AC on that enzyme. Namely, amino acid substitutions near the entrance of the ligand pocket that may hinder the interaction of bulkier compounds. This highlights that not only modifications in the aromatic ring may influence protein-ligand interaction, which may be useful to guide the development of selective AOX inhibitors, especially important in agricultural settings where both plant and pathogen contain AOX genes. Additionally, we have previously demonstrated that MpAOX inhibition by *N*-phenylbenzamide derivatives has a protective effect in plants against *M. perniciosa* [6], albeit with a high dosage of 200 μM. Therefore, we expect that AF and CB analogues, which have a much lower IC_{50} on rMpAOX will be more potent antifungal agents against the witches' broom disease of cocoa.

As observed with other AOXs, the selection of the detergent for protein purification is critical to ensure maximal enzymatic activity at the end of the process [11,12]. Here, we demonstrate that FC12 is the best choice for rMpAOX when compared to DDM and C12E8. Other detergents have been tested, but without improvement on yield and activity recovery (data not shown). Moreover, adding 0.0125% C12E8 to the reaction medium increased rMpAOX activity by 3.5 times and allowed the determination of kinetic parameters, in agreement with reports with TAO and SgAOX [11,12].

The specific activity of solubilized rMpAOX has been determined as 432.4 ± 19.3 nmol Q_1H_2 min^{-1} mg^{-1}, which is three orders of magnitude lower than TAO, the fastest AOX identified to date. Indeed, it has been pointed out that fungal AOXs display lower reaction rates than AOXs from other organisms [29]. The rMpAOX K_M for Q_1H_2 is 53.4 ± 6.5 μM and is within the range of values reported for other AOXs [11,12,21,30].

In conclusion, we present insights on inhibitors of a fungal AOX and we hope that our results will aid the development of novel antifungal agents targeted at *M. perniciosa* and other fungal phytopathogens.

5. Acknowledgements

This work was supported by The São Paulo Research Foundation (FAPESP) through research grants 2015/07653-5 and 2016/10498-4, and scholarships 2014/15339-6 and 2017/12852-2. This work was also supported by the National Council for Scientific and Technological Development (CNPq) grant 475535/2013-8 and scholarship 142358/2014-2.

6. Bibliography

[1] L.W. Meinhardt, J. Rincones, B.A. Bailey, M.C. Aime, G.W. Griffith, D. Zhang, G.A.G. Pereira, Moniliophthora perniciosa, the causal agent of witches' broom disease of cacao: what's new from this old foe?, Mol. Plant Pathol. 9 (2008) 577–88. doi:10.1111/j.1364-3703.2008.00496.x.

[2] P.J.P.L. Teixeira, D.P. de T. Thomazella, G.A.G. Pereira, Time for Chocolate: Current Understanding and New Perspectives on Cacao Witches' Broom Disease Research, PLoS Pathog. 11 (2015) e1005130. doi:10.1371/journal.ppat.1005130.

[3] J.M.C. Mondego, M.F. Carazzolle, G.G.L. Costa, E.F. Formighieri, L.P. Parizzi, J. Rincones, C. Cotomacci, D.M. Carraro, A.F. Cunha, H. Carrer, R.O. Vidal, R.C. Estrela, O. García, D.P.T. Thomazella, B. V de Oliveira, A.B. Pires, M.C.S. Do Rio, M.R.R. Araújo, M.H. de Moraes, L.A.B. Castro, K.P. Gramacho, M.S. Gonçalves, J.P.M. Neto, A.G. Neto, L. V Barbosa, M.J. Guiltinan, B.A. Bailey, L.W. Meinhardt, J.C.M. Cascardo, G.A.G. Pereira, A genome survey of Moniliophthora perniciosa gives new insights into Witches' Broom Disease of cacao., BMC Genomics. 9 (2008) 548. doi:10.1186/1471-2164-9-548.

[4] D.P.T. Thomazella, P.J.P.L. Teixeira, H.C. Oliveira, E.E. Saviani, J. Rincones, I.M. Toni, O. Reis, O. Garcia, L.W. Meinhardt, I. Salgado, G. a G. Pereira, The hemibiotrophic cacao pathogen Moniliophthora perniciosa depends on a mitochondrial alternative oxidase for biotrophic development., New Phytol. 194 (2012) 1025–34. doi:10.1111/j.1469-8137.2012.04119.x.

[5] A.L. Moore, T. Shiba, L. Young, S. Harada, K. Kita, K. Ito, Unraveling the heater: new

insights into the structure of the alternative oxidase., Annu. Rev. Plant Biol. 64 (2013) 637–63. doi:10.1146/annurev-arplant-042811-105432.

[6] M.R. Barsottini, B.A. Pires, M.L. Vieira, J.G. Pereira, P.C. Costa, J. Sanitá, A. Coradini, F. Mello, C. Marschalk, E.M. Silva, D. Paschoal, A. Figueira, F.H. Rodrigues, A.T. Cordeiro, P.C. Miranda, P.S. Oliveira, M.L. Sforça, M.F. Carazzolle, S.A. Rocco, G.A. Pereira, Synthesis and testing of novel alternative oxidase (AOX) inhibitors with antifungal activity against Moniliophthora perniciosa (Stahel), the causal agent of witches' broom disease of cocoa, and other phytopathogens, Pest Manag. Sci. (2018). doi:10.1002/ps.5243.

[7] P.M. Wood, D.W. Hollomon, A critical evaluation of the role of alternative oxidase in the performance of strobilurin and related fungicides acting at the Qo site of complex III., Pest Manag. Sci. 59 (2003) 499–511. doi:10.1002/ps.655.

[8] D. Fernández-Ortuño, J.A. Torés, A. de Vicente, A. Pérez-García, Mechanisms of resistance to QoI fungicides in phytopathogenic fungi., Int. Microbiol. 11 (2008) 1–9. doi:10.2436/20.1501.01.38.

[9] J.K. Lang, K. Gohil, L. Packer, Simultaneous determination of tocopherols, ubiquinols, and ubiquinones in blood, plasma, tissue homogenates, and subcellular fractions., Anal. Biochem. 157 (1986) 106–16. doi:10.1016/0003-2697(86)90203-4.

[10] T.N. Petersen, S. Brunak, G. von Heijne, H. Nielsen, SignalP 4.0: discriminating signal peptides from transmembrane regions., Nat. Methods. 8 (2011) 785–6. doi:10.1038/nmeth.1701.

[11] Y. Kido, K. Sakamoto, K. Nakamura, M. Harada, T. Suzuki, Y. Yabu, H. Saimoto, F. Yamakura, D. Ohmori, A. Moore, S. Harada, K. Kita, Purification and kinetic characterization of recombinant alternative oxidase from Trypanosoma brucei brucei., Biochim. Biophys. Acta. 1797 (2010) 443–50. doi:10.1016/j.bbabio.2009.12.021.

[12] C. Elliott, L. Young, B. May, J. Shearman, M.S. Albury, Y. Kido, K. Kita, A.L. Moore, Purification and characterisation of recombinant DNA encoding the alternative oxidase from Sauromatum guttatum, Mitochondrion. 19 (2014) 261–268. doi:10.1016/j.mito.2014.03.002.

[13] U.K. Laemmli, Cleavage of Structural Proteins during the Assembly of the Head of Bacteriophage T4, Nature. 227 (1970) 680–685. doi:10.1038/227680a0.

[14] M.M. Bradford, A rapid and sensitive method for the quantitation of microgram quantities of protein utilizing the principle of protein-dye binding, Anal. Biochem. 72 (1976) 248–254. doi:10.1016/0003-2697(76)90527-3.

[15] H. Saimoto, Y. Kido, Y. Haga, K. Sakamoto, K. Kita, Pharmacophore identification of ascofuranone, potent inhibitor of cyanide-insensitive alternative oxidase of Trypanosoma brucei, J. Biochem. 153 (2013) 267–273. doi:10.1093/jb/mvs135.

[16] A.M. Waterhouse, J.B. Procter, D.M.A. Martin, M. Clamp, G.J. Barton, Jalview Version 2--a multiple sequence alignment editor and analysis workbench, Bioinformatics. 25 (2009) 1189–1191. doi:10.1093/bioinformatics/btp033.

[17] S. Bienert, A. Waterhouse, T.A.P. de Beer, G. Tauriello, G. Studer, L. Bordoli, T. Schwede, The SWISS-MODEL Repository—new features and functionality, Nucleic Acids Res. 45 (2017) D313–D319. doi:10.1093/nar/gkw1132.

[18] T. Shiba, Y. Kido, K. Sakamoto, D.K. Inaoka, C. Tsuge, R. Tatsumi, G. Takahashi, E.O. Balogun, T. Nara, T. Aoki, T. Honma, A. Tanaka, M. Inoue, S. Matsuoka, H. Saimoto, A.L. Moore, S. Harada, K. Kita, Structure of the trypanosome cyanide-insensitive alternative oxidase, Proc. Natl. Acad. Sci. U. S. A. 110 (2013) 4580–4585. doi:10.1073/pnas.1218386110.

[19] S.H. Oliveira, F.A. Ferraz, R. V Honorato, J. Xavier-Neto, T.J. Sobreira, P.S. de Oliveira, KVFinder: steered identification of protein cavities as a PyMOL plugin, BMC Bioinformatics. 15 (2014) 197. doi:10.1186/1471-2105-15-197.

[20] T. Omura, Mitochondria-targeting sequence, a multi-role sorting sequence recognized at all steps of protein import into mitochondria., J. Biochem. 123 (1998) 1010–6. http://www.ncbi.nlm.nih.gov/pubmed/9603986.

[21] G.U. Ebiloma, T.D. Ayuga, E.O. Balogun, L.A. Gil, A. Donachie, M. Kaiser, T. Herraiz, D.K. Inaoka, T. Shiba, S. Harada, K. Kita, H.P. de Koning, C. Dardonville, Inhibition of trypanosome alternative oxidase without its N-terminal mitochondrial targeting signal (ΔMTS-TAO) by cationic and non-cationic 4-hydroxybenzoate and 4-alkoxybenzaldehyde derivatives active against T. brucei and T. congolense, Eur. J. Med. Chem. 150 (2018) 385–402. doi:10.1016/j.ejmech.2018.02.075.

[22] A.L. Umbach, M.A. Gonzàlez-Meler, C.R. Sweet, J.N. Siedow, Activation of the plant mitochondrial alternative oxidase: insights from site-directed mutagenesis, Biochim. Biophys. Acta - Bioenerg. 1554 (2002) 118–128. doi:10.1016/S0005-2728(02)00219-0.

[23] A.G. Medentsev, A.Y. Arinbasarova, V.K. Akimenko, Reactivation of the alternative oxidase of Yarrowia lipolytica by nucleoside monophosphates, FEMS Yeast Res. 5 (2004) 231–236. doi:10.1016/j.femsyr.2004.08.003.

[24] G.U. Ebiloma, T.D. Ayuga, E.O. Balogun, L.A. Gil, A. Donachie, M. Kaiser, T. Herraiz, D.K. Inaoka, T. Shiba, S. Harada, K. Kita, H.P. de Koning, C. Dardonville, Inhibition of trypanosome alternative oxidase without its N-terminal mitochondrial targeting signal (ΔMTS-TAO) by cationic and non-cationic 4-hydroxybenzoate and 4-alkoxybenzaldehyde derivatives active against T. brucei and T. congolense, Eur. J. Med. Chem. 150 (2018) 385–402. doi:10.1016/j.ejmech.2018.02.075.

[25] R.A. West, T. Cunningham, L.E. Pennicott, S.P.S. Rao, S.E. Ward, Toward More Drug Like Inhibitors of Trypanosome Alternative Oxidase, ACS Infect. Dis. 4 (2018) 592–604. doi:10.1021/acsinfecdis.7b00218.

[26] R.A. Copeland, Tight Binding Inhibitors, in: R.A. Copeland (Ed.), Enzym. A Pract. Introd. to Struct. Mech. Data Anal., 2nd ed., John Wiley & Sons, Inc., New York, USA, 2000: pp. 305–317. doi:10.1002/0471220639.ch9.

[27] J. Vanderleyden, E. Van Den Eynde, H. Verachtert, Nature of the effect of adenosine 5'-monophosphate on the cyanide-insensitive respiration in mitochondria of Moniliella tomentosa, Biochem. J. 186 (1980) 309–316. doi:10.1042/bj1860309.

[28] A.L. Umbach, J.N. Siedow, The Cyanide-Resistant Alternative Oxidases from the Fungi Pichia stipitis and Neurospora crassa Are Monomeric and Lack Regulatory Features of the Plant Enzyme, Arch. Biochem. Biophys. 378 (2000) 234–245. doi:10.1006/abbi.2000.1834.

[29] B. May, L. Young, A.L. Moore, Structural insights into the alternative oxidases: are all oxidases made equal?, Biochem. Soc. Trans. 45 (2017) 731–740.

doi:10.1042/BST20160178.

[30] R.A. West, O.G. O'Doherty, T. Askwith, J. Atack, P. Beswick, J. Laverick, M. Paradowski, L.E. Pennicott, S.P.S. Rao, G. Williams, S.E. Ward, African trypanosomiasis: Synthesis & SAR enabling novel drug discovery of ubiquinol mimics for trypanosome alternative oxidase, Eur. J. Med. Chem. 141 (2017) 676–689. doi:10.1016/j.ejmech.2017.09.067.

Supplementary information

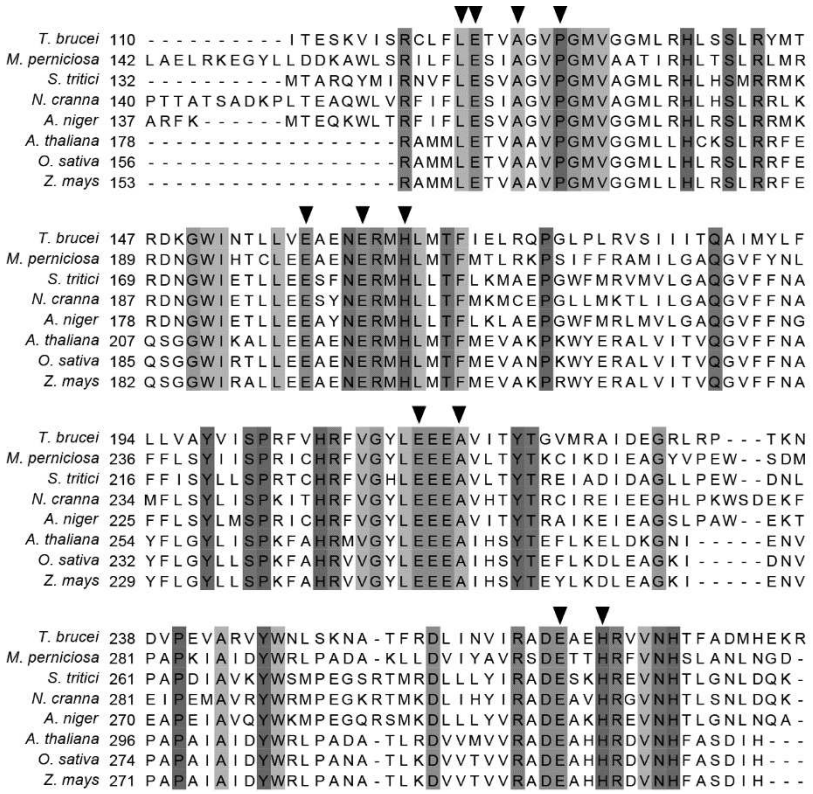

Supplementary fig. S1. Sequence alignment of AOXs from several organisms. Numbers on the left indicate the amino acid numbering for each sequence. Arrows show residues important for substrate binding and coordination of the two ferrous ions in the AOX catalytic site, and shaded regions indicate 100% identity regions.

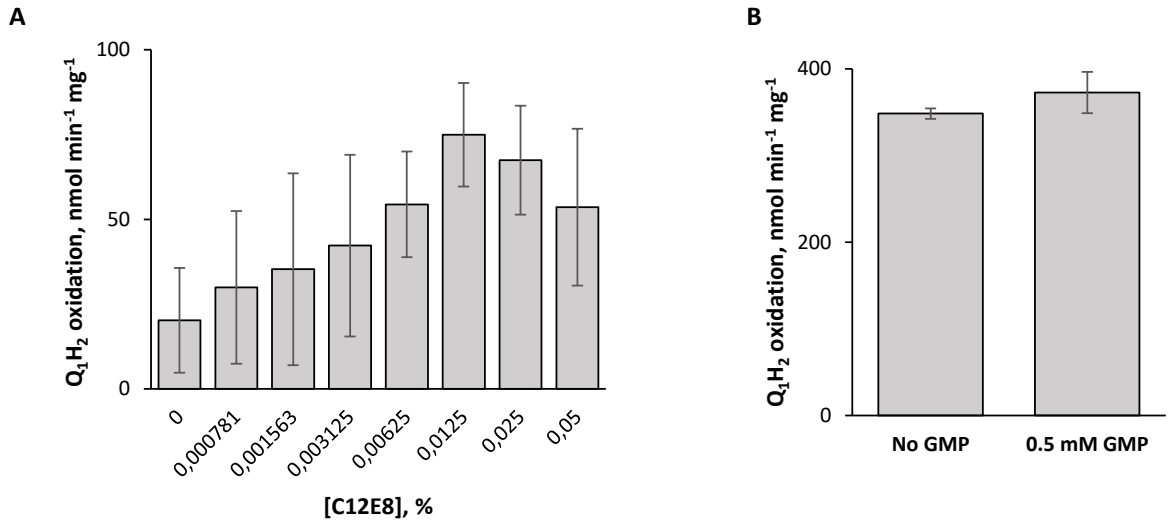

Supplementary fig. S2. Purified rMpAOX enzymatic assays. **(A)** Titration of the detergent C12E8 in reaction buffer. **(B)** Testing of the effect of GMP on purified rMpAOX.

DISCUSSÃO GERAL

A respiração alternativa, historicamente reconhecida como a respiração resistente a inibidores dos complexos III e IV, foi descrita pela primeira vez em 1937 em plantas termogênicas. Em 1971 se identificou a enzima responsável pelo fenômeno e com atividade de oxidase terminal: a AOX [29,140]. Desde então, novas informações sobre a distribuição filogenética da AOX e a função biológica trouxeram crescente interesse para esta enzima, tanto na investigação de aspectos básicos da biologia, quanto em aplicações de cunho tecnológico, tais como desenvolvimento de medicamentos [121,122], melhoramento vegetal para a resistência a estresse biótico e abiótico [141–144], terapia gênica para condições de disfunção mitocondrial [145,146] e de defensivos agrícolas.

Em relação aos fungos fitopatógenos, a AOX ganhou destaque após a identificação do seu papel na resistência a fungicidas. Estrobilurinas são inibidores do complexo III comercializados desde a década de 1990 que alcançaram sucesso mundial como defensivo agrícola. Por exemplo, a azoxistrobina atingiu o patamar de fungicida mais comercializado mundialmente apenas 4 anos após seu lançamento, e em 10 anos as estrobilurinas ocupavam 20% do mercado global de fungicidas. Ou seja, relatos de resistência causam alarde em igual proporção ao sucesso das estrobilurinas [97,147], especialmente quando se trata de fungos que ameçam a segurança alimentar mundial, como *Magnaporthe grisea* [99], *Mycosphaerella graminicola* [100,101], *Sclerotinia sclerotiorum* [102] e *Venturia inaequalis* [103].

Paralelamente, *M. perniciosa* foi o primeiro fitopatógeno no qual a AOX foi associada ao processo infeccioso em si. Similarmente ao observado em *T. brucei*, *M. perniciosa* parece ser exclusivamente dependente da MpAOX durante a colonização do hospedeiro vivo (hifas monocarióticas), o que torna esta enzima um interessante alvo para fungicidas direcionados. Não obstante, a MpAOX também confere resistência às estrobilurinas para *M. perniciosa* [9].

Dada a relevância da AOX de fungos, bem como o potencial impacto econômico e social de um fungicida baseado na inibição desta enzima, este trabalho teve como objetivo gerar informações relevantes para o desenvolvimento de novos inibidores da AOX para o uso em campo. Para tanto, a MpAOX foi escolhida como modelo.

O primeiro capítulo é um manuscrito já aceito para publicação e sintetiza esforços voltados à padronização de novas metodologias úteis para o desenvolvimento, a triagem e a caracterização de novos inibidores da AOX com atividade antifúngica. Em primeiro lugar, a

fácil síntese dos NPD representa uma vantagem em relação aos derivados da ascofuranona. Ademais, a levedura *P. pastoris* demonstrou ser um modelo adequado para a triagem da biblioteca de moléculas sintetizadas, visto que possui uma AOX endógena que suporta o seu crescimento na presença de inibidores da respiração principal. Ademais, foi estabelecido um ensaio miniaturizado capaz de quantificar o crescimento da *P. pastoris*, o que possibilitou a comparação de um grande número de moléculas, seguido da identificação do NPD 7J-41 como um promissor inibidor da AOX e com ação antifúngica. De fato, demonstrou-se que o NPD 7j-41 bloqueia a germinação de esporos de *M. perniciosa* e impede o surgimento de sintomas da VDB *in planta*.

Outro ponto de interesse é o estudo das relações estrutura-atividade dos inibidores da AOX a fim de direcionar o planejamento racional de novas moléculas. A fácil síntese dos NPD permitiu gerar um grande conjunto de moléculas, e os resultados obtidos apoiaram a criação de um modelo computacional de interação proteína-ligante. Observou-se que átomos de halogênio nos NPD favorecem a interação do inibidor com a enzima através da interação com o ferro no sítio ativo, enquanto que grupos doadores de elétrons foram menos potentes. Isto está de acordo com resultados obtidos para derivados da ascofuranona e a AOX de *T. brucei*, sugerindo que a presença de halogênios seja essencial para boa interação entre proteína e ligante [137].

Por outro lado, os valores de IC_{50} da ascofuranona (~10 nM; Capítulo 2) e do NPD 7J-41 (~200 μM; Capítulo 1) denotam uma grande diferença na potência destes dois compostos, sugerindo os NPD possam ser aprimorados. Como o anel benzênico da ascofuranona é totalmente substituído, ao contrário dos NPD, é possível que modificações adicionais nos NPD aumentem sua potência frente à MpAOX e os torne mais eficazes *in vivo*. Por exemplo, na ascofuranona ocorre uma hidroxila na posição *para* em relação ao cloro, a qual também favorece a interação da ascofuranona com a AOX [137].

Já o segundo capítulo apresenta um manuscrito em fase final de preparação que aborda a expressão heteróloga e a caracterização funcional da MpAOX recombinante, juntamente com a caracterização de inibidores da classe da ascofuranona. Dado que a ascofuranona e derivados haviam sido testados apenas na AOX de parasitas e plantas, foi essencial averiguar se estes compostos seriam igualmente ativos sobre a AOX de um fungo. Confirmou-se que a MpAOX é sensível à ascofuranona e a coletoclorina B, condizente com a alta identidade dos resíduos na cavidade hidrofóbica entre a MpAOX e outras AOX. No entanto, houve uma grande divergência em relação à potência da ascoclorina, o que suscitou uma investigação mais detalhada deste fenômeno.

A presença da cicloexanona trissubstituída na cauda isoprênica da ascoclorina afetou a seletividade deste composto entre a MpAOX e a TAO. Após a comparação do sítio de ligação entre ambas AOX, tal divergência é possivelmente decorrente de dois resíduos de aminoácido na entrada da cavidade hidrofóbica da AOX que são mais volumosos na MpAOX do que na TAO. Interessantemente, diferenças na cauda isoprênica também estão associadas à modulação do efeito biológico em outros sistemas. Por exemplo, a ascofuranona é menos tóxica em camundongos do que a ascoclorina e a coletoclorina B, possivelmente devido à interação da ascoclorina e da coletoclorina B com o complexo III da respiração celular [28,148,149].

Nesse sentido, um dos desafios para o desenvolvimento de inibidores seletivos para a AOX é o fato de que outras enzimas mitocondriais têm o ubiquinol como substrato ou produto. Ou seja, há chance de que um inibidor da AOX competitivo para este substrato também interaja com outras enzimas. A ascoclorina e a coletoclorina B se ligam no complexo III eucarioto, bem como com em complexos respiratórios bacterianos [150]. A ascoclorina e a ascofuranona também inibem a diidroorotato desidrogenase humana (hDHODH) [151]; e a ascofuranona age sobre a glicerol-3-fosdato desidrogenase de *T. brucei* [129]. Outros compostos, como a cloroquina, o UHDBT e a auraquina C inibem tanto a AOX como a via principal da respiração quando avaliados em extratos de mitocôndrias [131,132,134].

Paralelamente, há relatos de interação da ascofuranona e da ascoclorina com proteínas que não relacionadas ao ubiquinol. Sabe-se que estas moléculas possuem ação antitumoral, imunossupressora, hipolipidêmica e anti-hipertensiva [152–158]. Estes efeitos estão possivelmente relacionados à ativação do PPARγ, um receptor hormonal nuclear envolvido na diferenciação celular e na regulação do metabolismo energético [159]. Outros análogos da ascoclorina são reconhecidos agonistas de receptores nucleares ou inibidores da enzima testosterona 5α redutase [160,161].

Os NPD ora identificados não são exceção. Por exemplo, fluopyram, flutolanil e benodanil são fungicidas inibidores do complexo II altamente semelhantes ao 7J-41 **(Figura 10)**. A principal diferença é que o anel benzênico ligado ao oxigênio é substituído em *orto* nos inibiores do complexo II, e não em *meta*. Inclusive, esta similaridade pode ter relação com os compostos inespecíficos para a AOX que foram identificados durante a triagem dos derivados de NPD.

Finalmente, outro fator crítico que influencia nas características farmacológicas de um inibidor da AOX é o tamanho da cauda carbônica ligada ao anel benzênico. Derivados da

ascofuranona com uma cadeia carbônica mais longa são mais potentes, conforme observado entre a coletoclorina B e a coletoclorina D neste trabalho, bem como para outros compostos investigados [135,137,139]. Contudo, a alta lipofilicidade necessária para a interação com a TAO pode representar um problema em sistemas *in vivo* devido a problemas relacionados à administração e à distribuição sistêmica de um composto altamente hidrofóbico [126,162].

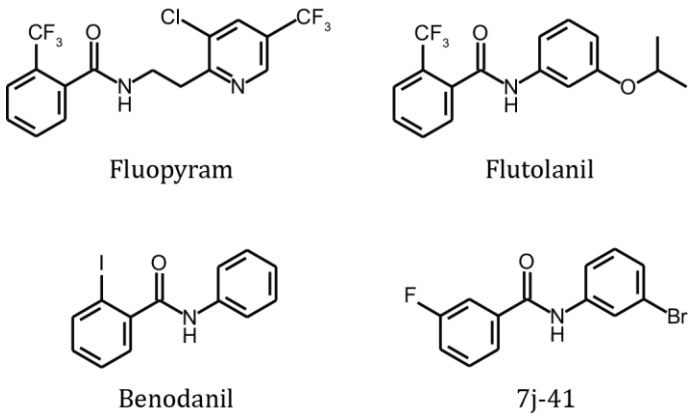

Figura 10. Fungicidas comerciais inibidores do complexo II e o NPD 7j-41. Fonte: *Fungicide Resistance Action Committee* (FRAC, 2018).

CONCLUSÃO

Os objetivos propostos para este trabalho foram alcançados com sucesso. As informações geradas serão fundamentais para o desenvolvimento de novos agentes antifúngicos que atuam sinergisticamente com inibidores da via principal da respiração, para o controle da vassoura de bruxa do cacaueiro, bem como outras doenças que atacam culturas ao redor do mundo, como batata, tomate, café, feijão, soja, frutas cítricas, manga, uva, dentre outras.

Com auxílio da levedura modelo *P. pastoris*, se desenvolveu um novo método para a triagem e caracterização de inibidores da AOX com ação antifúngica. Isto permitiu a identificação de um novo composto ativo contra a AOX: o NPD 7J-41, cuja obtenção é mais fácil e rápida do que os derivados da ascofuranona conhecidos até o momento.

7J-41 inibiu a germinação de esporos de *M. perniciosa* e preveniu o desenvolvimento de sintomas da vassoura de bruxa. Isto representa um importante avanço rumo ao tratamento da VBD e outras doenças causadas por fungos dependentes da AOX.

A MpAOX recombinante foi purificada com sucesso na sua forma ativa, porém o ambiente hidrofóbico (possivelmente a membrana fosfolipídica ou o substrato natural, Q_{10}) é necessário para máxima atividade e para a regulação pós-traducional por GMP.

A ascofuranona e derivados inibem a MpAOX, e a ascoclorina exibiu menor potência entre os compostos testados. Isto é possivelmente atribuído a restrições estéricas impostas pela volumosa cicloexanona ligada à cadeia isoprênica. Este fato será útil para o desenvolvimento de inibidores seletivos entre isoformas da AOX ou entre as AOX de diferentes organismos (por exemplo *M. perniciosa* e o cacaueiro).

PERSPECTIVAS

Frente aos resultados ora apresentados, as próximas etapas poderão abordar:

1. A otimização de inibidores da AOX baseados nos NPD, especialmente direcionados por modelos de interação proteína-ligante gerados com base nos dados ora disponíveis.
2. Confirmar se a fraca interação da ascoclorina com a MpAOX realmente se deve aos resíduos de aminoácido sugeridos (I167 e F232), por exemplo por mutação sítio-dirigida
3. A obtenção da estrutura cristalográfica da MpAOX será de grande valia para o desenho racional de ligantes, bem como poderá trazer luz sobre o mecanismo de ativação por GMP.
4. Averiguar a atividade sobre os NPD e outros inibidores sobre a AOX do cacaueiro, especialmente o transcrito CGD0008991 que foi detectado em todos os tecidos **(Figura 8)**.
5. Avaliar os inibidores da AOX quanto a outros parâmetros de interesse para o uso comercial, como: eficácia de tratamentos preventivo e curativo contra a VDB; toxicidade em plantas e animais; distribuição sistêmica em plantas e animais, permanência no meio-ambiente; permanência em produtos oriundos do cacaueiro; entre outros.

REFERÊNCIAS BIBLIOGRÁFICAS

1. Meinhardt, L.W., Rincones, J., Bailey, B.A., Aime, M.C., Griffith, G.W., Zhang, D., and Pereira, G.A.G. (2008) Moniliophthora perniciosa, the causal agent of witches' broom disease of cacao: what's new from this old foe? *Mol. Plant Pathol.*, **9** (5), 577–88.

2. Hebbar, P.K. (2007) Cacao diseases: a global perspective from an industry point of view. *Phytopathology*, **97** (12), 1658–63.

3. Martins, P.T.. (2007) Os reflexos da crise da lavoura cacueira nos ecossistemas de manguezal do município de Ilhéus, Bahia. *Geogr. – Univ. Estadual Londrina, Dep. Geociências*, **16** (1), 39–50.

4. Griffith, G.W., Nicholson, J., Nenninger, A., Birch, R.N., and Hedger, J.N. (2003) Witches' brooms and frosty pods: Two major pathogens of cacao. *New Zeal. J. Bot.*, **41** (3), 423–435.

5. Purdy, L.H., and Schmidt, R.A. (1996) Status of cacao witches' broom: biology, epidemiology, and management. *Annu. Rev. Phytopathol.*, **34**, 573–94.

6. de Oliveira Ceita, G., Macêdo, J.N.A., Santos, T.B., Alemanno, L., da Silva Gesteira, A., Micheli, F., Mariano, A.C., Gramacho, K.P., da Costa Silva, D., Meinhardt, L., Mazzafera, P., Pereira, G.A.G., and de Mattos Cascardo, J.C. (2007) Involvement of calcium oxalate degradation during programmed cell death in Theobroma cacao tissues triggered by the hemibiotrophic fungus Moniliophthora perniciosa. *Plant Sci.*, **173** (2), 106–117.

7. Zaparoli, G., Barsottini, M.R. de O., de Oliveira, J.F., Dyszy, F., Teixeira, P.J.P.L., Barau, J.G., Garcia, O., Costa-Filho, A.J., Ambrosio, A.L.B., Pereira, G.A.G., and Dias, S.M.G. (2011) The Crystal Structure of Necrosis- and Ethylene-Inducing Protein 2 from the Causal Agent of Cacao's Witches' Broom Disease Reveals Key Elements for Its Activity. *Biochemistry*, **50** (45), 9901–9910.

8. Barau, J., Grandis, A., Carvalho, V.M.D.A., Teixeira, G.S., Zaparoli, G.H.A., do Rio, M.C.S., Rincones, J., Buckeridge, M.S., and Pereira, G.A.G. (2015) Apoplastic and intracellular plant sugars regulate developmental transitions in witches' broom disease of cacao. *J. Exp. Bot.*, **66** (5), 1325–1337.

9. Thomazella, D.P.T., Teixeira, P.J.P.L., Oliveira, H.C., Saviani, E.E., Rincones, J., Toni, I.M., Reis, O., Garcia, O., Meinhardt, L.W., Salgado, I., and Pereira, G. a G. (2012) The hemibiotrophic cacao pathogen Moniliophthora perniciosa depends on a mitochondrial alternative oxidase for biotrophic development. *New Phytol.*, **194** (4), 1025–34.

10. Sellem, C.H., Bovier, E., Lorin, S., and Sainsard-Chanet, A. (2009) Mutations in Two Zinc-Cluster Proteins Activate Alternative Respiratory and Gluconeogenic Pathways and Restore Senescence in Long-Lived Respiratory Mutants of Podospora anserina. *Genetics*, **182** (1), 69–78.

11. Fioravanti, C.H., and Velho, L. (2011) Fungos, fazendeiros e cientistas em luta contra a vassoura-de-bruxa. *Sociologias*, **13** (27), 256–283.

12. Medeiros, F.H.V., Pomella, A.W.V., de Souza, J.T., Niella, G.R., Valle, R., Bateman, R.P., Fravel, D., Vinyard, B., and Hebbar, P.K. (2010) A novel, integrated method for management of witches' broom disease in Cacao in Bahia, Brazil. *Crop Prot.*, **29** (7), 704–711.

13. Mondego, J.M.C., Carazzolle, M.F., Costa, G.G.L., Formighieri, E.F., Parizzi, L.P., Rincones, J., Cotomacci, C., Carraro, D.M., Cunha, A.F., Carrer, H., Vidal, R.O., Estrela, R.C., García, O., Thomazella, D.P.T., de Oliveira, B. V, Pires, A.B., Rio, M.C.S. Do, Araújo, M.R.R., de Moraes, M.H., Castro, L.A.B., Gramacho, K.P., Gonçalves, M.S., Neto, J.P.M., Neto, A.G., Barbosa, L. V, Guiltinan, M.J., Bailey, B.A., Meinhardt, L.W., Cascardo, J.C.M., and Pereira, G.A.G. (2008) A genome survey of Moniliophthora perniciosa gives new insights into Witches' Broom Disease of cacao. *BMC Genomics*, **9**, 548.

14. Teixeira, P.J.P.L., Thomazella, D.P. de T., Reis, O., do Prado, P.F.V., do Rio, M.C.S., Fiorin, G.L., José, J., Costa, G.G.L., Negri, V.A., Mondego, J.M.C., Mieczkowski, P., and Pereira, G.A.G. (2014) High-Resolution Transcript Profiling of the Atypical Biotrophic Interaction between Theobroma cacao and the Fungal Pathogen Moniliophthora perniciosa. *Plant Cell*, **26** (11), 4245–4269.

15. Engelbrecht, C.J., Harrington, T.C., and Alfenas, A. (2007) Ceratocystis wilt of cacao-a disease of increasing importance. *Phytopathology*, **97** (12), 1648–1649.

16. Silva, S.D.V.M., Pinto, L.R.M., Oliveira, B.F. De, Damaceno, V.O., Pires, J.L., and Dias, C.T. dos S. (2012) Resistência de progênies de cacaueiro à murcha-de-

Ceratocystis. *Trop. Plant Pathol.*, **37** (3), 191–195.

17. Santos, R.M.F., Silva, S.D.V.M., Sena, K., Micheli, F., and Gramacho, K.P. (2013) Kinetics and Histopathology of the Cacao-Ceratocystis cacaofunesta Interaction. *Trop. Plant Biol.*, **6** (1), 37–45.

18. Nelson, D.L., and Cox, M.M. (2004) Oxidative Phosphorylation and Photophosphorylation, in *Lehninger Principles of Biochemistry*, 4thed., New York, pp. 690–750.

19. McDonald, A.E., and Gospodaryov, D. V. (2018) Alternative NAD(P)H dehydrogenase and alternative oxidase: Proposed physiological roles in animals. *Mitochondrion*.

20. Takaya, N. (2003) Hybrid Respiration in the Denitrifying Mitochondria of Fusarium oxysporum. *J. Biochem.*, **133** (4), 461–465.

21. Uchimura, H., Enjoji, H., Seki, T., Taguchi, A., Tsakaya, N., and Shoun+, H. (2002) Nitrate Reductase-Formate Dehydrogenase Couple Involved in the Fungal Denitrification by Fusarium oxysporum. *J. Biochem.*, **131** (4), 579–586.

22. Ma, W.K., Farrell, R.E., and Siciliano, S.D. (2008) Soil Formate Regulates the Fungal Nitrous Oxide Emission Pathway. *Appl. Environ. Microbiol.*, **74** (21), 6690–6696.

23. McDonald, A.E., and Vanlerberghe, G.C. (2006) Origins, evolutionary history, and taxonomic distribution of alternative oxidase and plastoquinol terminal oxidase. *Comp. Biochem. Physiol. Part D Genomics Proteomics*, **1** (3), 357–364.

24. McDonald, A.E. (2008) Alternative oxidase: an inter-kingdom perspective on the function and regulation of this broadly distributed “cyanide-resistant” terminal oxidase. *Funct. Plant Biol.*, **35** (7), 535.

25. McDonald, A.E. (2009) Alternative oxidase: What information can protein sequence comparisons give us? *Physiol. Plant.*, **137** (4), 328–341.

26. Nargang, F.E., Adames, K., Rüb, C., Cheung, S., Easton, N., Nargang, C.E., and Chae, M.S. (2012) Identification of Genes Required for Alternative Oxidase Production in the Neurospora crassa Gene Knockout Library. *G3 Genes|Genomes|Genetics*, **2** (11), 1345–1356.

27. Siedow, J.N., Umbach, A.L., and Moore, A.L. (1995) The active site of the cyanide-

resistant oxidase from plant mitochondria contains a binuclear iron center. *FEBS Lett.*, **362** (1), 10–14.

28. Shiba, T., Kido, Y., Sakamoto, K., Inaoka, D.K., Tsuge, C., Tatsumi, R., Takahashi, G., Balogun, E.O., Nara, T., Aoki, T., Honma, T., Tanaka, A., Inoue, M., Matsuoka, S., Saimoto, H., Moore, A.L., Harada, S., and Kita, K. (2013) Structure of the trypanosome cyanide-insensitive alternative oxidase. *Proc. Natl. Acad. Sci. U. S. A.*, **110** (12), 4580–4585.

29. Moore, A.L., Shiba, T., Young, L., Harada, S., Kita, K., and Ito, K. (2013) Unraveling the heater: new insights into the structure of the alternative oxidase. *Annu. Rev. Plant Biol.*, **64**, 637–63.

30. Young, L., May, B., Pendlebury-Watt, A., Shearman, J., Elliott, C., Albury, M.S., Shiba, T., Inaoka, D.K., Harada, S., Kita, K., and Moore, A.L. (2014) Probing the ubiquinol-binding site of recombinant Sauromatum guttatum alternative oxidase expressed in E. coli membranes through site-directed mutagenesis. *Biochim. Biophys. Acta - Bioenerg.*, **1837** (7), 1219–1225.

31. Fukai, Y., Amino, H., Hirawake, H., Yabu, Y., Ohta, N., Minagawa, N., Sakajo, S., Yoshimoto, A., Nagai, K., Takamiya, S., Kojima, S., and Kita, K. (1999) Functional expression of the ascofuranone-sensitive Trypanosoma brucei brucei alternative oxidase in the cytoplasmic membrane of Escherichia coli. *Comp. Biochem. Physiol. Part C Pharmacol. Toxicol. Endocrinol.*, **124** (2), 141–148.

32. Kido, Y., Sakamoto, K., Nakamura, K., Harada, M., Suzuki, T., Yabu, Y., Saimoto, H., Yamakura, F., Ohmori, D., Moore, A., Harada, S., and Kita, K. (2010) Purification and kinetic characterization of recombinant alternative oxidase from Trypanosoma brucei brucei. *Biochim. Biophys. Acta - Bioenerg.*, **1797** (4), 443–450.

33. Elliott, C., Young, L., May, B., Shearman, J., Albury, M.S., Kido, Y., Kita, K., and Moore, A.L. (2014) Purification and characterisation of recombinant DNA encoding the alternative oxidase from Sauromatum guttatum. *Mitochondrion*, **19**, 261–268.

34. Rich, P.R. (1978) Quinol oxidation in Arum maculatum mitochondria and its application to the assay, solubilisation and partial purification of the alternative oxidase. *FEBS Lett.*, **96** (2), 252–256.

35. May, B., Young, L., and Moore, A.L. (2017) Structural insights into the alternative

oxidases: are all oxidases made equal? *Biochem. Soc. Trans.*, **45** (3), 731–740.

36. Gelhaye, E., Rouhier, N., Gerard, J., Jolivet, Y., Gualberto, J., Navrot, N., Ohlsson, P.-I., Wingsle, G., Hirasawa, M., Knaff, D.B., Wang, H., Dizengremel, P., Meyer, Y., and Jacquot, J.-P. (2004) A specific form of thioredoxin h occurs in plant mitochondria and regulates the alternative oxidase. *Proc. Natl. Acad. Sci. U. S. A.*, **101** (40), 14545–14550.

37. Marti, M.C., Olmos, E., Calvete, J.J., Diaz, I., Barranco-Medina, S., Whelan, J., Lazaro, J.J., Sevilla, F., and Jimenez, A. (2009) Mitochondrial and Nuclear Localization of a Novel Pea Thioredoxin: Identification of Its Mitochondrial Target Proteins. *Plant Physiol.*, **150** (2), 646–657.

38. Umbach, A.L., and Siedow, J.N. (1993) Covalent and Noncovalent Dimers of the Cyanide-Resistant Alternative Oxidase Protein in Higher Plant Mitochondria and Their Relationship to Enzyme Activity. *Plant Physiol.*, **103** (3), 845–854.

39. Umbach, A.L., and Siedow, J.N. (2000) The Cyanide-Resistant Alternative Oxidases from the Fungi Pichia stipitis and Neurospora crassa Are Monomeric and Lack Regulatory Features of the Plant Enzyme. *Arch. Biochem. Biophys.*, **378** (2), 234–245.

40. Umbach, A.L., Gonzàlez-Meler, M.A., Sweet, C.R., and Siedow, J.N. (2002) Activation of the plant mitochondrial alternative oxidase: insights from site-directed mutagenesis. *Biochim. Biophys. Acta - Bioenerg.*, **1554** (1–2), 118–128.

41. Jarmuszkiewicz, W., Wagner, A.M., Wagner, M.J., and Hryniewiecka, L. (1997) Immunological identification of the alternative oxidase of Acanthamoeba castellanii mitochondria. *FEBS Lett.*, **411** (1), 110–114.

42. Vanlerberghe, G.C. (1998) Molecular Localization of a Redox-Modulated Process Regulating Plant Mitochondrial Electron Transport. *Plant Cell*, **10** (9), 1551–1560.

43. Rhoads, D.M., Umbach, a. L., Sweet, C.R., Lennon, a. M., Rauch, G.S., and Siedow, J.N. (1998) Regulation of the Cyanide-resistant Alternative Oxidase of Plant Mitochondria: Identification of the Cysteine Residue Involved in -Keto Acid Stimulation and Intersubunit Disulfide Bond Formation. *J. Biol. Chem.*, **273** (46), 30750–30756.

44. Umbach, A.L., Wiskich, J.T., and Siedow, J.N. (1994) Regulation of alternative oxidase kinetics by pyruvate and intermolecular disulfide bond redox status in soybean seedling mitochondria. *FEBS Lett.*, **348** (2), 181–184.

45. Umbach, A.L., Ng, V.S., and Siedow, J.N. (2006) Regulation of plant alternative oxidase activity: A tale of two cysteines. *Biochim. Biophys. Acta - Bioenerg.*, **1757** (2), 135–142.

46. Crichton, P.G., Albury, M.S., Affourtit, C., and Moore, A.L. (2010) Mutagenesis of the Sauromatum guttatum alternative oxidase reveals features important for oxygen binding and catalysis. *Biochim. Biophys. Acta - Bioenerg.*, **1797** (6–7), 732–737.

47. Crichton, P.G., Affourtit, C., Albury, M.S., Carré, J.E., and Moore, A.L. (2005) Constitutive activity of Sauromatum guttatum alternative oxidase in Schizosaccharomyces pombe implicates residues in addition to conserved cysteines in α-keto acid activation. *FEBS Lett.*, **579** (2), 331–336.

48. Djajanegara, I., Holtzapffel, R., Finnegan, P.M., Hoefnagel, M.H.N., Berthold, D.A., Wiskich, J.T., and Day, D.A. (1999) A single amino acid change in the plant alternative oxidase alters the specificity of organic acid activation. *FEBS Lett.*, **454** (3), 220–224.

49. Holtzapffel, R.C., Castelli, J., Finnegan, P.M., Millar, A.H., Whelan, J., and Day, D.A. (2003) A tomato alternative oxidase protein with altered regulatory properties. *Biochim. Biophys. Acta - Bioenerg.*, **1606** (1–3), 153–162.

50. Yukioka, H., Inagaki, S., Tanaka, R., Katoh, K., Miki, N., Mizutani, A., and Masuko, M. (1998) Transcriptional activation of the alternative oxidase gene of the fungus *Magnaporthe grisea* by a respiratory-inhibiting fungicide and hydrogen peroxide. *Biochim. Biophys. Acta*, **1442** (2–3), 161–169.

51. Sakajo, S., Minagawa, N., and Yoshimoto, A. (1997) Effects of Nucleotides on Cyanide-resistant Respiratory Activity in Mitochondria Isolated from Antimycin A-treated Yeast Hansenula anomala. *Biosci. Biotechnol. Biochem.*, **61** (2), 396–399.

52. Milani, G., Jarmuszkiewicz, W., Sluse-Goffart, C.M., Schreiber, A.Z., Vercesi, A.E., and Sluse, F.E. (2001) Respiratory chain network in mitochondria of Candida parapsilosis : ADP/O appraisal of the multiple electron pathways. *FEBS Lett.*, **508** (2), 231–235.

53. Medentsev, A.G., Arinbasarova, A.Y., and Akimenko, V.K. (2004) Reactivation of the alternative oxidase of Yarrowia lipolytica by nucleoside monophosphates. *FEMS Yeast Res.*, **5** (3), 231–236.

54. Vanderleyden, J., Peeters, C., Verachtert, H., and Bertrand, H. (1980) Stimulation of the alternative oxidase of Neurospora crassa by Nucleoside phosphates. *Biochem. J.*, **188**

(1), 141–144.

55. Sierra-Campos, E., Velázquez, I., Matuz-Mares, D., Villavicencio-Queijeiro, A., and Pardo, J.P. (2009) Functional properties of the Ustilago maydis alternative oxidase under oxidative stress conditions. *Mitochondrion*, **9** (2), 96–102.

56. Vanderleyden, J., Van Den Eynde, E., and Verachtert, H. (1980) Nature of the effect of adenosine 5'-monophosphate on the cyanide-insensitive respiration in mitochondria of Moniliella tomentosa. *Biochem. J.*, **186** (1), 309–316.

57. Doussière, J., and Vignais, P. V (1984) AMP-dependence of the cyanide-insensitive pathway in the respiratory chain of Paramecium tetraurelia. *Biochem. J.*, **220** (3), 787–794.

58. Sharpless, T.K., and Butow, R.A. (1970) An inducible alternate terminal oxidase in Euglena gracilis mitochondria. *J. Biol. Chem.*, **245** (1), 58–70.

59. Dry, I.B., Moore, A.L., Day, D.A., and Wiskich, J.T. (1989) Regulation of alternative pathway activity in plant mitochondria: Nonlinear relationship between electron flux and the redox poise of the quinone pool. *Arch. Biochem. Biophys.*, **273** (1), 148–157.

60. Moore, A.L., Dry, I.B., and Wiskich, J.T. (1988) Measurement of the redox state of the ubiquinone pool in plant mitochondria. *FEBS Lett.*, **235** (1–2), 76–80.

61. Meeuse, B.J.D. (1975) Thermogenic Respiration in Aroids. *Annu. Rev. Plant Physiol.*, **26** (1), 117–126.

62. Ito, K., Ogata, T., Kakizaki, Y., Elliott, C., Albury, M.S., and Moore, A.L. (2011) Identification of a Gene for Pyruvate-Insensitive Mitochondrial Alternative Oxidase Expressed in the Thermogenic Appendices in Arum maculatum. *Plant Physiol.*, **157** (4), 1721–1732.

63. Bovier, E., Sellem, C.H., Humbert, A., and Sainsard-Chanet, A. (2014) Genetic and Functional Investigation of Zn 2 Cys 6 Transcription Factors RSE2 and RSE3 in Podospora anserina. *Eukaryot. Cell*, **13** (1), 53–65.

64. Chae, M.S., Nargang, C.E., Cleary, I.A., Lin, C.C., Todd, A.T., and Nargang, F.E. (2007) Two Zinc-Cluster Transcription Factors Control Induction of Alternative Oxidase in Neurospora crassa. *Genetics*, **177** (4), 1997–2006.

65. Qi, Z., Smith, K.M., Bredeweg, E.L., Bosnjak, N., Freitag, M., and Nargang, F.E. (2017) Alternative Oxidase Transcription Factors AOD2 and AOD5 of Neurospora crassa Control the Expression of Genes Involved in Energy Production and Metabolism. *G3 Genes|Genomes|Genetics*, **7** (2), 449–466.

66. Suzuki, Y., Murray, S.L., Wong, K.H., Davis, M.A., and Hynes, M.J. (2012) Reprogramming of carbon metabolism by the transcriptional activators AcuK and AcuM in Aspergillus nidulans. *Mol. Microbiol.*, **84** (5), 942–964.

67. Vanlerberghe, G.C., and Mclntosh, L. (1996) Signals Regulating the Expression of the Nuclear Gene Encoding Alternative Oxidase of Plant Mitochondria. *Plant Physiol.*, **111** (2), 589–595.

68. Selinski, J., Hartmann, A., Kordes, A., Deckers-Hebestreit, G., Whelan, J., and Scheibe, R. (2017) Analysis of Posttranslational Activation of Alternative Oxidase Isoforms. *Plant Physiol.*, **174** (4), 2113–2127.

69. Leiter, É., Park, H.-S., Kwon, N.-J., Han, K.-H., Emri, T., Oláh, V., Mészáros, I., Dienes, B., Vincze, J., Csernoch, L., Yu, J.-H., and Pócsi, I. (2016) Characterization of the aodA, dnmA, mnSOD and pimA genes in Aspergillus nidulans. *Sci. Rep.*, **6** (1), 20523.

70. Molnár, Á.P., Németh, Z., Fekete, E., Flipphi, M., Keller, N.P., and Karaffa, L. (2018) Analysis of the relationship between alternative respiration and sterigmatocystin formation in Aspergillus nidulans. *Toxins (Basel).*, **10** (4).

71. Karaffa, L., Sándor, E., Kozma, J., Kubicek, C.P., and Szentirmai, A. (1999) The role of the alternative respiratory pathway in the stimulation of cephalosporin C formation by soybean oil in Acremonium chrysogenum. *Appl. Microbiol. Biotechnol.*, **51** (5), 633–638.

72. Cvetkovska, M., and Vanlerberghe, G.C. (2012) Alternative oxidase modulates leaf mitochondrial concentrations of superoxide and nitric oxide. *New Phytol.*, **195** (1), 32–39.

73. Kern, A., Hartner, F.S., Freigassner, M., Spielhofer, J., Rumpf, C., Leitner, L., Frohlich, K.-U., and Glieder, A. (2007) Pichia pastoris “just in time” alternative respiration. *Microbiology*, **153** (4), 1250–1260.

74. El-Osta, H., and Circu, M.L. (2016) Mitochondrial ROS and Apoptosis, in

Mitochondrial Mechanisms of Degeneration and Repair in Parkinson's Disease, Springer International Publishing, Cham, pp. 1–23.

75. Maxwell, D.P., Nickels, R., and McIntosh, L. (2002) Evidence of mitochondrial involvement in the transduction of signals required for the induction of genes associated with pathogen attack and senescence. *Plant J.*, **29** (3), 269–279.

76. Norman, C. (2004) Salicylic Acid Is an Uncoupler and Inhibitor of Mitochondrial Electron Transport. *Plant Physiol.*, **134** (1), 492–501.

77. Xie, Z., and Chen, Z. (1999) Salicylic Acid Induces Rapid Inhibition of Mitochondrial Electron Transport and Oxidative Phosphorylation in Tobacco Cells. *Plant Physiol.*, **120** (1), 217–226.

78. Polidoros, A.N., Mylona, P. V., Pasentsis, K., Scandalios, J.G., and Tsaftaris, A.S. (2005) The maize alternative oxidase 1a (Aox1a) gene is regulated by signals related to oxidative stress. *Redox Rep.*, **10** (2), 71–78.

79. Simons, B.H., Millenaar, F.F., Mulder, L., Van Loon, L.C., and Lambers, H. (1999) Enhanced Expression and Activation of the Alternative Oxidase during Infection of Arabidopsis with Pseudomonas syringae pv tomato. *Plant Physiol.*, **120** (2), 529–538.

80. Lennon, A.M., Neuenschwander, U.H., Ribas-Carbo, M., Giles, L., Ryals, J.A., and Siedow, J.N. (1997) The Effects of Salicylic Acid and Tobacco Mosaic Virus Infection on the Alternative Oxidase of Tobacco. *Plant Physiol.*, **115** (2), 783–791.

81. Chivasa, S. (1997) Salicylic Acid Interferes with Tobacco Mosaic Virus Replication via a Novel Salicylhydroxamic Acid-Sensitive Mechanism. *Plant Cell*, **9** (4), 547–557.

82. Chivasa, S. (1998) Cyanide Restores N GeneMediated Resistance to Tobacco Mosaic Virus in Transgenic Tobacco Expressing Salicylic Acid Hydroxylase. *Plant Cell*, **10** (9), 1489–1498.

83. Shkolnik-Inbar, D., and Bar-Zvi, D. (2011) Expression of ABSCISIC ACID INSENSITIVE 4 (ABI4) in developing Arabidopsis seedlings. *Plant Signal. Behav.*, **6** (5), 694–696.

84. Takumi, S., Tomioka, M., Eto, K., Naydenov, N., and Nakamura, C. (2002) Characterization of two non-homoeologous nuclear genes encoding mitochondrial alternative oxidase in common wheat. *Genes Genet. Syst.*, **77** (2), 81–88.

85. Giraud, E., Ho, L.H.M., Clifton, R., Carroll, A., Estavillo, G., Tan, Y.-F., Howell, K.A., Ivanova, A., Pogson, B.J., Millar, A.H., and Whelan, J. (2008) The Absence of ALTERNATIVE OXIDASE1a in Arabidopsis Results in Acute Sensitivity to Combined Light and Drought Stress. *Plant Physiol.*, **147** (2), 595–610.

86. Costa, J.H., Jolivet, Y., Hasenfratz-Sauder, M.-P., Orellano, E.G., da Guia Silva Lima, M., Dizengremel, P., and Fernandes de Melo, D. (2007) Alternative oxidase regulation in roots of Vigna unguiculata cultivars differing in drought/salt tolerance. *J. Plant Physiol.*, **164** (6), 718–727.

87. Yip, J.Y.H., and Vanlerberghe, G.C. (2001) Mitochondrial alternative oxidase acts to dampen the generation of active oxygen species during a period of rapid respiration induced to support a high rate of nutrient uptake. *Physiol. Plant.*, **112** (3), 327–333.

88. Pasqualini, S., Paolocci, F., Borgogni, A., Morettini, R., and Ederli, L. (2007) The overexpression of an alternative oxidase gene triggers ozone sensitivity in tobacco plants. *Plant, Cell Environ.*, **30** (12), 1545–1556.

89. Clifton, R., Millar, A.H., and Whelan, J. (2006) Alternative oxidases in Arabidopsis: A comparative analysis of differential expression in the gene family provides new insights into function of non-phosphorylating bypasses. *Biochim. Biophys. Acta - Bioenerg.*, **1757** (7), 730–741.

90. Saika, H., Ohtsu, K., Hamanaka, S., Nakazono, M., Tsutsumi, N., and Hirai, A. (2002) AOX1c, a novel rice gene for alternative oxidase; comparison with rice AOX1a and AOX1b. *Genes Genet. Syst.*, **77** (1), 31–38.

91. Saisho, D., Nakazono, M., Lee, K.-H., Tsutsumi, N., Akita, S., and Hirai, A. (2001) The gene for alternative oxidase-2 (AOX2) from Arabidopsis thaliana consists of five exons unlike other AOX genes and is transcribed at an early stage during germination. *Genes Genet. Syst.*, **76** (2), 89–97.

92. Finnegan, P.M., Whelan, J., Millar, A.H., Zhang, Q., Smith, M.K., Wiskich, J.T., and Day, D.A. (1997) Differential Expression of the Multigene Family Encoding the Soybean Mitochondrial Alternative Oxidase. *Plant Physiol.*, **114** (2), 455–466.

93. McCabe, T.C., Finnegan, P.M., Harvey Millar, A., Day, D.A., and Whelan, J. (1998) Differential Expression of Alternative Oxidase Genes in Soybean Cotyledons during Postgerminative Development. *Plant Physiol.*, **118** (2), 675–682.

94. Karpova, O. V. (2002) Differential Expression of Alternative Oxidase Genes in Maize Mitochondrial Mutants. *Plant Cell*, **14** (12), 3271–3284.

95. Rogov, A.G., Sukhanova, E.I., Uralskaya, L.A., Aliverdieva, D.A., and Zvyagilskaya, R.A. (2014) Alternative oxidase: Distribution, induction, properties, structure, regulation, and functions. *Biochem.*, **79** (13), 1615–1634.

96. Vanlerberghe, G. (2013) Alternative Oxidase: A Mitochondrial Respiratory Pathway to Maintain Metabolic and Signaling Homeostasis during Abiotic and Biotic Stress in Plants. *Int. J. Mol. Sci.*, **14** (4), 6805–6847.

97. Wood, P.M., and Hollomon, D.W. (2003) A critical evaluation of the role of alternative oxidase in the performance of strobilurin and related fungicides acting at the Qo site of Complex III. *Pest Manag. Sci.*, **59** (5), 499–511.

98. Fernández-Ortuño, D., Torés, J.A., de Vicente, A., and Pérez-García, A. (2008) Mechanisms of resistance to QoI fungicides in phytopathogenic fungi. *Int. Microbiol.*, **11** (1), 1–9.

99. Avila-Adame, C., and Köller, W. (2002) Disruption of the alternative oxidase gene in Magnaporthe grisea and its impact on host infection. *Mol. plant-microbe Interact.*, **15** (5), 493–500.

100. Affourtit, C., Heaney, S.P., and Moore, A.L. (2000) Mitochondrial electron transfer in the wheat pathogenic fungus Septoria tritici: on the role of alternative respiratory enzymes in fungicide resistance. *Biochim. Biophys. Acta - Bioenerg.*, **1459** (2–3), 291–298.

101. Miguez, M., Reeve, C., Wood, P.M., and Hollomon, D.W. (2004) Alternative oxidase reduces the sensitivity of Mycosphaerella graminicola to QOI fungicides. *Pest Manag. Sci.*, **60** (1), 3–7.

102. Xu, T., Wang, Y.-T., Liang, W.-S., Yao, F., Li, Y.-H., Li, D.-R., Wang, H., and Wang, Z.-Y. (2013) Involvement of alternative oxidase in the regulation of sensitivity of Sclerotinia sclerotiorum to the fungicides azoxystrobin and procymidone. *J. Microbiol.*, **51** (3), 352–358.

103. Olaya, G., Zheng, D., and Köller, W. (1998) Differential responses of germinating Venturia inaequalis conidia to kresoxim-methyl. *Pestic. Sci.*, **54** (3), 230–236.

104. Barsottini, M.R., Pires, B.A., Vieira, M.L., Pereira, J.G., Costa, P.C., Sanitá, J., Coradini, A., Mello, F., Marschalk, C., Silva, E.M., Paschoal, D., Figueira, A., Rodrigues, F.H., Cordeiro, A.T., Miranda, P.C., Oliveira, P.S., Sforça, M.L., Carazzolle, M.F., Rocco, S.A., and Pereira, G.A. (2018) Synthesis and testing of novel alternative oxidase (AOX) inhibitors with antifungal activity against Moniliophthora perniciosa (Stahel), the causal agent of witches' broom disease of cocoa, and other phytopathogens. *Pest Manag. Sci.*

105. Joseph-Horne, T., Wood, P.M., Wood, C.K., Moore, A.L., Headrick, J., and Hollomon, D. (1998) Characterization of a split respiratory pathway in the wheat "take-all" fungus, Gaeumannomyces graminis var. tritici. *J. Biol. Chem.*, **273** (18), 11127–11133.

106. Walker, A.-S., Auclair, C., Gredt, M., and Leroux, P. (2009) First occurrence of resistance to strobilurin fungicides in Microdochium nivale and Microdochium majus from French naturally infected wheat grains. *Pest Manag. Sci.*, **65** (8), 906–915.

107. Hayashi, K., Watanabe, M., Tanaka, T., and Uesugi, Y. (1996) Cyanide-insensitive Respiration of Phytopathogenic Fungi Demonstrated by Antifungal Joint Action of Respiration Inhibitors. *J. Pestic. Sci.*, **21** (4), 399–403.

108. Fujimura, M. (2010) Mechanism of action of dicarboximide and phenylpyrrole on the stress-response signal transduction pathway. *J. Pestic. Sci.*, **35** (3), 351–353.

109. Yan, L., Li, M., Cao, Y., Gao, P., Cao, Y., Wang, Y., and Jiang, Y. (2009) The alternative oxidase of Candida albicans causes reduced fluconazole susceptibility. *J. Antimicrob. Chemother.*, **64** (4), 764–773.

110. Strippoli, V., D'Auria, F.D., Tecca, M., Callari, A., and Simonetti, G. (2000) Propyl gallate increases in vitro antifungal imidazole activity against Candida albicans. *Int. J. Antimicrob. Agents*, **16** (1), 73–76.

111. Martins, V.P., Dinamarco, T.M., Soriani, F.M., Tudella, V.G., Oliveira, S.C., Goldman, G.H., Curti, C., and Uyemura, S.A. (2011) Involvement of an Alternative Oxidase in Oxidative Stress and Mycelium-to-Yeast Differentiation in Paracoccidioides brasiliensis. *Eukaryot. Cell*, **10** (2), 237–248.

112. Akhter, S., McDade, H.C., Gorlach, J.M., Heinrich, G., Cox, G.M., and Perfect, J.R. (2003) Role of Alternative Oxidase Gene in Pathogenesis of Cryptococcus neoformans. *Infect. Immun.*, **71** (10), 5794–5802.

113. Magnani, T., Soriani, F.M., Martins, V.D.P., Policarpo, A.C.D.F., Sorgi, C.A., Faccioli, L.H., Curti, C., and Uyemura, S.A. (2008) Silencing of mitochondrial alternative oxidase gene of Aspergillus fumigatus enhances reactive oxygen species production and killing of the fungus by macrophages. *J. Bioenerg. Biomembr.*, **40** (6), 631–636.

114. Guedouari, H., Gergondey, R., Bourdais, A., Vanparis, O., Bulteau, A.L., Camadro, J.M., and Auchère, F. (2014) Changes in glutathione-dependent redox status and mitochondrial energetic strategies are part of the adaptive response during the filamentation process in Candida albicans. *Biochim. Biophys. Acta - Mol. Basis Dis.*, **1842** (9), 1855–1869.

115. Chaudhuri, M., Ajayi, W., and Hill, G. (1998) Biochemical and molecular properties of the Trypanosoma brucei alternative oxidase. *Mol. Biochem. Parasitol.*, **95** (1), 53–68.

116. Roberts, C.W., Roberts, F., Henriquez, F.L., Akiyoshi, D., Samuel, B.U., Richards, T. a, Milhous, W., Kyle, D., McIntosh, L., Hill, G.C., Chaudhuri, M., Tzipori, S., and McLeod, R. (2004) Evidence for mitochondrial-derived alternative oxidase in the apicomplexan parasite Cryptosporidium parvum: a potential anti-microbial agent target. *Int. J. Parasitol.*, **34** (3), 297–308.

117. Williams, B.A.P., Elliot, C., Burri, L., Kido, Y., Kita, K., Moore, A.L., and Keeling, P.J. (2010) A broad distribution of the alternative oxidase in microsporidian parasites. *PLoS Pathog.*, **6** (2), 1–8.

118. Schonbaum, G.R., Bonner, W.D., Storey, B.T., and Bahr, J.T. (1971) Specific Inhibition of the Cyanide-insensitive Respiratory Pathway in Plant Mitochondria by Hydroxamic Acids. *Plant Physiol.*, **47** (1), 124–128.

119. Siedow, J.N., and Girvin, M.E. (1980) Alternative Respiratory Pathway: Its Role in Seed Respiration and Its Inhibition by Propyl Gallate. *Plant Physiol.*, **65** (4), 669–674.

120. Janes, H.W., and Wiest, S.C. (1982) Inhibition of O2 Consumption Resistant to Cyanide and Its Development by N-Propyl Gallate and Salicylhydroxamic Acid. *Plant Physiol.*, **70** (3), 853–857.

121. Menzies, S.K., Tulloch, L.B., Florence, G.J., and Smith, T.K. (2018) The trypanosome alternative oxidase: a potential drug target? *Parasitology*, **145** (2), 175–183.

122. Chaudhuri, M., Ott, R.D., and Hill, G.C. (2006) Trypanosome alternative oxidase: from

molecule to function. *Trends Parasitol.*, **22** (10), 484–491.

123. Clarkson, A., and Brohn, F. (1976) Trypanosomiasis: an approach to chemotherapy by the inhibition of carbohydrate catabolism. *Science (80-.).*, **194** (4261), 204–206.

124. Clarkson, A.B., Grady, R.W., Grossman, S.A., McCallum, R.J., and Brohn, F.H. (1981) Trypanosoma brucei brucei: A systematic screening for alternatives to the salicylhydroxamic acid-glycerol combination. *Mol. Biochem. Parasitol.*, **3** (5), 271–291.

125. Clarkson, A.B., Bienen, E.J., Pollakis, G., and Grady, R.W. (1989) Trypanocidal CoQ analogues: Their effect on other mitochondrial systems. *Comp. Biochem. Physiol. Part B Comp. Biochem.*, **94** (2), 245–251.

126. Grady, R.W., Bienen, E.J., and Clarkson, A.B. (1986) p-alkyloxybenzhydroxamic acids, effective inhibitors of the trypanosome glycerol-3-phosphate oxidase. *Mol. Biochem. Parasitol.*, **19** (3), 231–240.

127. Grady, R.W., Bienen, E.J., and Clarkson, A.B. (1986) Esters of 3,4-dihydroxybenzoic acid, highly effective inhibitors of the sn-glycerol-3-phosphate oxidase of Trypanosoma brucei brucei. *Mol. Biochem. Parasitol.*, **21** (1), 55–63.

128. Grady, R.W., Bienen, E.J., Dieck, H.A., Saric, M., and Clarkson, A.B. (1993) N-n-alkyl-3,4-dihydroxybenzamides as inhibitors of the trypanosome alternative oxidase: activity in vitro and in vivo. *Antimicrob. Agents Chemother.*, **37** (5), 1082–1085.

129. Minagawa, N., Yabu, Y., Kita, K., Nagai, K., Ohta, N., Meguro, K., Sakajo, S., and Yoshimoto, A. (1997) Erratum to “An antibiotic, ascofuranone, specifically inhibits respiration and in vitro growth of long slender bloodstream forms of Trypanosoma brucei brucei.” *Mol. Biochem. Parasitol.*, **84** (2), 271–280.

130. Hijikawa, Y., Matsuzaki, M., Suzuki, S., Inaoka, D.K., Tatsumi, R., Kido, Y., and Kita, K. (2017) Re-identification of the ascofuranone-producing fungus Ascochyta viciae as Acremonium sclerotigenum. *J. Antibiot. (Tokyo).*, **70** (3), 304–307.

131. James, T.W., and Spencer, M.S. (1982) Inhibition of Cyanide-Resistant Respiration in Pea Cotyledon Mitochondria by Chloroquine. *Plant Physiol.*, **69** (5), 1113–1115.

132. Cook, N.D., and Cammack, R. (1983) Effects of the quinone analogue 5-n-undecyl-6-hydroxy-4,7-dioxo benzothiazole on cyanide- sensitive and cyanide-insensitive plant mitochondria. *604th Meet. Cambridge*, **11**, 785.

133. Kay, C.J., and Palmer, J.M. (1985) Solubilization of the alternative oxidase of cuckoo-pint (Arum maculatum) mitochondria. Stimulation by high concentrations of ions and effects of specific inhibitors. *Biochem. J.*, **228** (2), 309–318.

134. Hoefnagel, M.H.N., Wiskich, J.T., Madgwick, S. a, Patterson, Z., Oettmeier, W., and Rich, P.R. (1995) New Inhibitors of the Ubiquinol Oxidase of Higher Plant Mitochondria. *Eur. J. Biochem.*, **233** (2), 531–537.

135. Ebiloma, G.U., Ayuga, T.D., Balogun, E.O., Gil, L.A., Donachie, A., Kaiser, M., Herraiz, T., Inaoka, D.K., Shiba, T., Harada, S., Kita, K., de Koning, H.P., and Dardonville, C. (2018) Inhibition of trypanosome alternative oxidase without its N-terminal mitochondrial targeting signal (ΔMTS-TAO) by cationic and non-cationic 4-hydroxybenzoate and 4-alkoxybenzaldehyde derivatives active against T. brucei and T. congolense. *Eur. J. Med. Chem.*, **150**, 385–402.

136. Yabu, Y., Yoshida, A., Suzuki, T., Nihei, C., Kawai, K., Minagawa, N., Hosokawa, T., Nagai, K., Kita, K., and Ohta, N. (2003) The efficacy of ascofuranone in a consecutive treatment on Trypanosoma brucei brucei in mice. *Parasitol. Int.*, **52** (2), 155–164.

137. Saimoto, H., Kido, Y., Haga, Y., Sakamoto, K., and Kita, K. (2013) Pharmacophore identification of ascofuranone, potent inhibitor of cyanide-insensitive alternative oxidase of Trypanosoma brucei. *J. Biochem.*, **153** (3), 267–273.

138. West, R.A., O'Doherty, O.G., Askwith, T., Atack, J., Beswick, P., Laverick, J., Paradowski, M., Pennicott, L.E., Rao, S.P.S., Williams, G., and Ward, S.E. (2017) African trypanosomiasis: Synthesis & SAR enabling novel drug discovery of ubiquinol mimics for trypanosome alternative oxidase. *Eur. J. Med. Chem.*, **141**, 676–689.

139. West, R.A., Cunningham, T., Pennicott, L.E., Rao, S.P.S., and Ward, S.E. (2018) Toward More Drug Like Inhibitors of Trypanosome Alternative Oxidase. *ACS Infect. Dis.*, **4** (4), 592–604.

140. Bendall, D.S., and Bonner, W.D. (1971) Cyanide-insensitive Respiration in Plant Mitochondria. *Plant Physiol.*, **47** (2), 236–245.

141. Arnholdt-Schmitt, B., Costa, J.H., and de Melo, D.F. (2006) AOX – a functional marker for efficient cell reprogramming under stress? *Trends Plant Sci.*, **11** (6), 281–287.

142. Vanlerberghe, G.C. (2013) Alternative oxidase: A mitochondrial respiratory pathway to maintain metabolic and signaling homeostasis during abiotic and biotic stress in plants. *Int. J. Mol. Sci.*, **14** (4), 6805–6847.

143. Vanlerberghe, G.C., Martyn, G.D., and Dahal, K. (2016) Alternative oxidase: a respiratory electron transport chain pathway essential for maintaining photosynthetic performance during drought stress. *Physiol. Plant.*, **157** (3), 322–337.

144. Kumar, S.R., and Sathishkumar, R. (2015) Gene technology applied for AOX functionality studies, in *Alternative respiratory pathways in higher plants* (eds.Gupta, K.J., Mur, L.A.J., and Neelwarne, B.), John Wiley & Sons, Ltd, Chichester, UK, pp. 287–297.

145. Camargo, A.F., Chioda, M.M., Rodrigues, A.P.C., Garcia, G.S., McKinney, E.A., Jacobs, H.T., and Oliveira, M.T. (2018) Xenotopic expression of alternative electron transport enzymes in animal mitochondria and their impact in health and disease. *Cell Biol. Int.*, **42** (6), 664–669.

146. Saari, S., Garcia, G.S., Bremer, K., Chioda, M.M., Andjelković, A., Debes, P. V., Nikinmaa, M., Szibor, M., Dufour, E., Rustin, P., Oliveira, M.T., and Jacobs, H.T. (2018) Alternative respiratory chain enzymes: Therapeutic potential and possible pitfalls. *Biochim. Biophys. Acta - Mol. Basis Dis.*

147. Fernández-Ortuño, D., Torés, J.A., de Vicente, A., and Pérez-García, A. (2010) The QoI fungicides, the rise and fall of a successful class of agricultural fungicides. *Fungicides*, 203–220.

148. Sasaki, H., Hosokawa, T., Sawada, M., and Ando, K. (1973) Isolation and structure of ascofuranone and ascofranol, antibiotics with hypolipidemic activity. *J. Antibiot. (Tokyo).*, **26** (11), 676–680.

149. Berry, E.A., Huang, L., Lee, D.-W., Daldal, F., Nagai, K., and Minagawa, N. (2010) Ascochlorin is a novel, specific inhibitor of the mitochondrial cytochrome bc1 complex. *Biochim. Biophys. Acta - Bioenerg.*, **1797** (3), 360–370.

150. Mogi, T., Ui, H., Shiomi, K., Ōmura, S., Miyoshi, H., and Kita, K. (2009) Antibiotics LL-Z1272 identified as novel inhibitors discriminating bacterial and mitochondrial quinol oxidases. *Biochim. Biophys. Acta - Bioenerg.*, **1787** (2), 129–133.

151. Shen, W., Ren, X., Zhu, J., Xu, Y., Lin, J., Li, Y., Zhao, F., Zheng, H., Li, R., Cui, X., Zhang, X., Lu, X., and Zheng, Z. (2016) Discovery of a new structural class of competitive h DHODH inhibitors with in vitro and in vivo anti-inflammatory, immunosuppressive effects. *Eur. J. Pharmacol.*, **791**, 205–212.

152. Hong, S., Park, K.-K., Magae, J., Ando, K., Lee, T.-S., Kwon, T.K., Kwak, J.-Y., Kim, C.-H., and Chang, Y.-C. (2005) Ascochlorin Inhibits Matrix Metalloproteinase-9 Expression by Suppressing Activator Protein-1-mediated Gene Expression through the ERK1/2 Signaling Pathway. *J. Biol. Chem.*, **280** (26), 25202–25209.

153. Hosokawa, T., Okutomi, T., Sawada, M., Ando, K., and Tamura, G. (1981) Unusual concentration of urine and prevention of polydipsia by fungal prenylphenols in doca hypertensive rats. *Eur. J. Pharmacol.*, **69** (4), 429–438.

154. Magae, J., Hosokawa, T., Ando, K., Nagai, K., and Tamura, G. (1982) Antitumor protective property of an isoprenoid antibiotic, ascofuranone. *J. Antibiot.*, **35** (11), 1547–1552.

155. Sawada, M., Hosokawa, T., Okutomi, T., and Ando, K. (1973) Hypolipidemic property of ascofuranone. *J. Antibiot. (Tokyo).*, **26** (11), 681–6.

156. Tamura, G., Suzuki, S., Takatsuki, A., Ando, K., and Arima, K. (1968) Ascochlorin, a new antibiotic, found by paper-disc agar-difusion method. I. *J. Antibiot. (Tokyo).*, **21** (9), 539–544.

157. Tsuruga, M., Nakajima, H., Ozawa, S., Togashi, M., Chang, Y.-C., Ando, K., and Magae, J. (2004) Characterization of 4-O-methyl-ascochlorin-induced apoptosis in comparison with typical apoptotic inducers in human leukemia cell lines. *Apoptosis*, **9** (4), 429–435.

158. Tsuruga, M., Nakajima, H., and Magae, J. (2007) Immunosuppressive Activity of 4-O-Methylascochlorin. *J. Antibiot. (Tokyo).*, **60** (1), 20–26.

159. Togashi, M., Masuda, H., Kawada, T., Tanaka, M., Saida, K., Ando, K., TAMURA, G., and MAGAE, J. (2002) PPAR.gamma Activation and Adipocyte Differentiation Induced by AS-6, a Prenyl-phenol Antidiabetic Antibiotic. *J. Antibiot. (Tokyo).*, **55** (4), 417–422.

160. Takamatsu, S., Rho, M.-C., Masuma, R., Hayashi, M., Komiyama, K., Tanaka, H., and Omura, S. (1994) A Novel Testosterone 5.ALPHA.-Reductase Inhibitor, 8',9'-Dehydroascochlorin Produced by Verticillium sp. FO-2787. *Chem. Pharm. Bull.*

(Tokyo)., **42** (4), 953–956.

161. Togashi, M., Ozawa, S., Abe, S., Nishimura, T., Tsuruga, M., Ando, K., Tamura, G., Kuwahara, S., Ubukata, M., and Magae, J. (2003) Ascochlorin Derivatives as Ligands for Nuclear Hormone Receptors. *J. Med. Chem.*, **46** (19), 4113–4123.

162. Grady, R.W., Bienen, E.J., and Clarkson, A.B. (1986) Esters of 3,4-dihydroxybenzoic acid, highly effective inhibitors of the sn-glycerol-3-phosphate oxidase of Trypanosoma brucei brucei. *Mol. Biochem. Parasitol.*, **21** (1), 55–63.

163. Teixeira, P.J.P.L., Thomazella, D.P. de T., and Pereira, G.A.G. (2015) Time for Chocolate: Current Understanding and New Perspectives on Cacao Witches' Broom Disease Research. *PLoS Pathog.*, **11** (10), e1005130.

164. El-Gebali, S., Mistry, J., Bateman, A., Eddy, S.R., Luciani, A., Potter, S.C., Qureshi, M., Richardson, L.J., Salazar, G.A., Smart, A., Sonnhammer, E.L.L., Hirsh, L., Paladin, L., Piovesan, D., Tosatto, S.C.E., and Finn, R.D. (2019) The Pfam protein families database in 2019. *Nucleic Acids Res.*, **47** (D1), D427–D432.

ANEXO 1

UNICAMP

INFORMAÇÃO

INFORMAMOS que o projeto **CIBio/IB No. 2011/03 - Genômica e Biotecnologia**, cujo pesquisador responsável é o Prof. Dr. Gonçalo Amarante Guimarães Pereira, sub-projeto "Desenvolvimento direcionado de inibidores da enzima mitocondrial Oxidase Alternativa (AOX) com ação antifúngica contra *Maniliophthora perniciosa*, fungo causador da vassoura de bruxa do cacaueiro", do pós-graduando Mário Ramos de Oliveira Barsottini, encontra-se devidamente aprovado e regularizado junto a CIBio/IB-UNICAMP e a CTNBio, conforme legislação vigente.

Cidade Universitária "Zeferino Vaz",
18 de março de 2019.

Prof. Dr. JOSÉ LUIZ PROENÇA MÓDENA
Presidente da CIBio
Instituto de Biologia – UNICAMP

CIBio/IB-Unicamp
Comissão Interna de Biossegurança
Instituto de Biologia - Unicamp
Caixa Postal 6109 - 13083-970 Campinas SP
Tel.: (19) 3521-6359 – e-mail: comisib@unicamp.br

ANEXO 2

Declaração

As cópias de artigos de minha autoria ou de minha co-autoria, já publicados ou submetidos para publicação em revistas científicas ou anais de congressos sujeitos a arbitragem, que constam da minha Dissertação/Tese de Mestrado/Doutorado, intitulada **Desenvolvimento direcionado de inibidores da enzima mitocondrial Oxidase Alternativa (AOX) com ação antifúngica contra Moniliophthora perniciosa, fungo causador da vassoura de bruxa do cacaueiro**, não infringem os dispositivos da Lei n.° 9.610/98, nem o direito autoral de qualquer editora.

Campinas, 11 de março de 2019

Assinatura : _____

Nome do(a) autor(a): **Mário Ramos de Oliveira Barsottini**

RG n.° 32.950.507-5

Assinatura : _____

Nome do(a) orientador(a): **Gonçalo Amarante Guimarães Pereira**

RG n.° 1713878